



The Hunt for Axion Dark Matter

Bradley J Kavanagh [he/him]

kavanagh@ifca.unican.es

Instituto de Física de Cantabria (CSIC-UC)

LSC Seminar

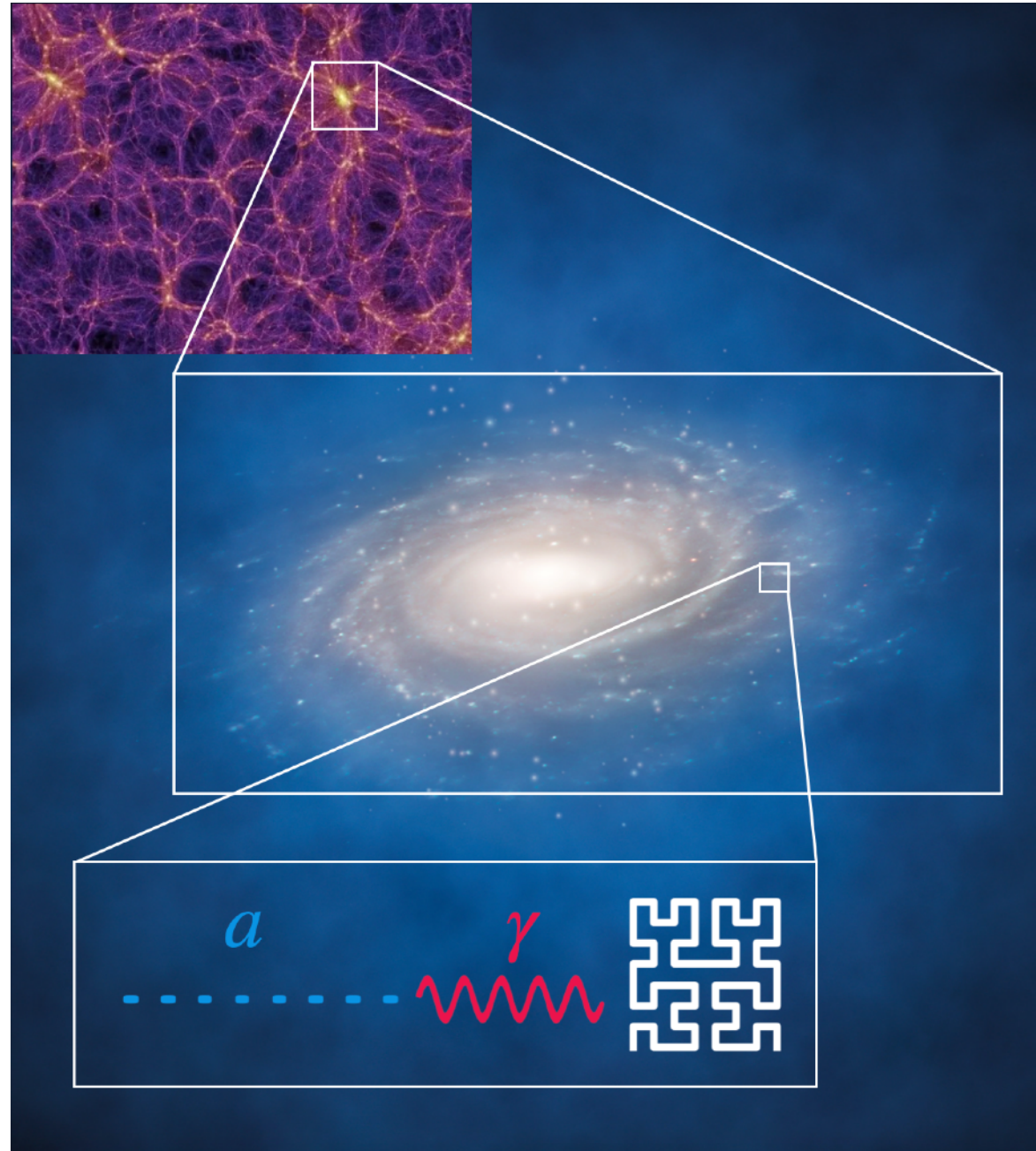
21 October 2025

Overview

- Dark Matter
- Axions as Dark Matter
- Axion Interactions and Constraints
- Axions in the Lab

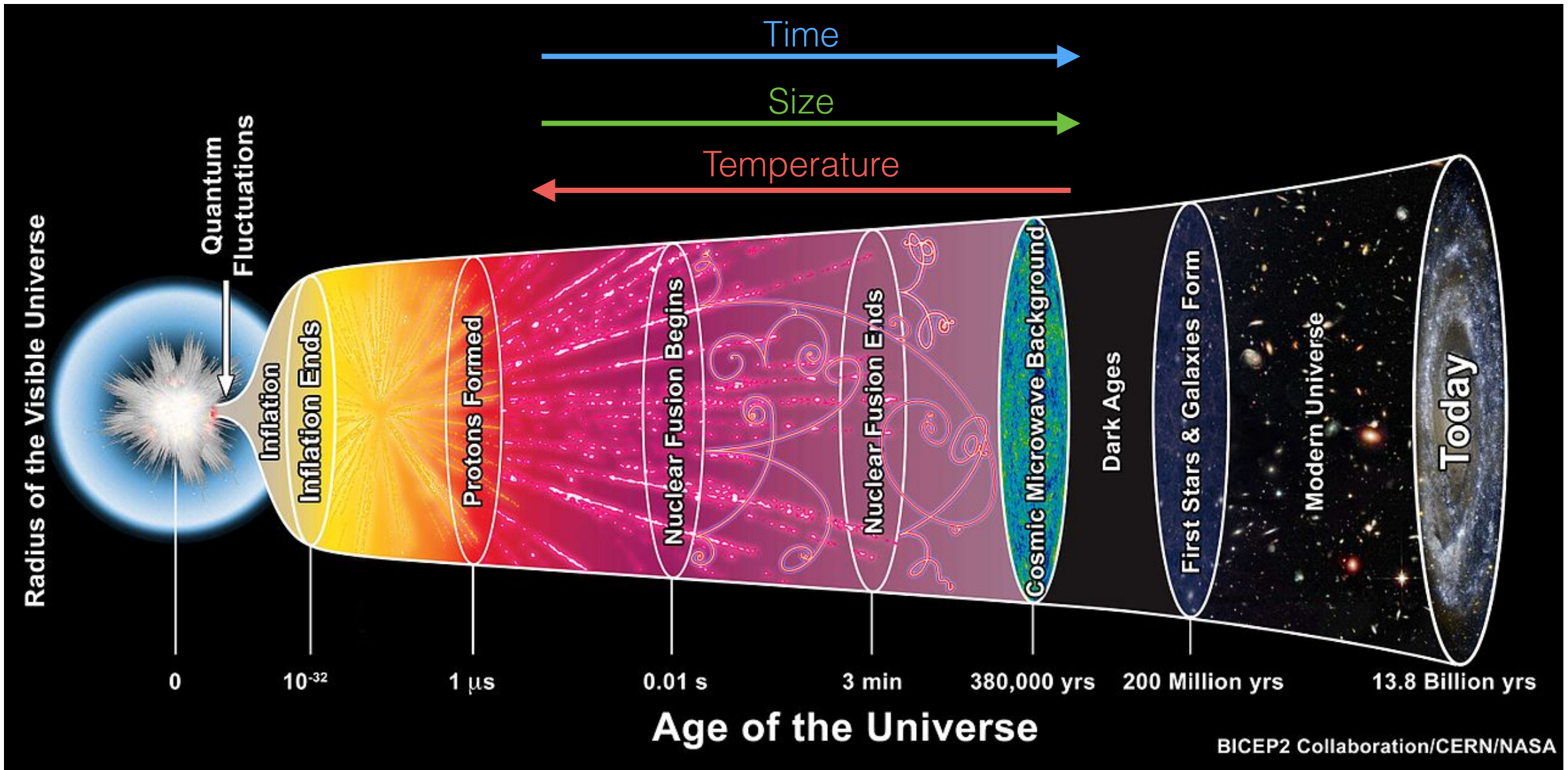


- (Complementary probes)



DARK MATTER

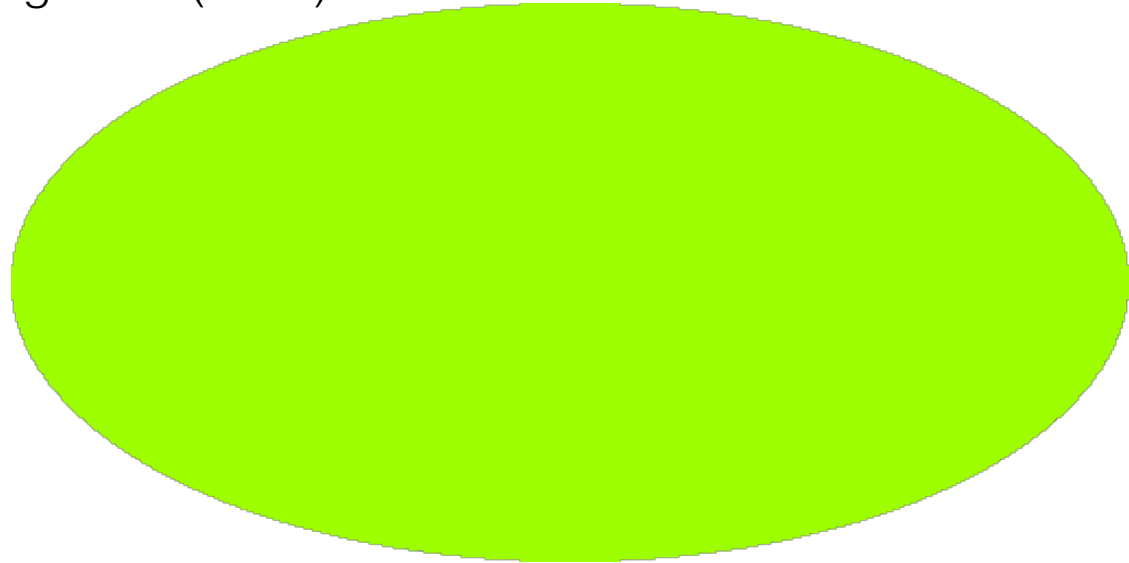
Everything, Everywhere, All at Once



Dark Matter in Cosmology

Cosmic Microwave
Background (CMB)

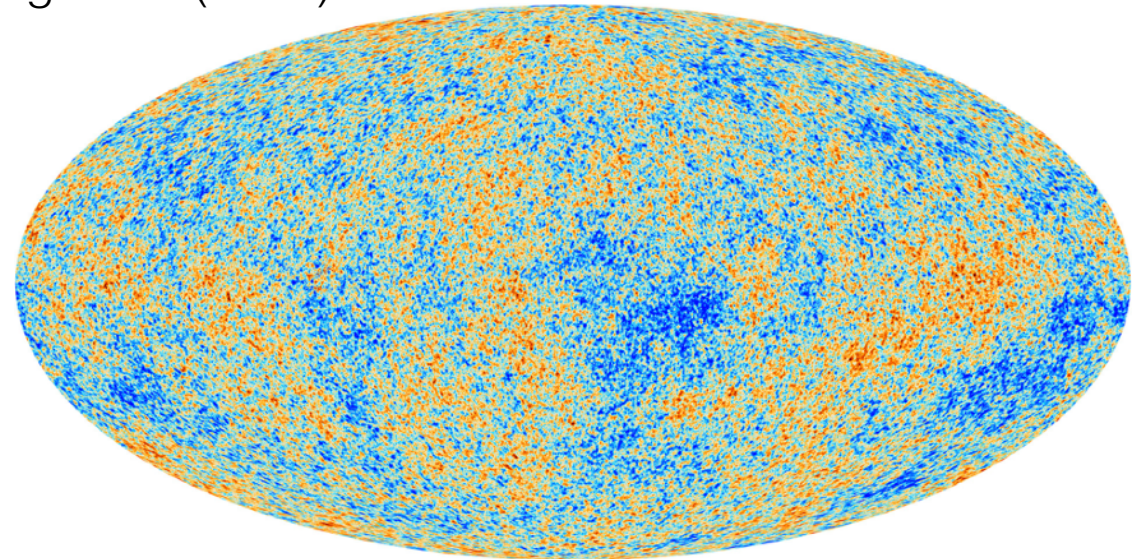
$$T_{\text{CMB}} = 2.73 \text{ K}$$



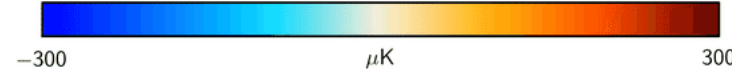
Dark Matter in Cosmology

Cosmic Microwave
Background (CMB)

$$T_{\text{CMB}} = 2.73 \text{ K}$$

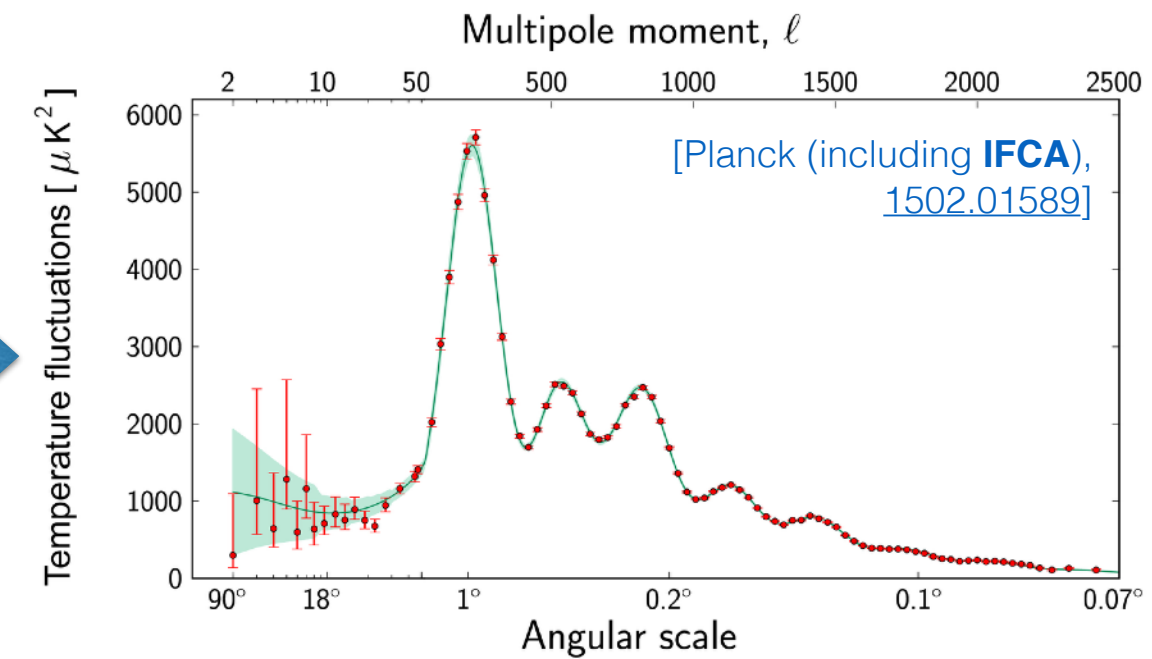
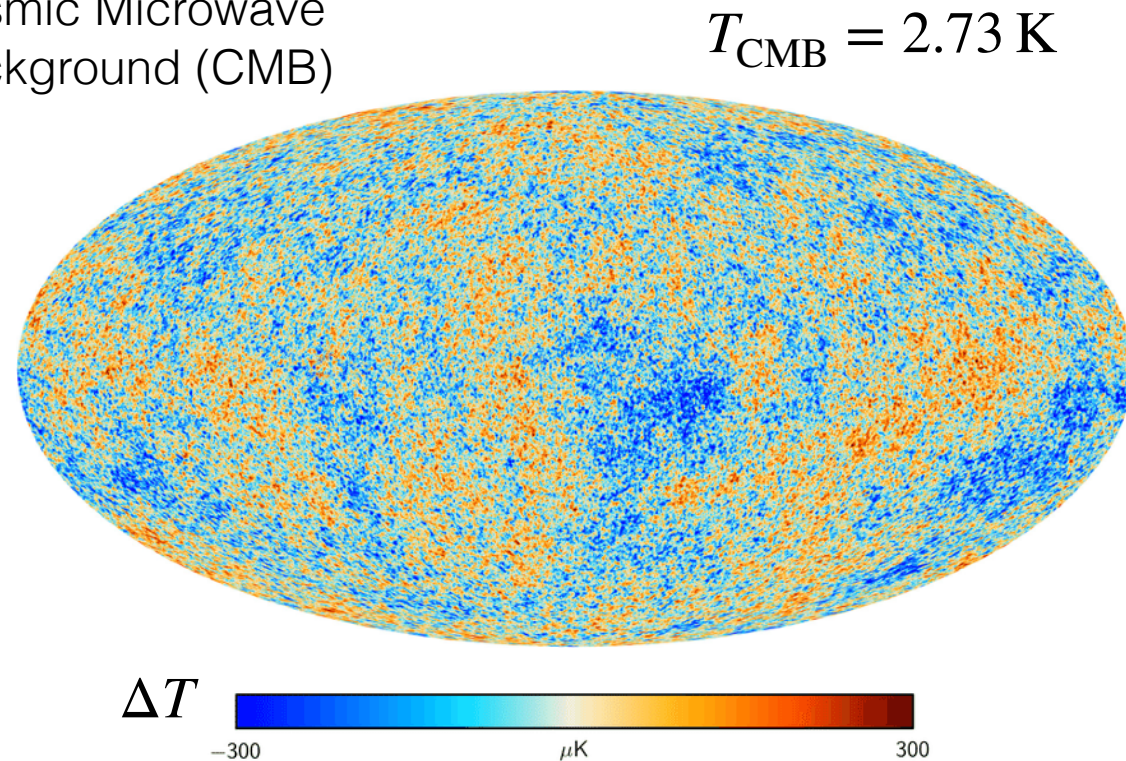


$$\Delta T$$



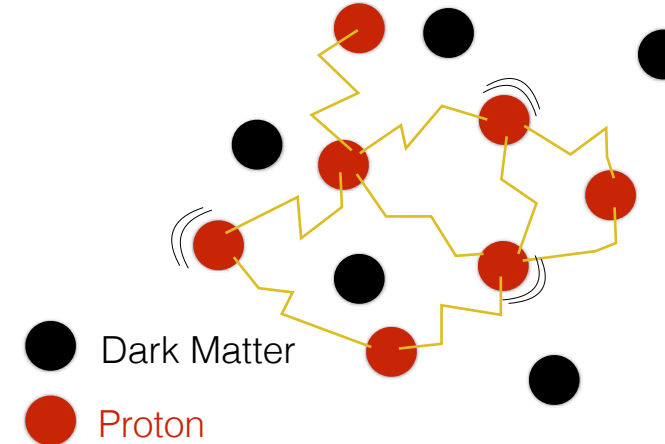
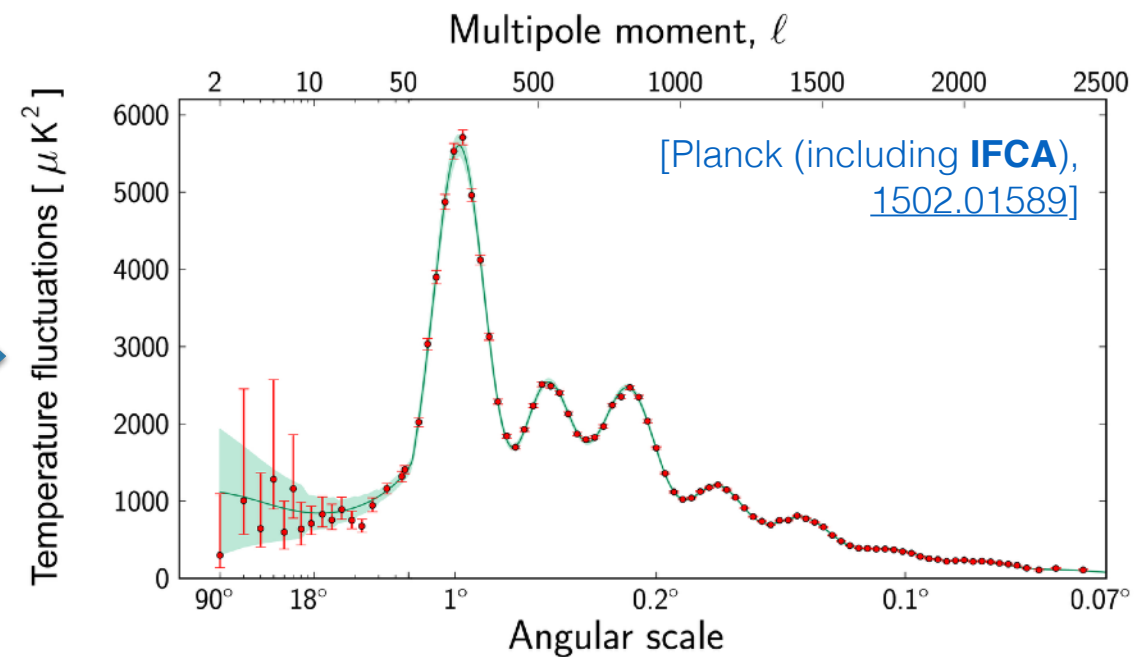
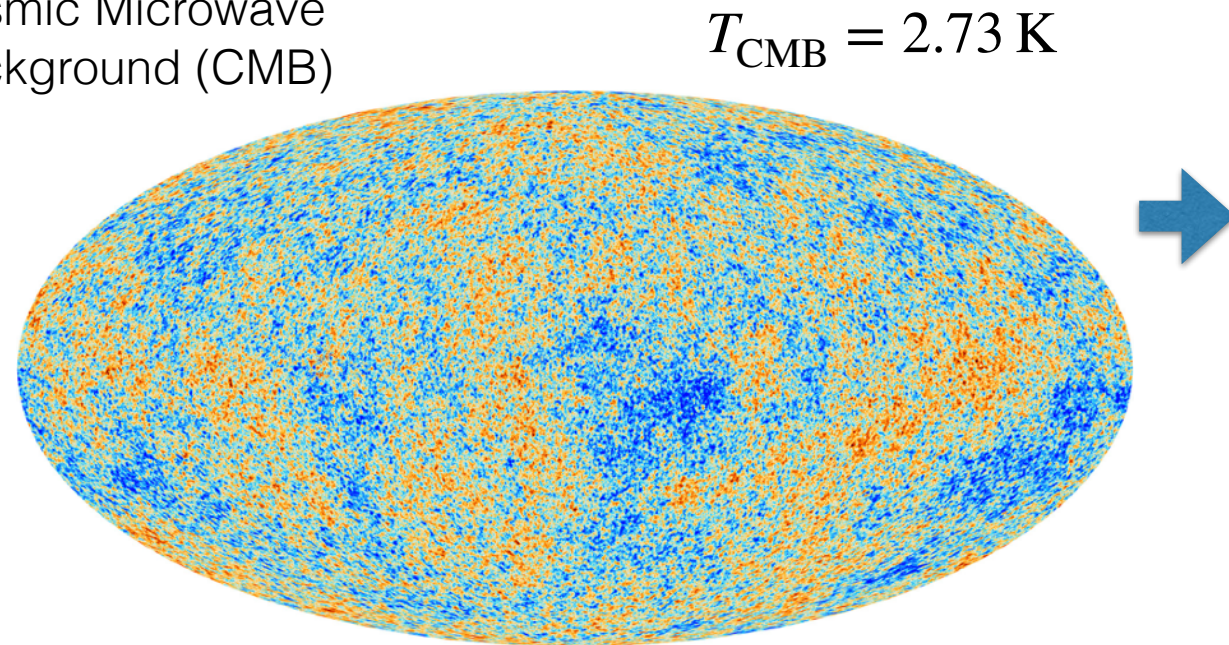
Dark Matter in Cosmology

Cosmic Microwave
Background (CMB)



Dark Matter in Cosmology

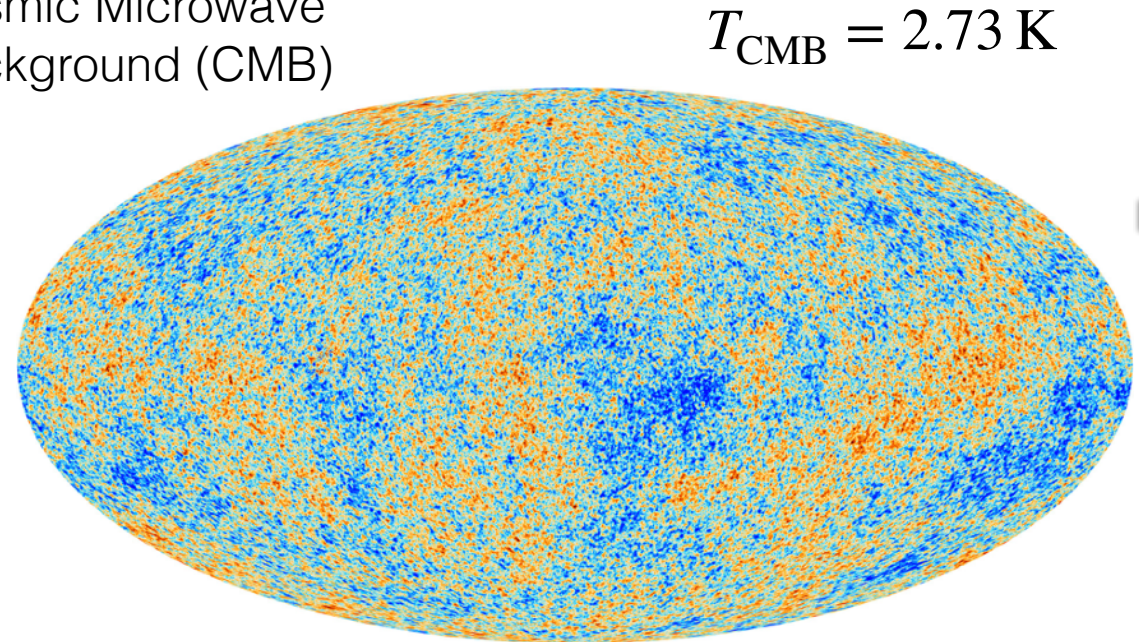
Cosmic Microwave
Background (CMB)



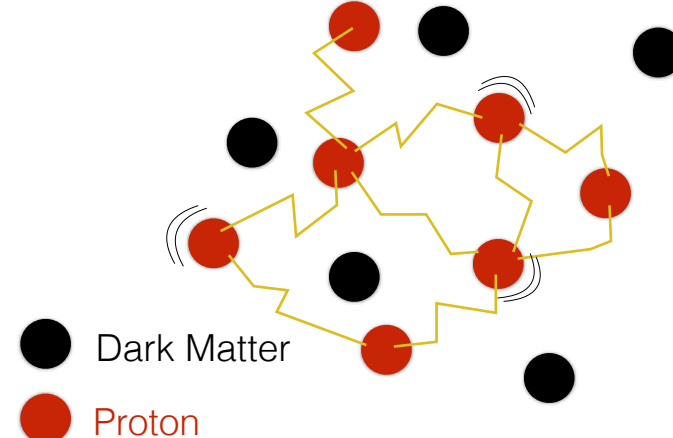
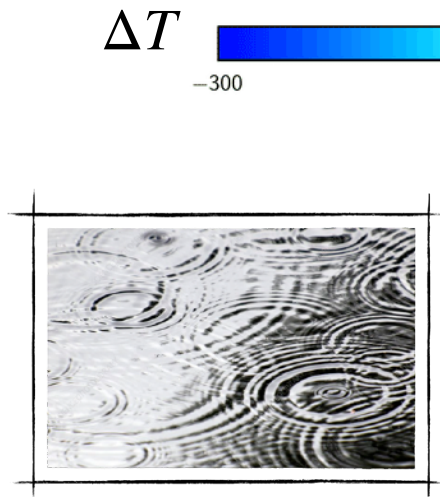
● Dark Matter
● Proton

Dark Matter in Cosmology

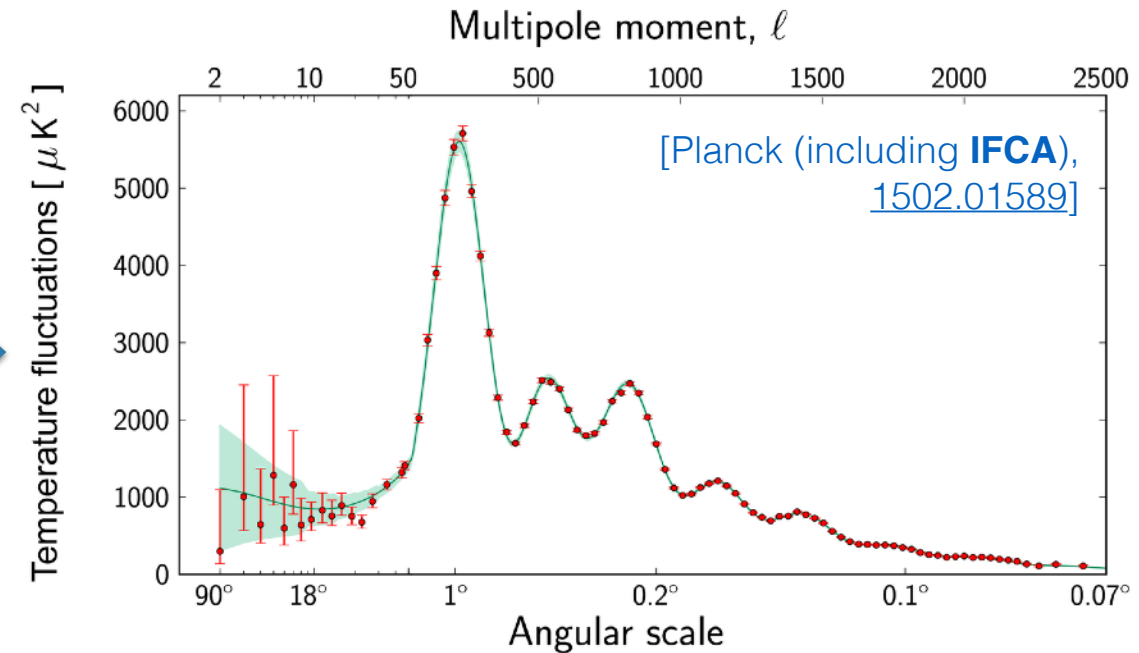
Cosmic Microwave
Background (CMB)



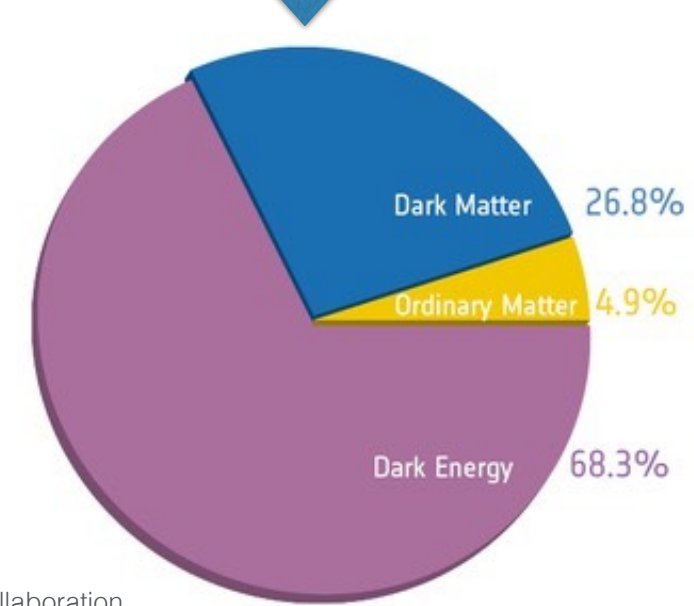
$$T_{\text{CMB}} = 2.73 \text{ K}$$



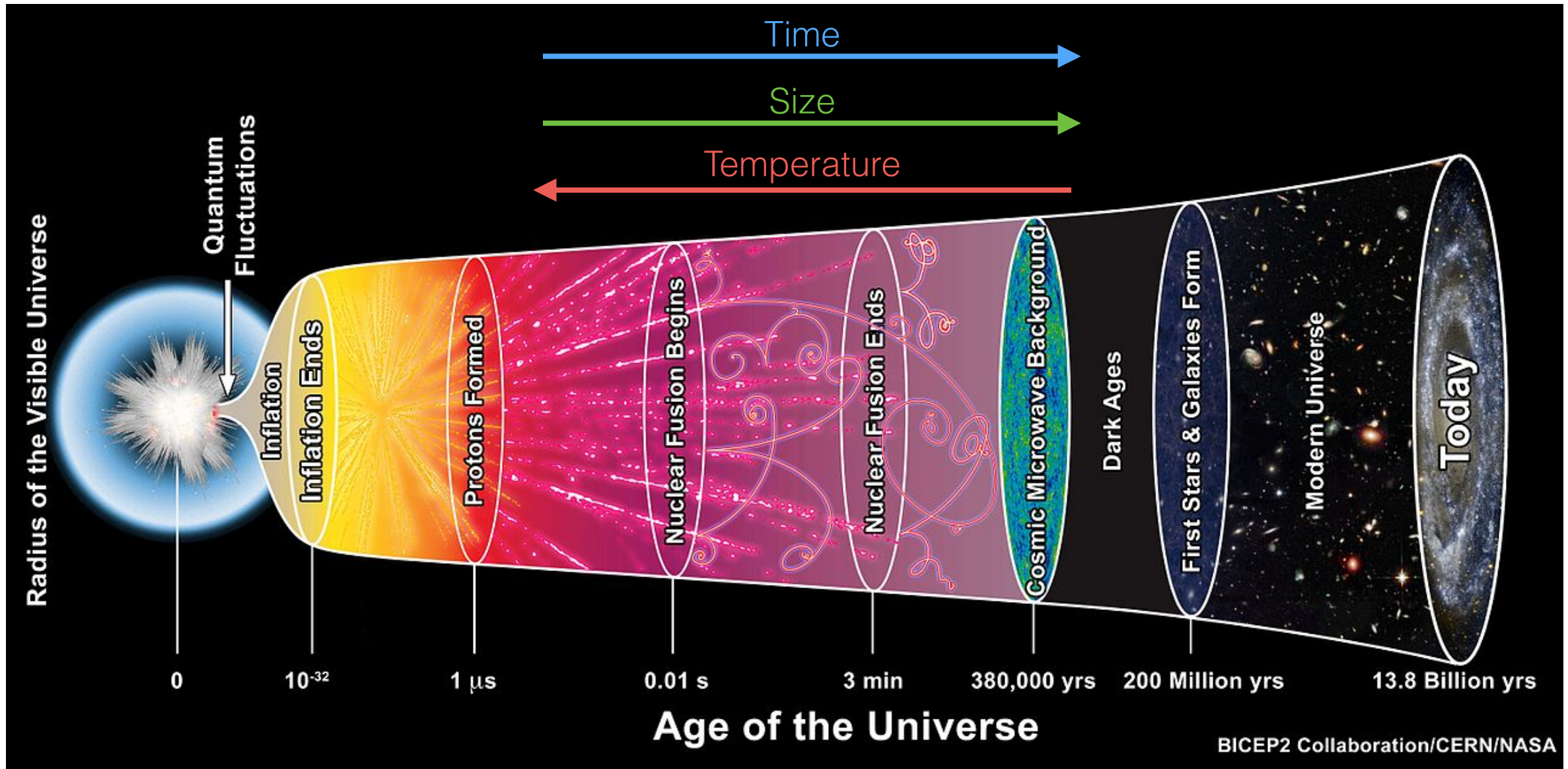
● Dark Matter
● Proton



Credit: ESA/Planck Collaboration



Everything, Everywhere, All at Once





Durham
University

Universiteit Leiden

THE EAGLE SIMULATION
icc.dur.ac.uk/Eagle

$t_{\text{age}} = 0.5 \text{ Gyr}$
Redshift = 10.11

[Video available [here](#)]

www.smcalpine.com



Universiteit Leiden



$t_{\text{age}} = 1.1 \text{ Gyr}$

Redshift = 5.24

[Video available [here](#)]

www.smcalpine.com



Universiteit Leiden



Durham
University

THE EAGLE SIMULATION
icc.dur.ac.uk/Eagle

$t_{\text{age}} = 1.7 \text{ Gyr}$
Redshift = 3.73

[Video available [here](#)]

www.smcalpine.com

Galaxies in Simulations

Dark matter has become an integral part of the standard cosmological model - the **Λ Cold Dark Matter (Λ CDM)** Model. DM plays a key role in our understanding of how Galaxies form, their properties and distributions.

Cosmological simulations can now produce realistic (and beautiful) Galaxies.



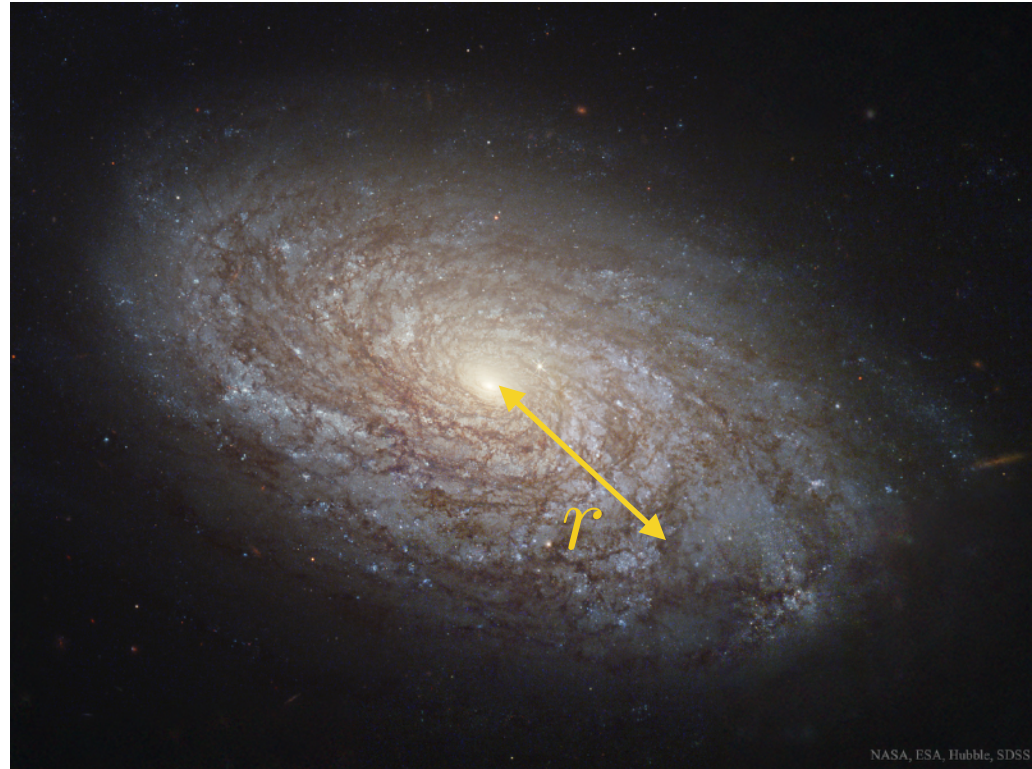
[IllustrisTNG simulation - [2101.12373](#)]

[See also e.g. Auriga Simulations - [1610.01159](#)]

Warning: Galaxy formation is messy and non-linear and still not fully understood

[E.g. [1609.05917](#) vs [1610.07663](#)]

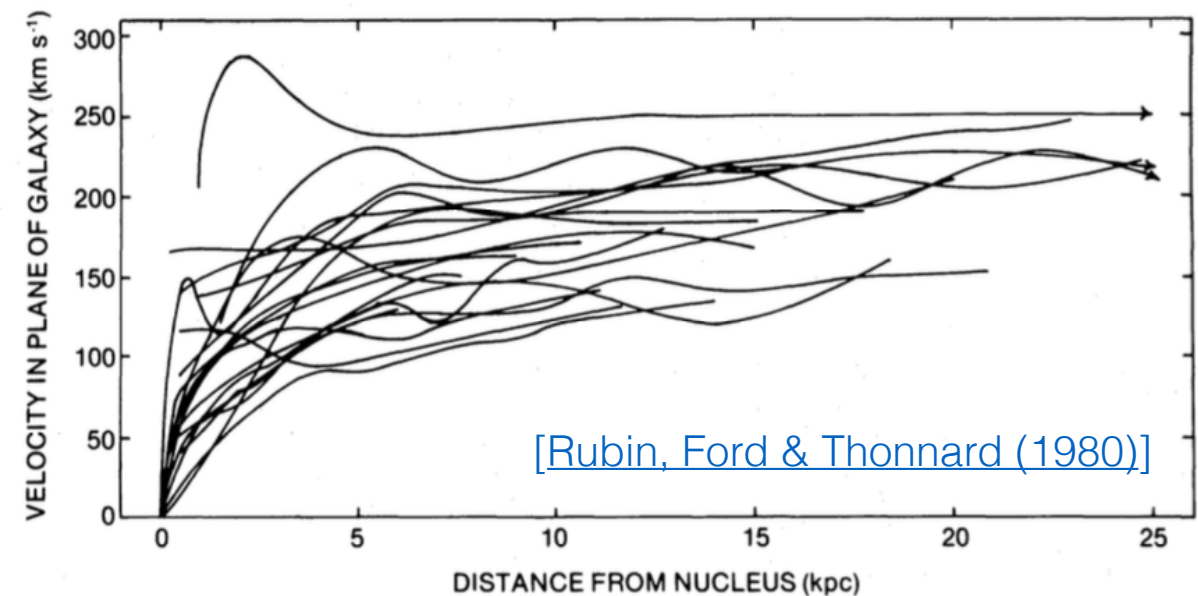
Dark Matter in Galaxies



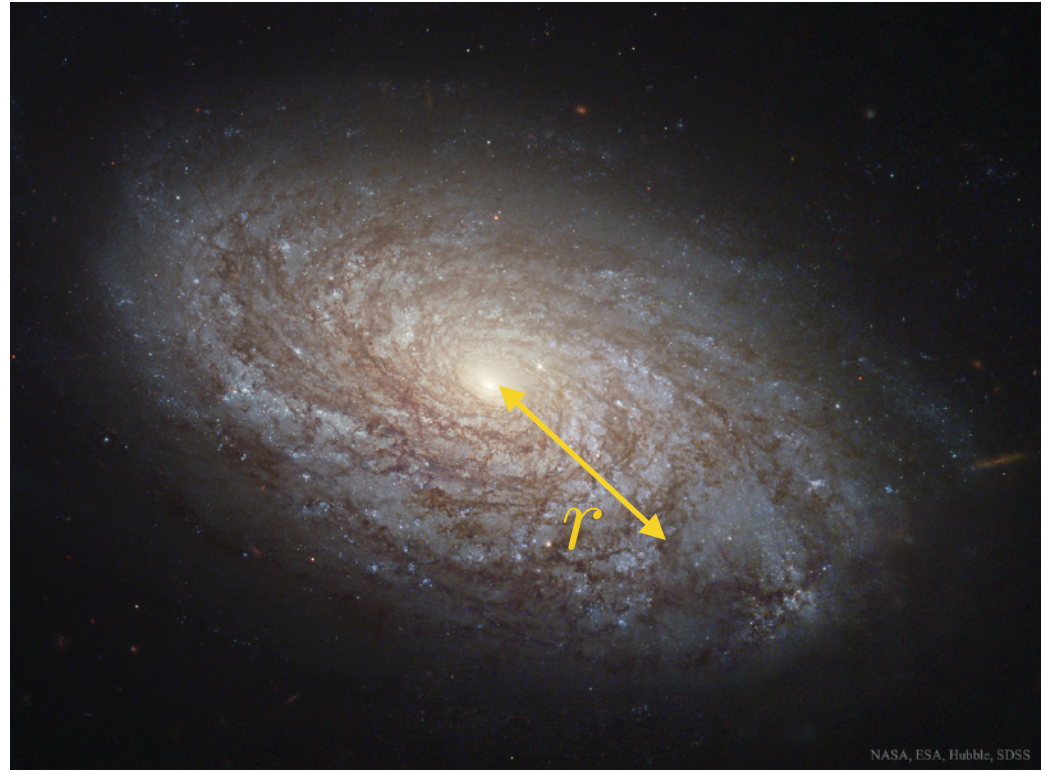
Rotational velocity $v_{\text{rot}}(r)$ of stars (and gas) in disk galaxies allows us to infer (in principle) the enclosed mass distribution.

$$v_{\text{rot}}(r) = \sqrt{\frac{GM_{\text{enc}}(r)}{r}}$$

Rotation curves flatten at large radii, which cannot be explained by mass of observed gas and stars (expect Keplerian $v_{\text{rot}}(r) \propto 1/\sqrt{r}$ at large radii).



Dark Matter in Galaxies



DM density at Earth:

$$\rho_\chi \sim 5 \times 10^{-25} \text{ g/cm}^3$$

$$\sim 0.3 \text{ GeV/cm}^3$$

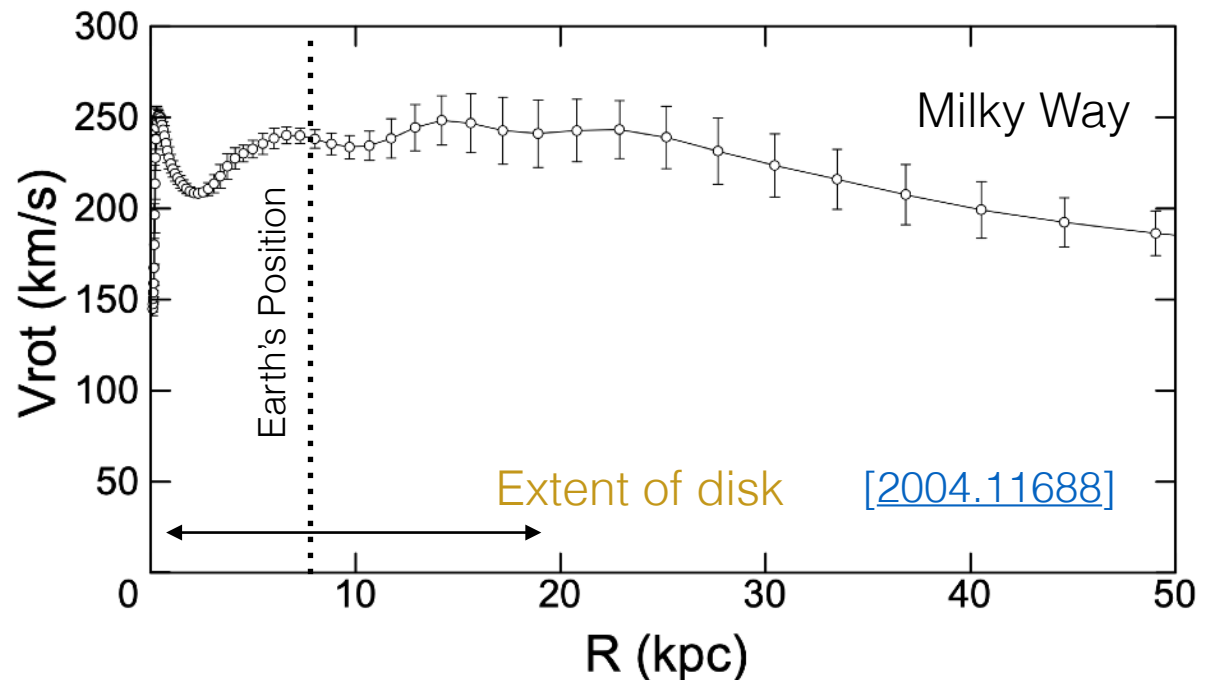
$$\sim 0.008 M_\odot/\text{pc}^3$$

[\[1404.1938\]](#)

Rotational velocity $v_{\text{rot}}(r)$ of stars (and gas) in disk galaxies allows us to infer (in principle) the enclosed mass distribution.

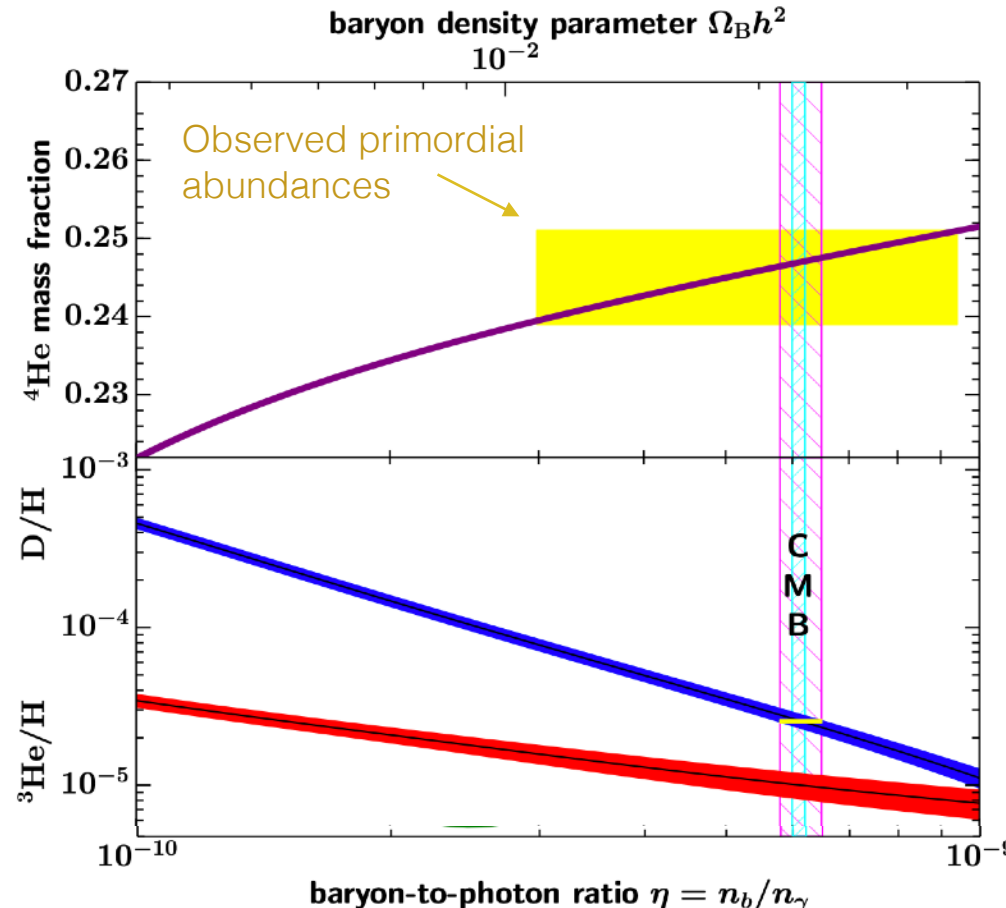
$$v_{\text{rot}}(r) = \sqrt{\frac{GM_{\text{enc}}(r)}{r}}$$

Rotation curves flatten at large radii, which cannot be explained by mass of observed gas and stars (expect Keplerian $v_{\text{rot}}(r) \propto 1/\sqrt{r}$ at large radii).



Dark Matter properties

Non-baryonic: Dark Matter cannot consist of baryonic matter (protons, neutrons, etc). In particular, it cannot participate in Big Bang Nucleosynthesis (BBN) at $T > 1 \text{ MeV}$, $t < 3 \text{ mins}$



Dark Matter Shopping List

- * Non-baryonic
- * 'Neutral'
- * 'Cold' (i.e. slow moving)
- * Produced in sufficient amounts

[0711.4996]

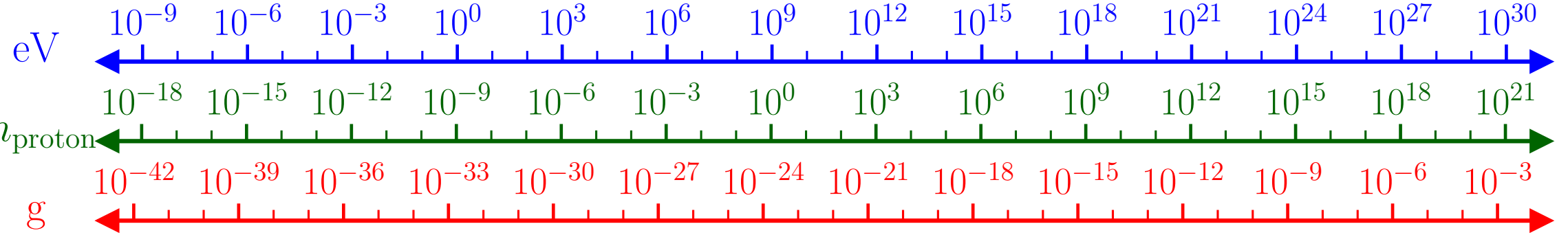
Neutral: Dark Matter cannot be charged*, otherwise it would couple to photons, affecting CMB anisotropies. It would also be able to dissipate energy (from visible stars/galaxies?)

*Strictly speaking, the Dark Matter cannot have a large charge-to-mass ratio (it could for example have a *millicharge*, much smaller than the electron charge).

Cold relic: It has to be produced in the correct abundance, with the correct 'temperature' in order to explain the observed distribution of structure in the Universe...

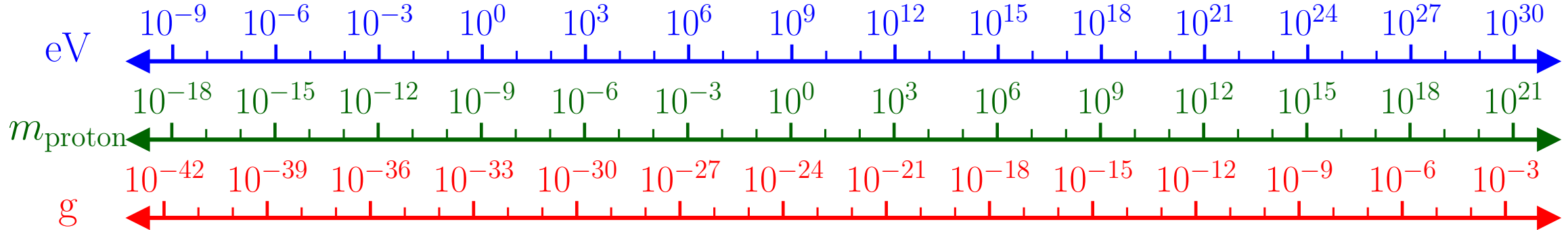
Dark Matter Mass Range

DM Mass

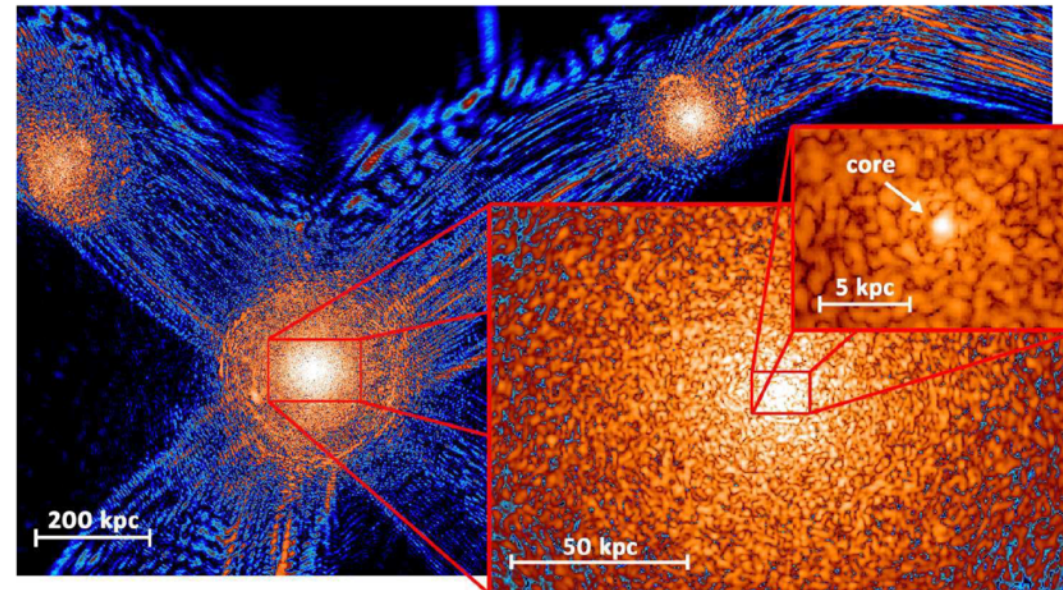


Dark Matter Mass Range

DM Mass

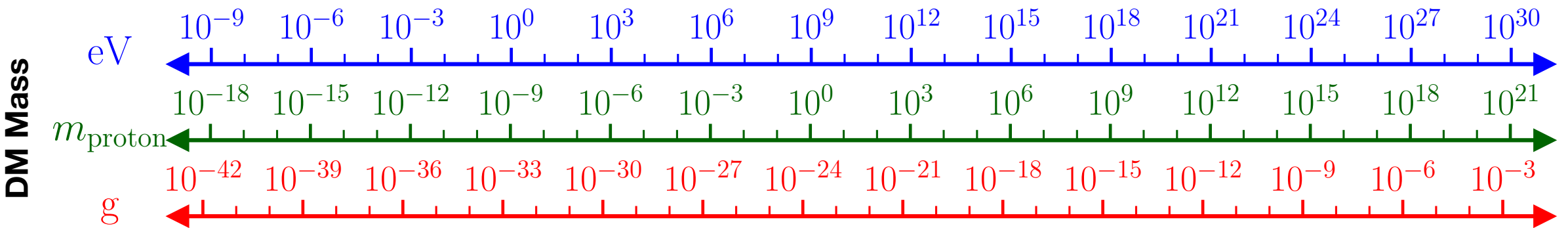


Very light DM ($\lesssim 10^{-22} \text{ eV}$)
has wave-like properties on
astrophysical scales,
spoiling galactic structure



[Schive et al (2014), [1406.6586](#)]

Dark Matter Mass Range



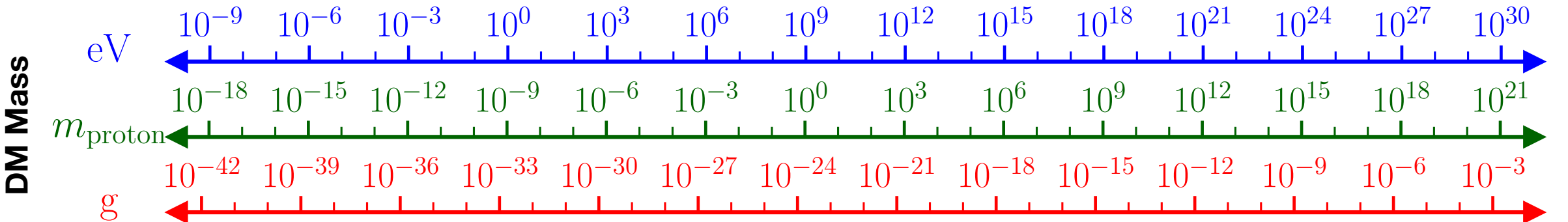
Very light DM ($\lesssim 10^{-22}$ eV)
has wave-like properties on
astrophysical scales,
spoiling galactic structure



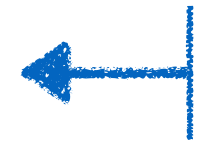
DM lighter than ~ 1 keV must
be bosonic (fermions cannot
be packed to high enough
densities in galaxies)

[Tremaine & Gunn (1979)]

Dark Matter Mass Range



Very light DM ($\lesssim 10^{-22} \text{ eV}$)
has wave-like properties on
astrophysical scales,
spoiling galactic structure



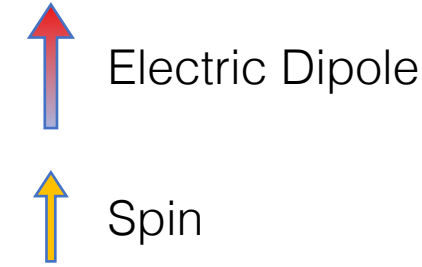
DM lighter than $\sim 1 \text{ keV}$ must
be bosonic (fermions cannot
be packed to high enough
densities in galaxies)

[Tremaine & Gunn (1979)]

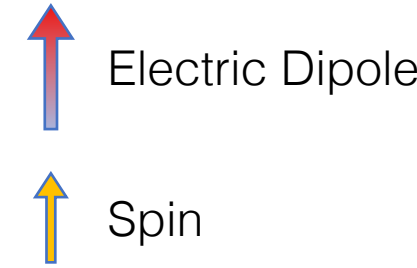
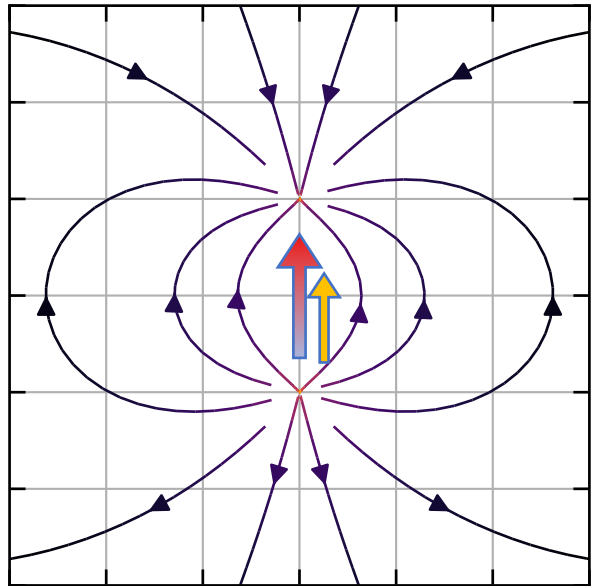
Very heavy DM ($\gtrsim 10^3 M_\odot$)
is ‘discrete’ on astrophysical
scales, spoiling galactic
structure

AXIONS AS DARK MATTER

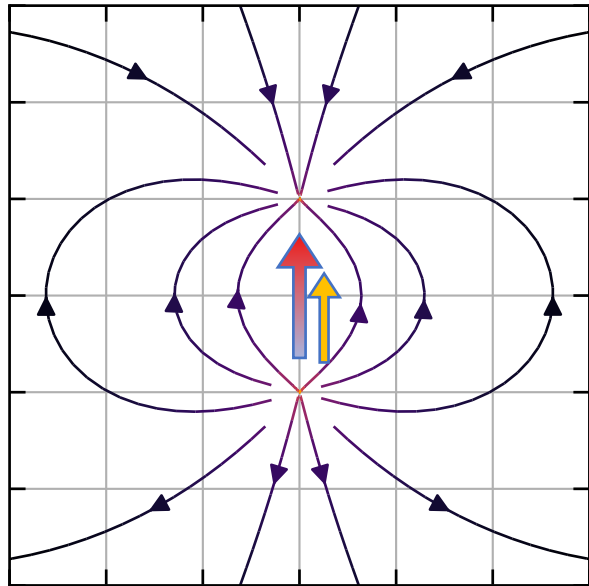
Charge-Parity Symmetry



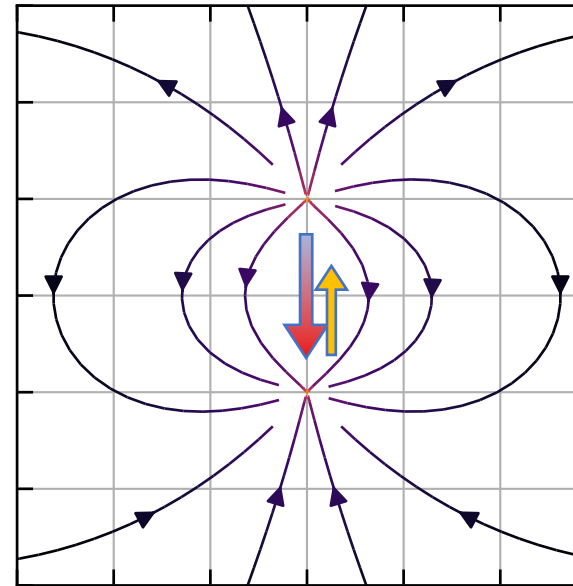
Charge-Parity Symmetry



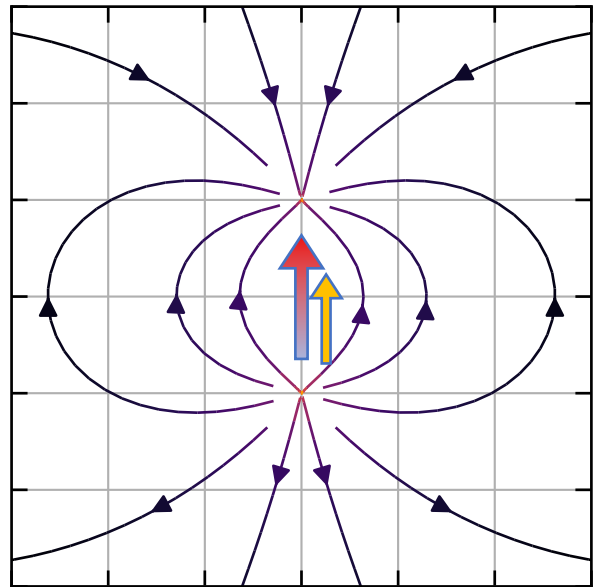
Charge-Parity Symmetry



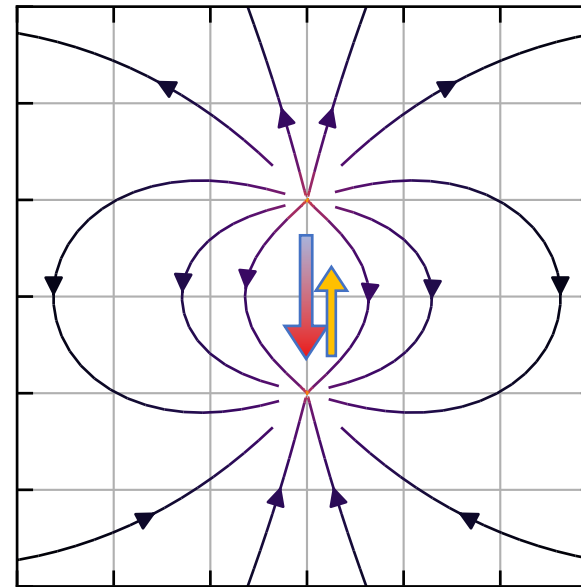
C →



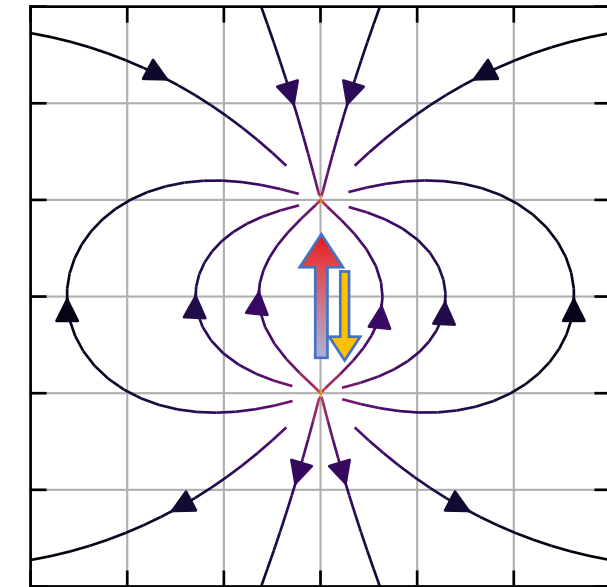
Charge-Parity Symmetry



C



P



Electric Dipole
Spin

The Strong CP Problem

Quantum Chromodynamics (QCD), the theory of the strong force, could have a large Charge-Parity (CP) violating term:

$$\mathcal{L}_{\text{QCD}} \supset \bar{\theta} \frac{1}{32\pi^2} G_{\mu\nu}^a \tilde{G}_a^{\mu\nu}$$

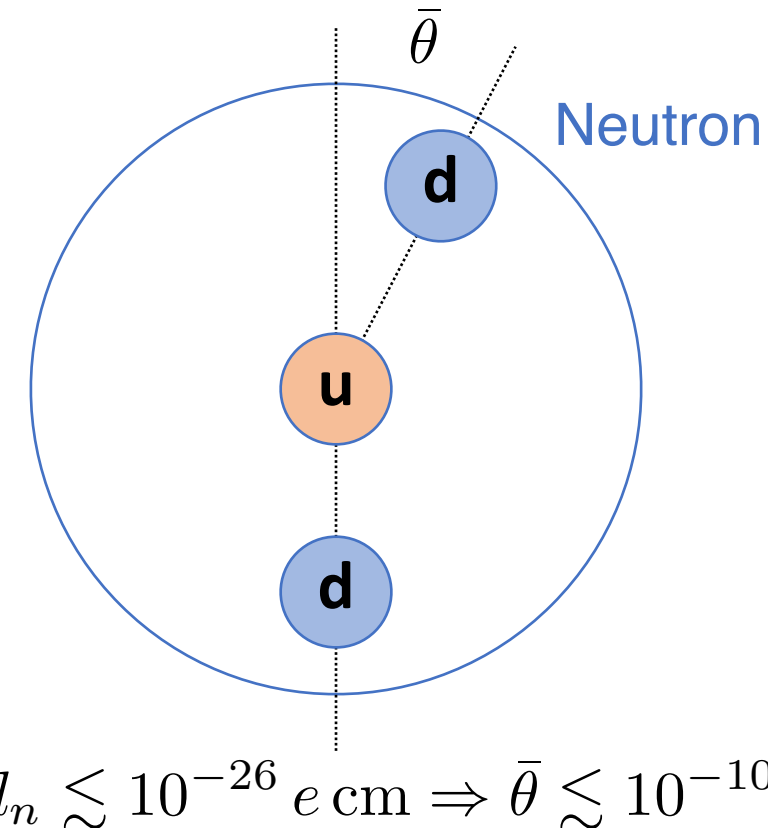
Gluon field strength

CP violation would give rise, for example, to a neutron electric dipole moment $d_n \sim 10^{-16} \bar{\theta} e \text{ cm}$. However, there is **no evidence of CP violation in Strong interactions.**

In QCD alone, the value of $\bar{\theta}$ is just a parameter of the theory, θ_{QCD} - it could in principle be $\mathcal{O}(1)$!

Much worse: the Weak Interactions *do* violate CP and this can be transferred to the Strong sector through non-perturbative effects related to the quark masses: $\theta_{\text{Weak}} = \text{Arg } |\mathbf{M}_q| \sim \mathcal{O}(1)$

Strong CP Problem: *why is $\bar{\theta} = \theta_{\text{QCD}} + \theta_{\text{Weak}}$ so small?!*



$$d_n \lesssim 10^{-26} e \text{ cm} \Rightarrow \bar{\theta} \lesssim 10^{-10}$$

The Strong CP Problem

Quantum Chromodynamics (QCD), the theory of the strong force, could have a large Charge-Parity (CP) violating term:

$$\mathcal{L}_{\text{QCD}} \supset \bar{\theta} \frac{1}{32\pi^2} G\tilde{G}$$

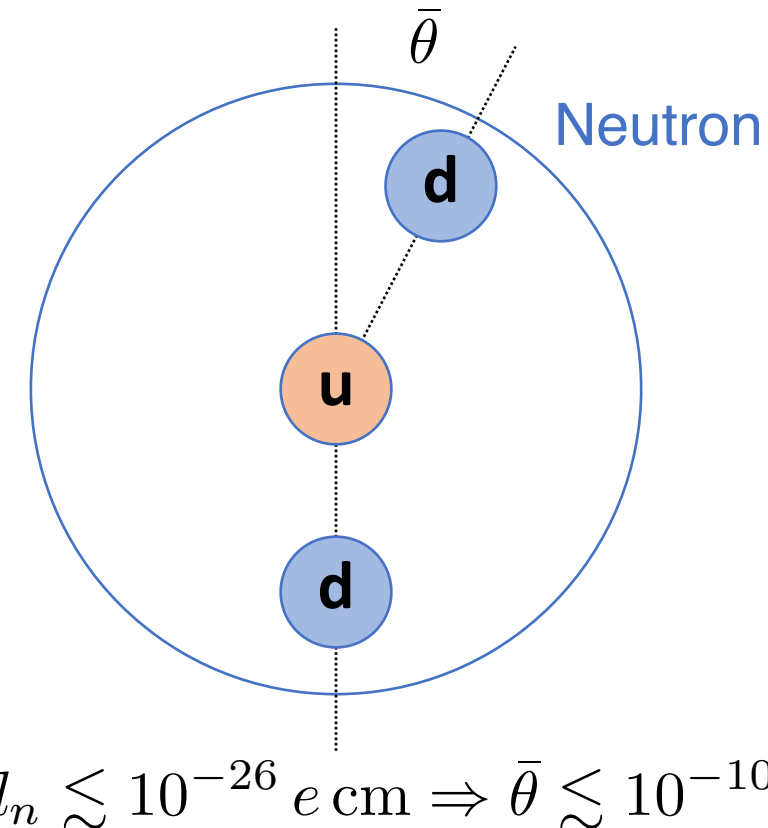
Gluon field strength

CP violation would give rise, for example, to a neutron electric dipole moment $d_n \sim 10^{-16} \bar{\theta} e \text{ cm}$. However, there is **no evidence of CP violation in Strong interactions.**

In QCD alone, the value of $\bar{\theta}$ is just a parameter of the theory, θ_{QCD} - it could in principle be $\mathcal{O}(1)$!

Much worse: the Weak Interactions *do* violate CP and this can be transferred to the Strong sector through non-perturbative effects related to the quark masses: $\theta_{\text{Weak}} = \text{Arg } |\mathbf{M}_q| \sim \mathcal{O}(1)$

Strong CP Problem: *why is $\bar{\theta} = \theta_{\text{QCD}} + \theta_{\text{Weak}}$ so small?!*

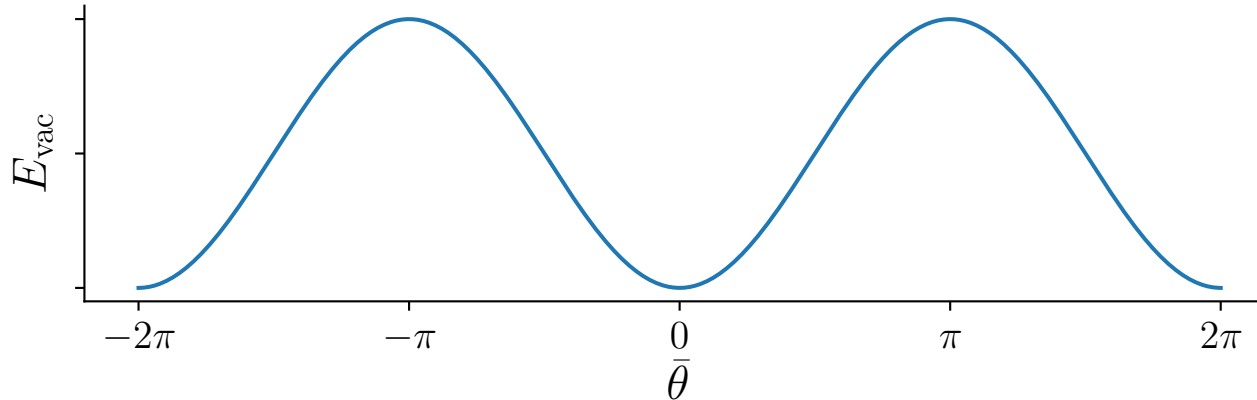


$$d_n \lesssim 10^{-26} e \text{ cm} \Rightarrow \bar{\theta} \lesssim 10^{-10}$$

Solving the Strong CP Problem

In fact, this CP violating term has an associated vacuum energy:

$$E_{\text{vac}} \sim \cos(\bar{\theta})$$



[Vafa & Witten (1984)]

But the parameter $\bar{\theta}$ is *static* so this doesn't help us...



Make $\bar{\theta}$ dynamical!

Peccei-Quinn (PQ) Mechanism: introduce a new complex scalar field φ , charged under a new global symmetry, $U_{\text{PQ}}(1)$ [Peccei & Quinn, 1977]

At low energy, the couplings of φ with the Standard Model introduce a new (dynamical) contribution to the CP violating term:

$$\mathcal{L}_{\text{QCD}} \supset \bar{\theta} \frac{1}{32\pi^2} G\tilde{G} + \mathcal{C}\theta \frac{1}{32\pi^2} G\tilde{G}$$

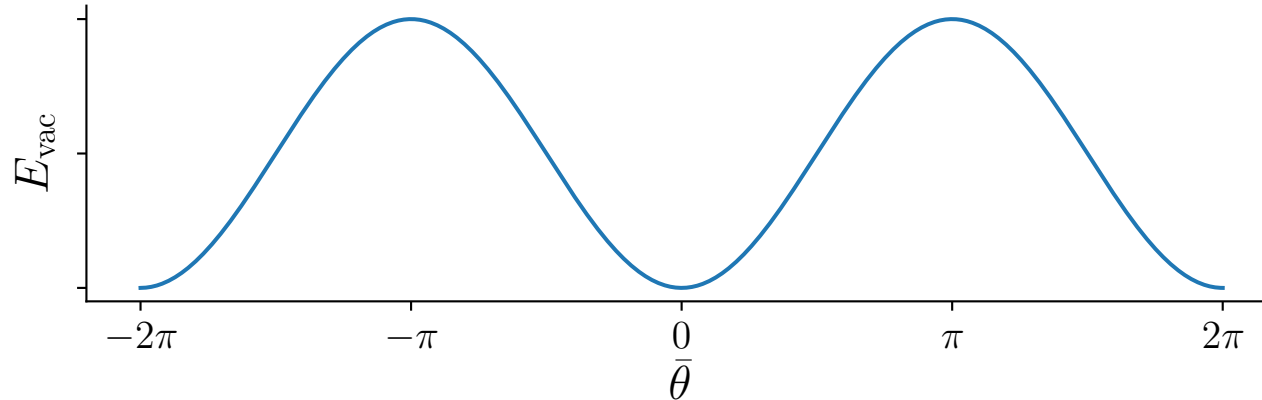
The 'colour anomaly' \mathcal{C} depends on exactly how the Standard Model is coupled to the new PQ symmetry (e.g. KSVZ, DFSZ)

Solving the Strong CP Problem

$$\mathcal{L}_{\text{QCD}} \supset \bar{\theta} \frac{1}{32\pi^2} G\tilde{G}$$

In fact, this CP violating term has an associated vacuum energy:

$$E_{\text{vac}} \sim \cos(\bar{\theta})$$



[Vafa & Witten (1984)]

But the parameter $\bar{\theta}$ is *static* so this doesn't help us...



Make $\bar{\theta}$ dynamical!

Peccei-Quinn (PQ) Mechanism: introduce a new complex scalar field φ , charged under a new global symmetry, $U_{\text{PQ}}(1)$ [Peccei & Quinn, 1977]

At low energy, the couplings of φ with the Standard Model introduce a new (dynamical) contribution to the CP violating term:

$$\mathcal{L}_{\text{QCD}} \supset \bar{\theta} \frac{1}{32\pi^2} G\tilde{G} + \mathcal{C}\theta \frac{1}{32\pi^2} G\tilde{G}$$

The 'colour anomaly' \mathcal{C} depends on exactly how the Standard Model is coupled to the new PQ symmetry (e.g. KSVZ, DFSZ)

Peccei-Quinn (PQ) Mechanism

The $U_{\text{PQ}}(1)$ symmetry is the **symmetry of a circle**.

At high energy (i.e. high temperatures in the early Universe), the $U_{\text{PQ}}(1)$ symmetry is preserved and the field φ is fixed to zero.



Peccei-Quinn (PQ) Mechanism

The $U_{\text{PQ}}(1)$ symmetry is the **symmetry of a circle**.

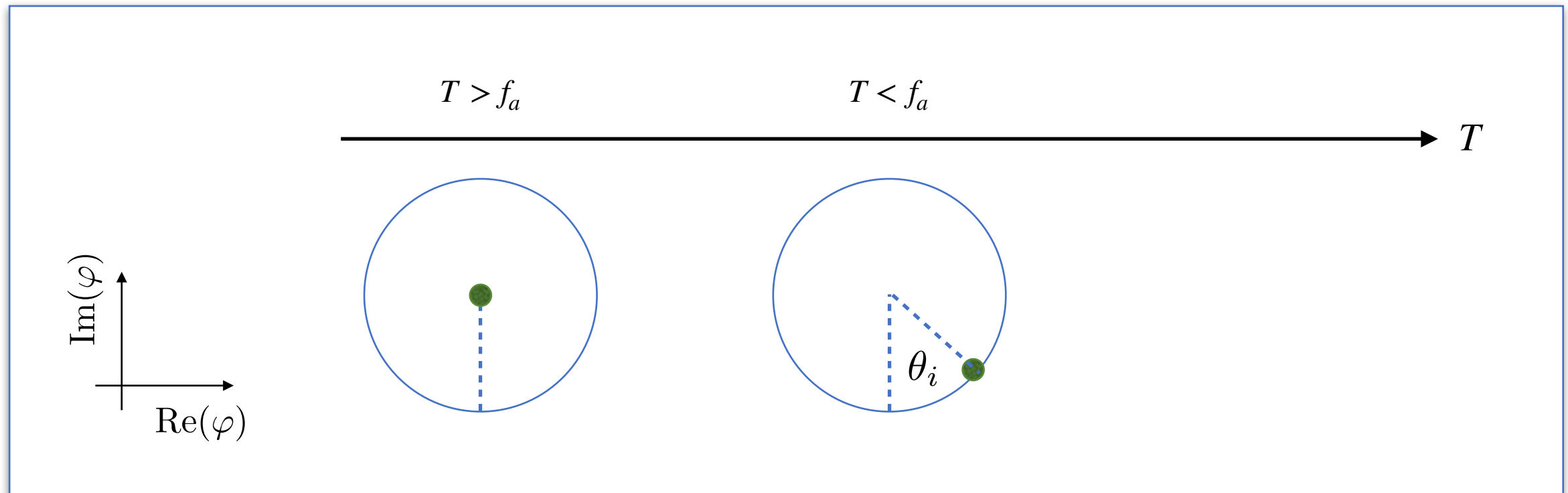
At high energy (i.e. high temperatures in the early Universe), the $U_{\text{PQ}}(1)$ symmetry is preserved and the field φ is fixed to zero.



Peccei-Quinn (PQ) Mechanism

As the Universe cools below the PQ scale f_a , the PQ symmetry is **spontaneously broken**.

$\varphi = 0$ is no longer the minimum-energy configuration. The field must choose some initial angle θ_i , but all angles are equally likely.



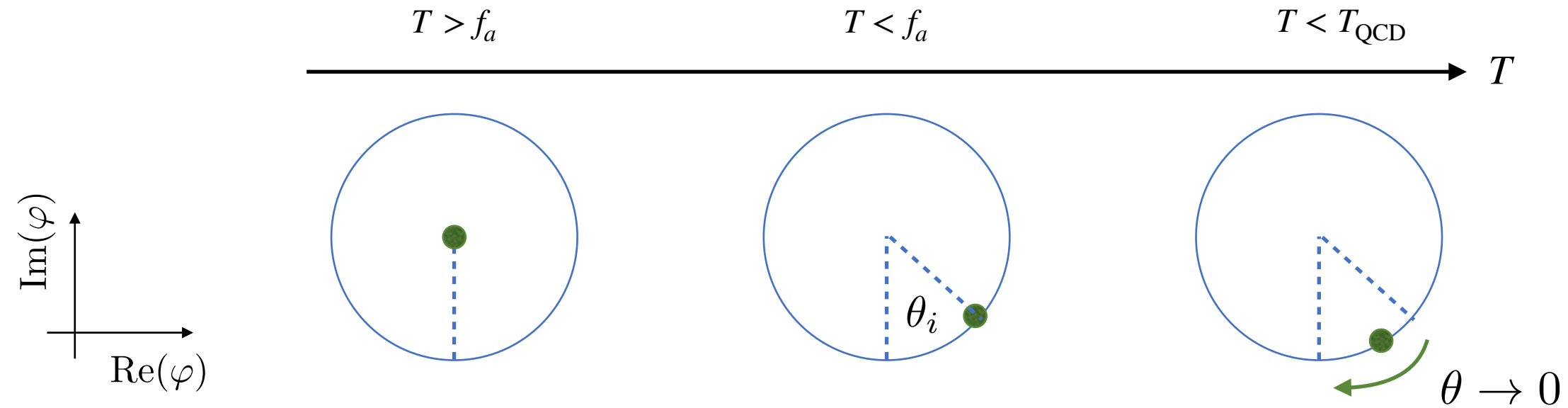
Peccei-Quinn (PQ) Mechanism

Once the Universe cools below the QCD phase transition, interactions with the Standard Model become important and induce a (dynamical) CP violating term:

$$\mathcal{L}_{\text{QCD}} \supset \frac{1}{32\pi^2} \left(\bar{\theta} + \mathcal{C} \frac{a}{f_a} \right) G\tilde{G}$$

The pseudoscalar field a is the **QCD axion!**

Strong CP problem can be solved dynamically! The vacuum energy $E_{\text{vac}} \sim \cos(\bar{\theta} + \mathcal{C}a/f_a)$ can be minimised by sending $a \rightarrow -f_a \bar{\theta}/\mathcal{C}$



Axions as Dark Matter

Below the QCD phase transition, the axion obtains a mass through its interactions with QCD:

$$m_a \approx f_\pi m_\pi / f_a \approx 5.7 \left(\frac{10^{12} \text{ GeV}}{f_a} \right) \mu\text{eV}$$

[1510.07633]

In general, if f_a is very large, then axions are very light, very weakly coupled and very long-lived!

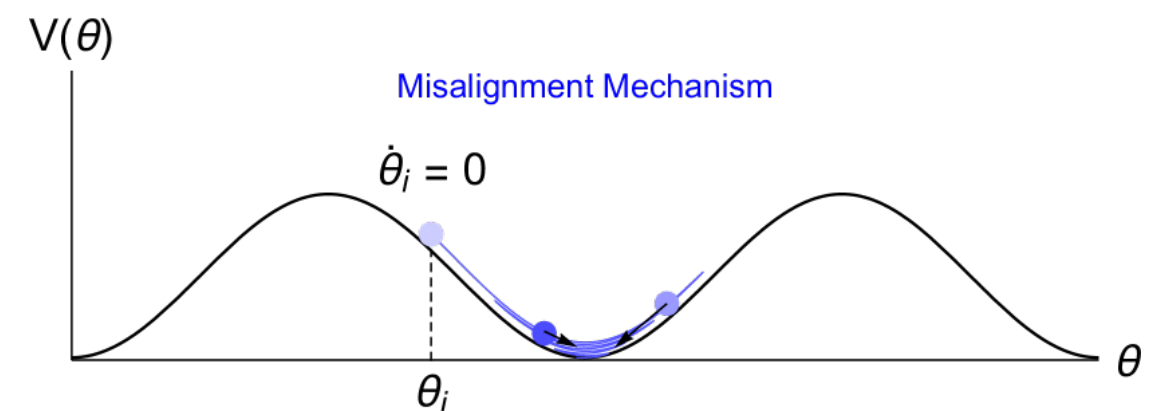
→ **Perfect DM Candidates!**

Below the QCD phase transition, the axion field evolves to give $\theta \rightarrow 0$, but the initial **misalignment angle** can take a random value $\theta_i = a/f_a \in [0, 2\pi]$.

The energy density stored in the axion field at this initial value $V(\theta_i)$ is converted into coherent oscillations of the axion field about the minimum — behaves as cold collisionless matter



Misalignment Mechanism



[1910.14152]

Pre- and post-inflationary axions

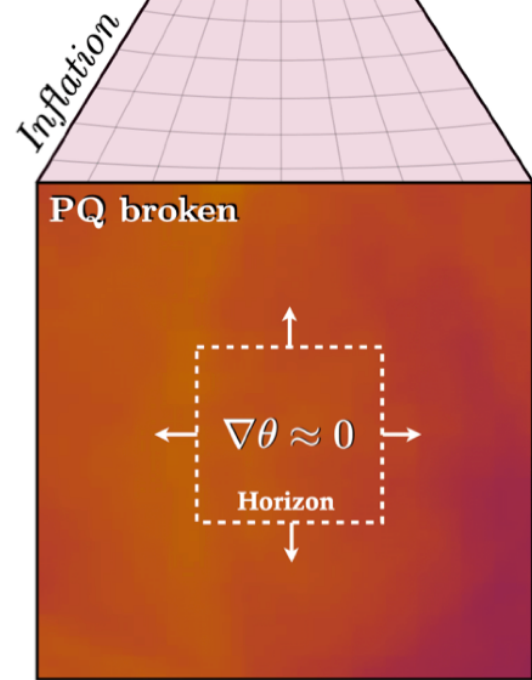
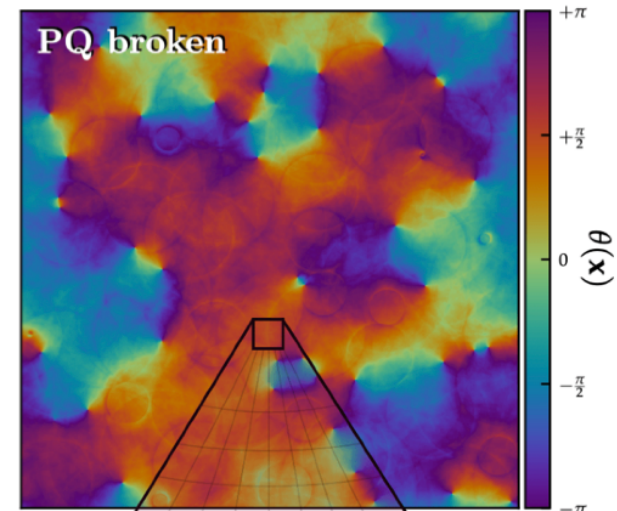
If the PQ symmetry is broken **before cosmic inflation**, then a small patch of the Universe with a given θ_i is inflated to become our observable Universe.

The axion abundance can be calculated as:

$$f_{\text{DM}} = \rho_a / \rho_{\text{DM}}$$
$$\approx \left(\frac{\theta_i}{2.155} \right)^2 \left(\frac{28 \mu\text{eV}}{m_a} \right)^{7/6}$$

...depends on the unknown parameter θ_i

Pre-inflationary scenario



$$\langle \theta_i^2 \rangle = \text{const.}$$

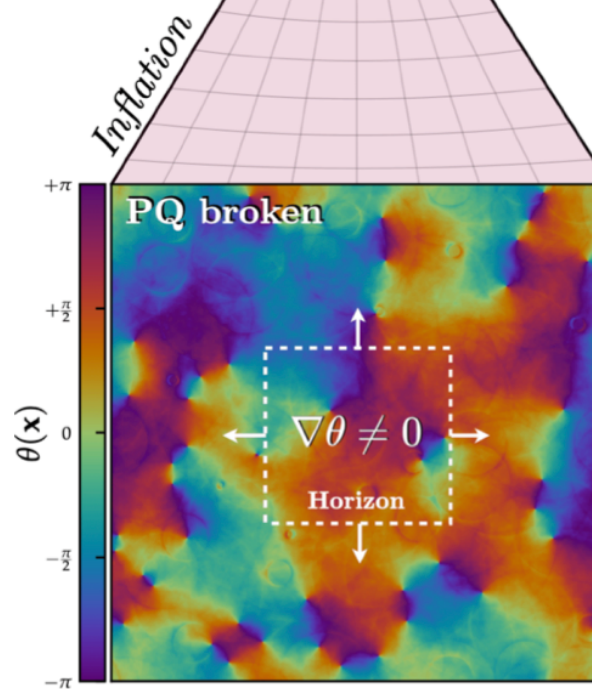
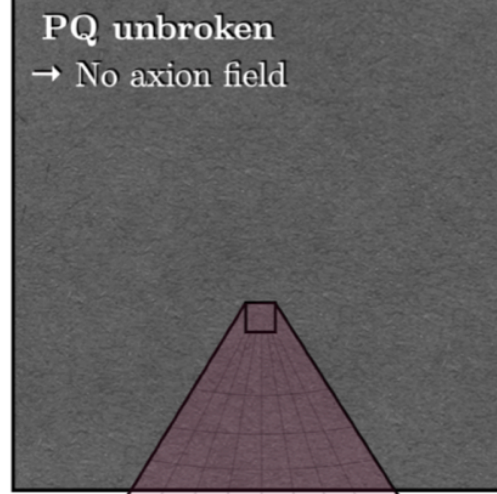
Pre- and post-inflationary axions

If the PQ symmetry is broken **after cosmic inflation**, then nearby patches of the Universe will have different initial misalignment angles.

Average misalignment angle $\langle \theta_i^2 \rangle$ is known so the axion abundance depends only on the axion mass.

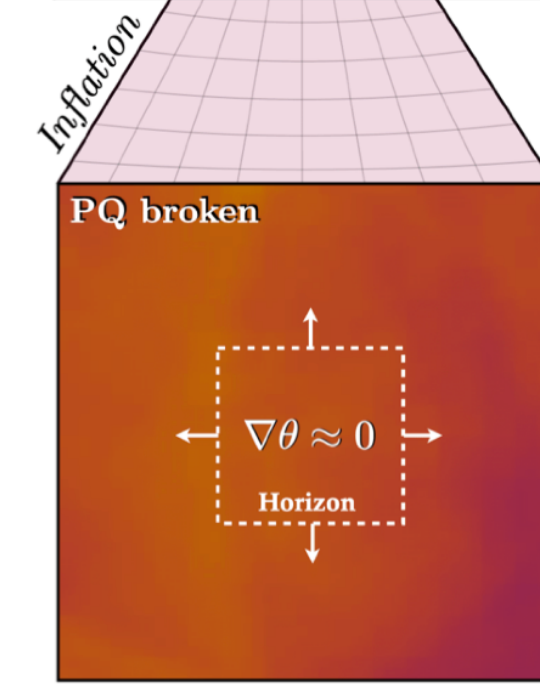
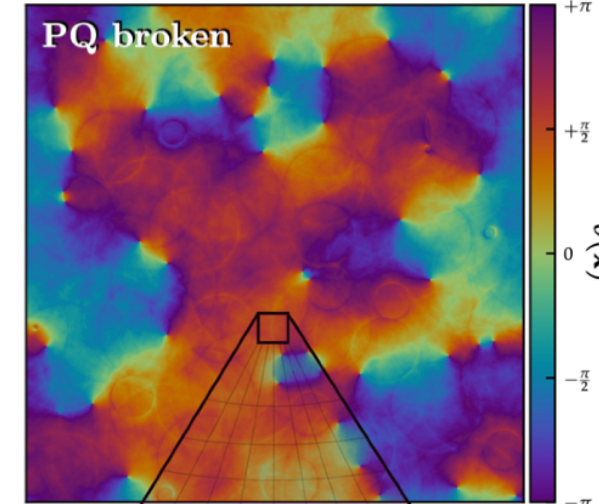
In principle, we can calculate the value of the axion mass required to explain all of the DM!

Post-inflationary scenario



$$\langle \theta_i^2 \rangle \approx \left(\frac{\pi}{\sqrt{3}} \right)^2$$

Pre-inflationary scenario

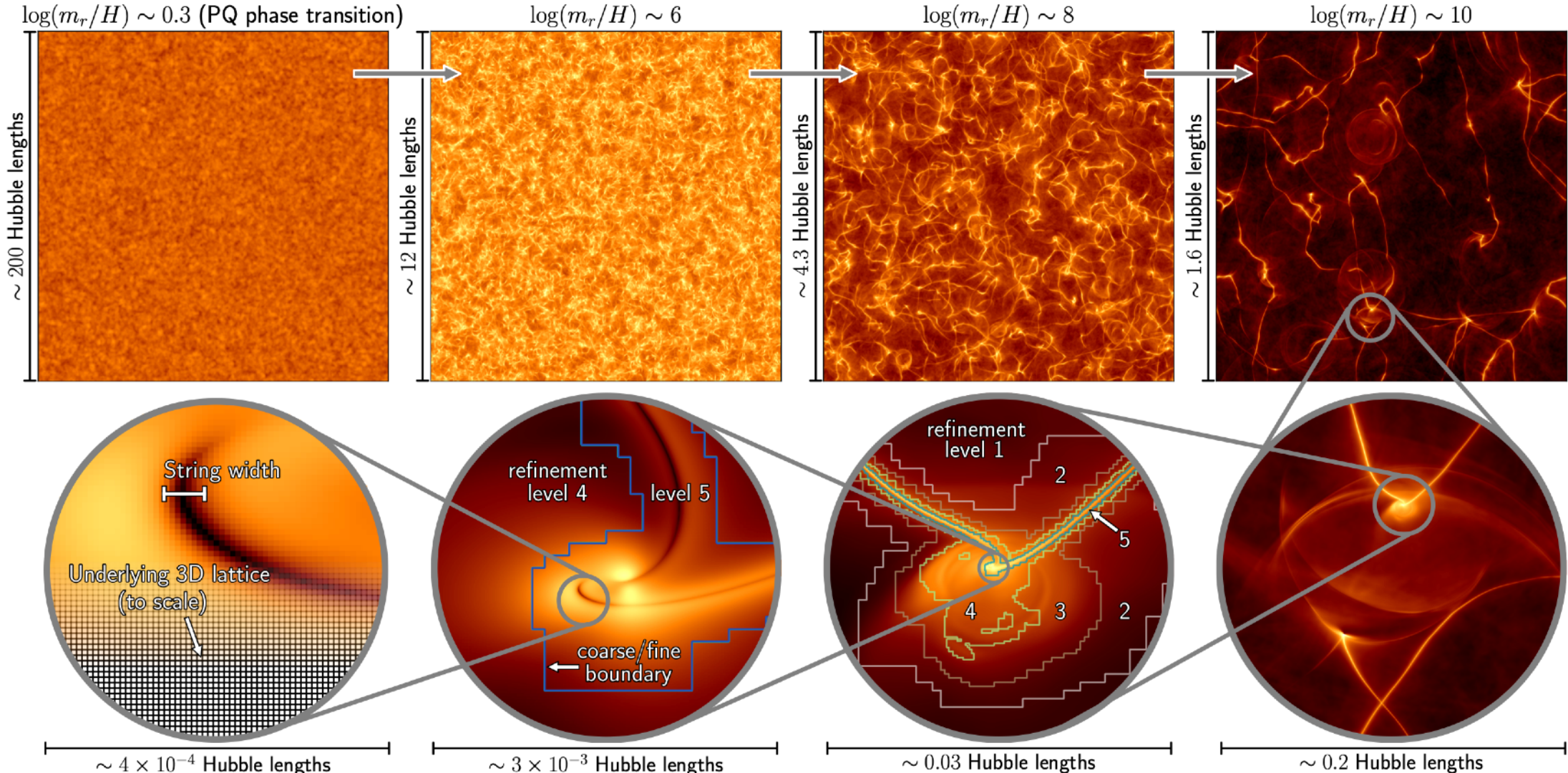


$$\langle \theta_i^2 \rangle = \text{const.}$$

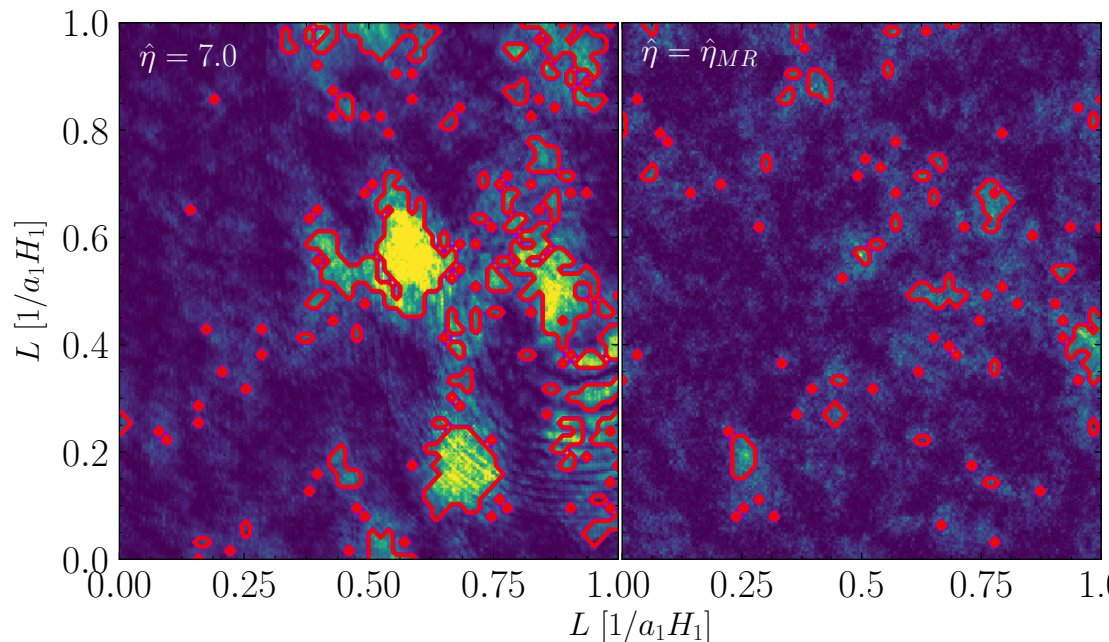
Axions, Strings and Walls

[2412.08699]

In practice, the calculation is very difficult... so the precise value of the axion mass is not known yet.



Axion Miniclusters



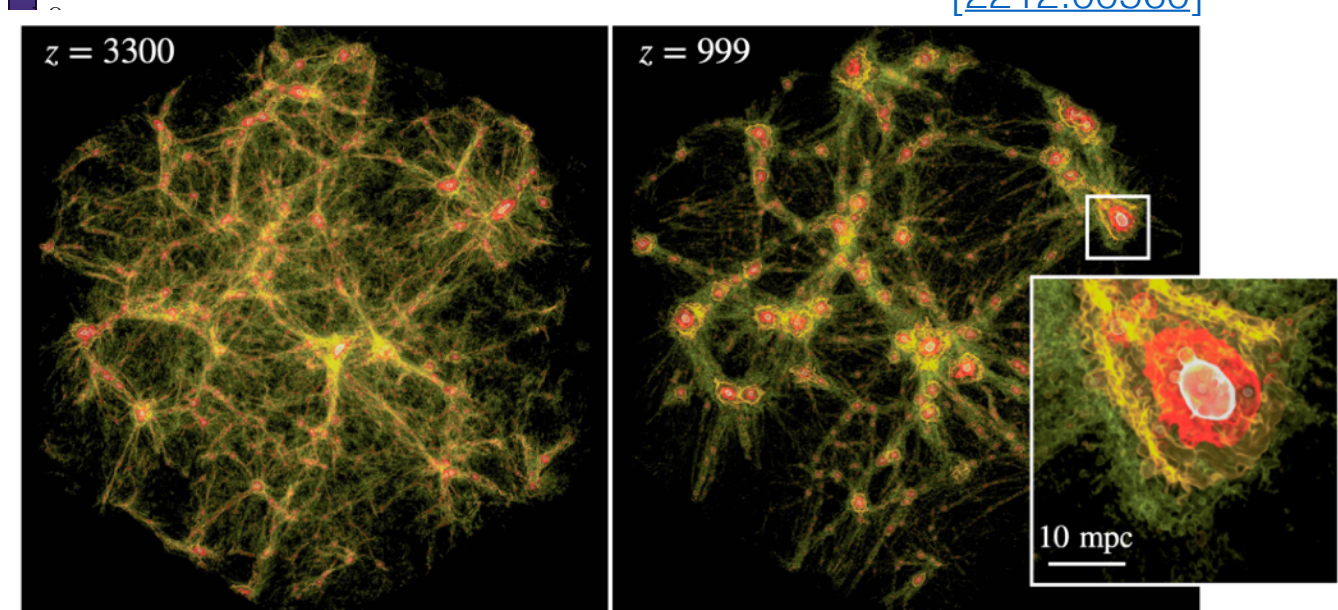
[Buschmann et al., [1906.00967](#)]

Born with masses $10^{-12} M_\odot$ but grow hierarchically to be much heavier!

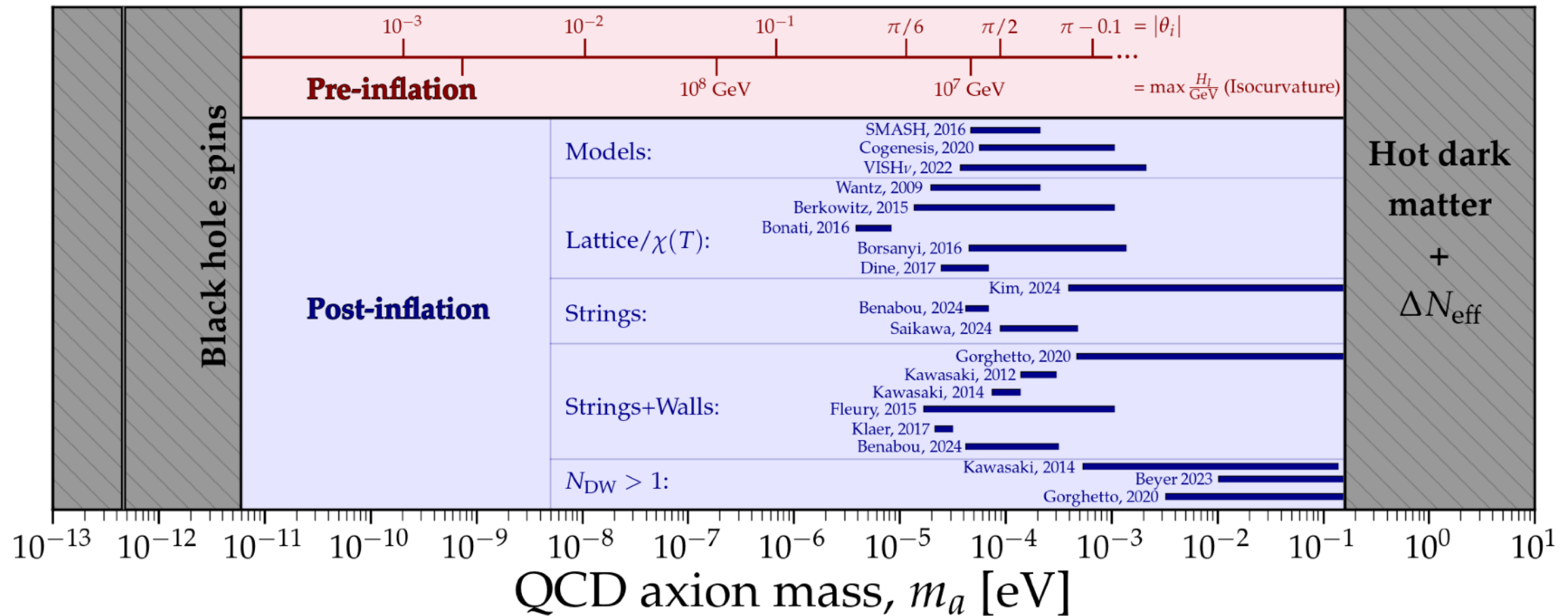
Axion density *in between* these AMCs could be <10% of the smooth average

In the post-inflationary scenario, initial overdensities in the axion field act as 'seeds' for the growth of "**axion miniclusters**" (AMCs)

[Kolb & Tkachev, [astro-ph/9403011](#)]

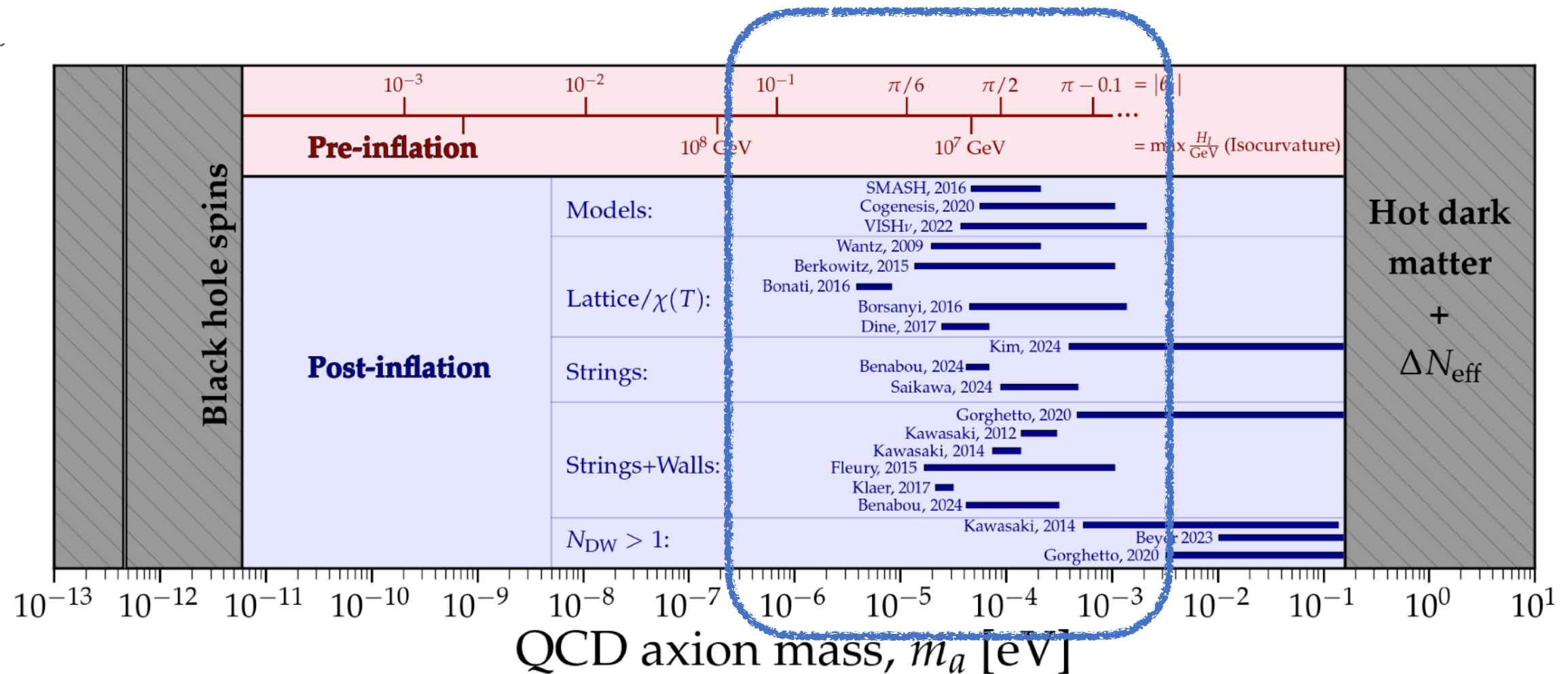


[See also Zurek et al., [astro-ph/0607341](#); Vaquero et al., [1809.09241](#); Eggemeier et al., [1911.09417](#)]



Axion Mass

[\[cajohare.github.io/AxionLimits/\]](https://cajohare.github.io/AxionLimits/)



AXION INTERACTIONS AND CONSTRAINTS

Axions couple to Standard Model:

*More model-dependent couplings to nucleons and electrons are also possible

Axion-Gluon

$$\mathcal{C} \frac{a}{f_a} \frac{1}{32\pi^2} G\tilde{G}$$

Axion-Photon

$$\mathcal{C} \frac{\alpha_{\text{EM}}}{32\pi^2} c_{a\gamma} \frac{a}{f_a} F\tilde{F}$$

Axions couple to Standard Model:

*More model-dependent couplings to nucleons and electrons are also possible

Axion-Gluon

$$\mathcal{C} \frac{a}{f_a} \frac{1}{32\pi^2} G\tilde{G}$$

Axion-Photon

$$\mathcal{C} \frac{\alpha_{\text{EM}}}{32\pi^2} c_{a\gamma} \frac{a}{f_a} F\tilde{F} \longrightarrow \frac{g_{a\gamma\gamma}}{4\pi} a(x) \mathbf{E} \cdot \mathbf{B}$$

with $g_{a\gamma\gamma} = \frac{\alpha_{\text{EM}} c_{a\gamma}}{2\pi(f_a/\mathcal{C})}$

$$\vec{\nabla} \cdot \vec{E} = \rho$$

$$\vec{\nabla} \cdot \vec{B} = 0$$

$$\vec{\nabla} \times \vec{E} = -\frac{\partial \vec{B}}{\partial t}$$

$$\vec{\nabla} \times \vec{B} = \frac{\partial \vec{E}}{\partial t} + \vec{J}$$

Axions couple to Standard Model:

*More model-dependent couplings to nucleons and electrons are also possible

Axion-Gluon

$$\mathcal{C} \frac{a}{f_a} \frac{1}{32\pi^2} G\tilde{G}$$

Axion-Photon

$$\mathcal{C} \frac{\alpha_{\text{EM}}}{32\pi^2} c_{a\gamma} \frac{a}{f_a} F\tilde{F} \longrightarrow \frac{g_{a\gamma\gamma}}{4\pi} a(x) \mathbf{E} \cdot \mathbf{B}$$

$$\text{with } g_{a\gamma\gamma} = \frac{\alpha_{\text{EM}} c_{a\gamma}}{2\pi(f_a/\mathcal{C})}$$

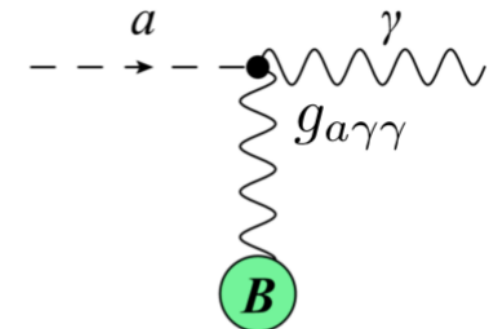
$$\vec{\nabla} \cdot \vec{E} = \rho - g_{a\gamma\gamma} \vec{B} \cdot \vec{\nabla} a$$

$$\vec{\nabla} \cdot \vec{B} = 0$$

$$\vec{\nabla} \times \vec{E} = - \frac{\partial \vec{B}}{\partial t}$$

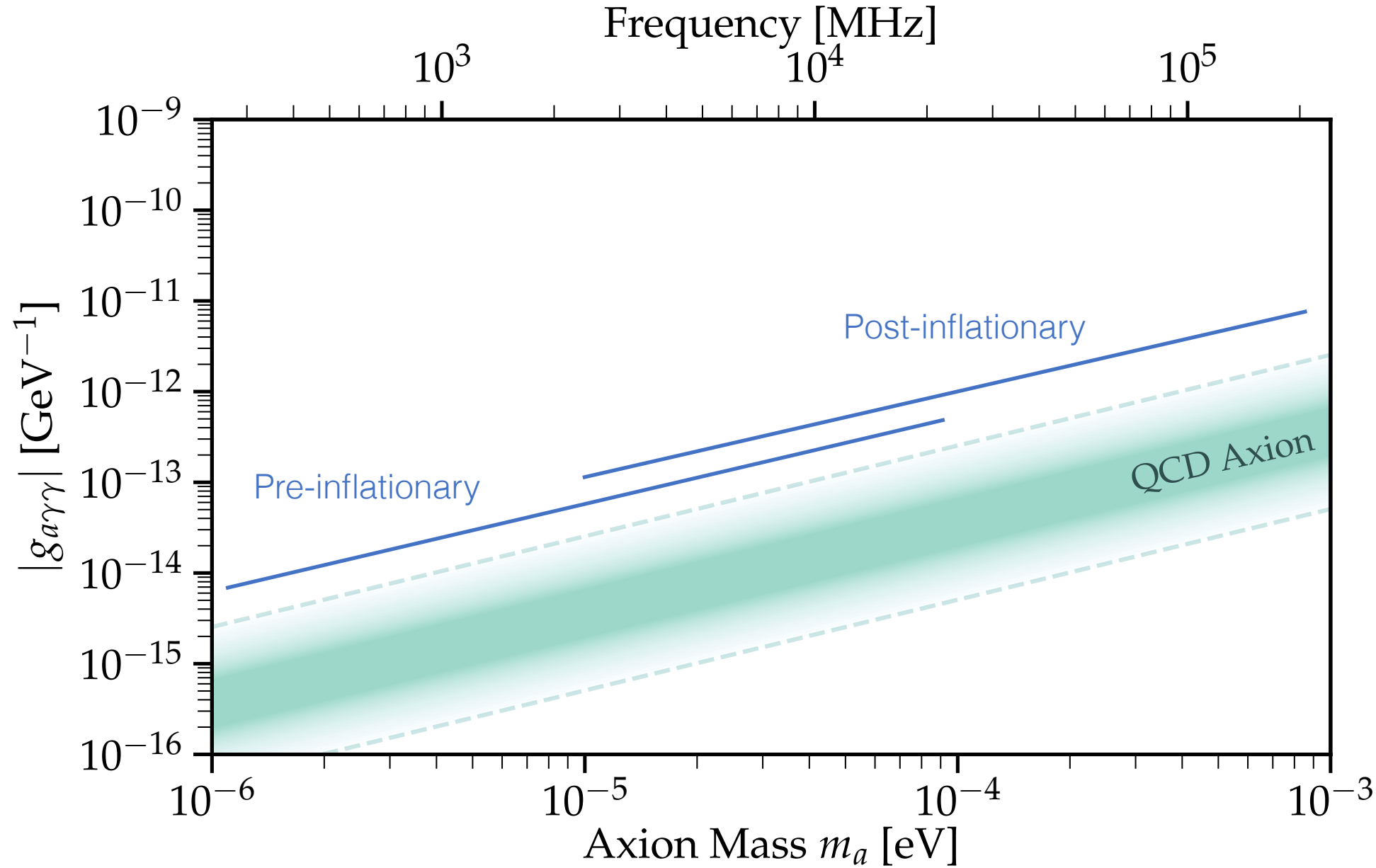
$$\vec{\nabla} \times \vec{B} = \frac{\partial \vec{E}}{\partial t} + \vec{J} - g_{a\gamma\gamma} \left(\vec{E} \times \vec{\nabla} a - \frac{\partial a}{\partial t} \vec{B} \right)$$

Leads to **Primakoff** process: the interconversion of axions and photons in a strong EM field:

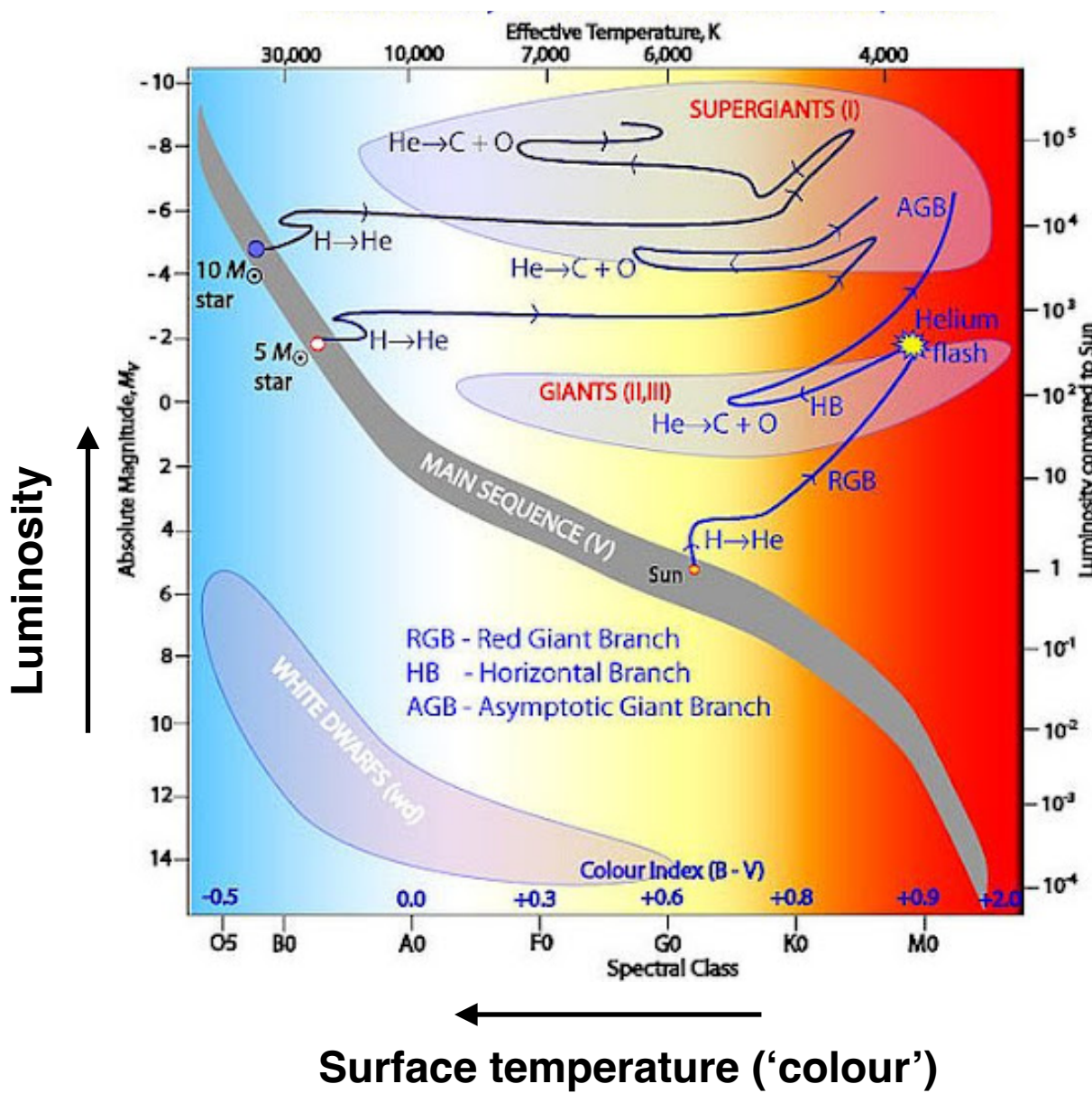


Axion (and ALP) Landscape

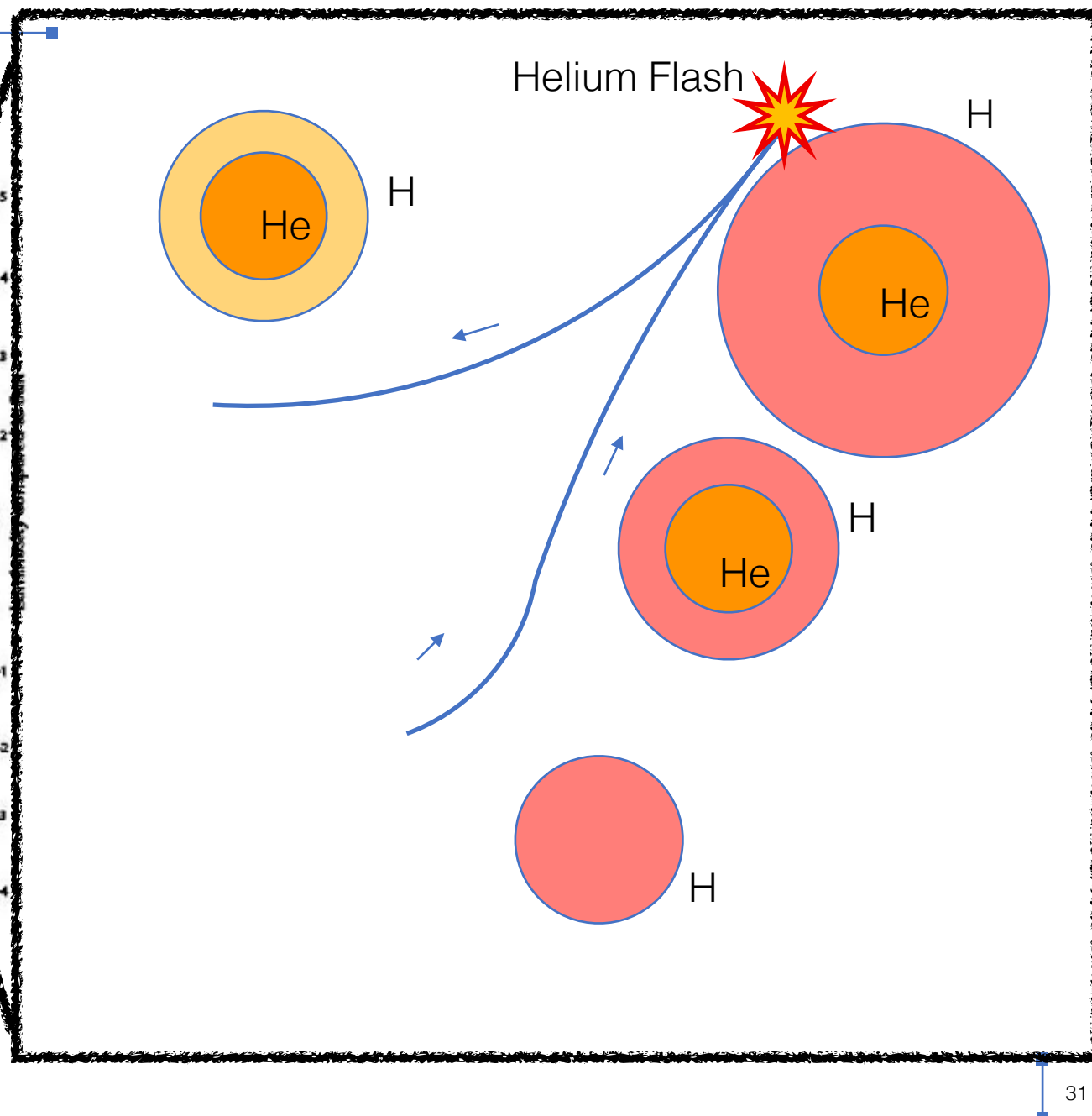
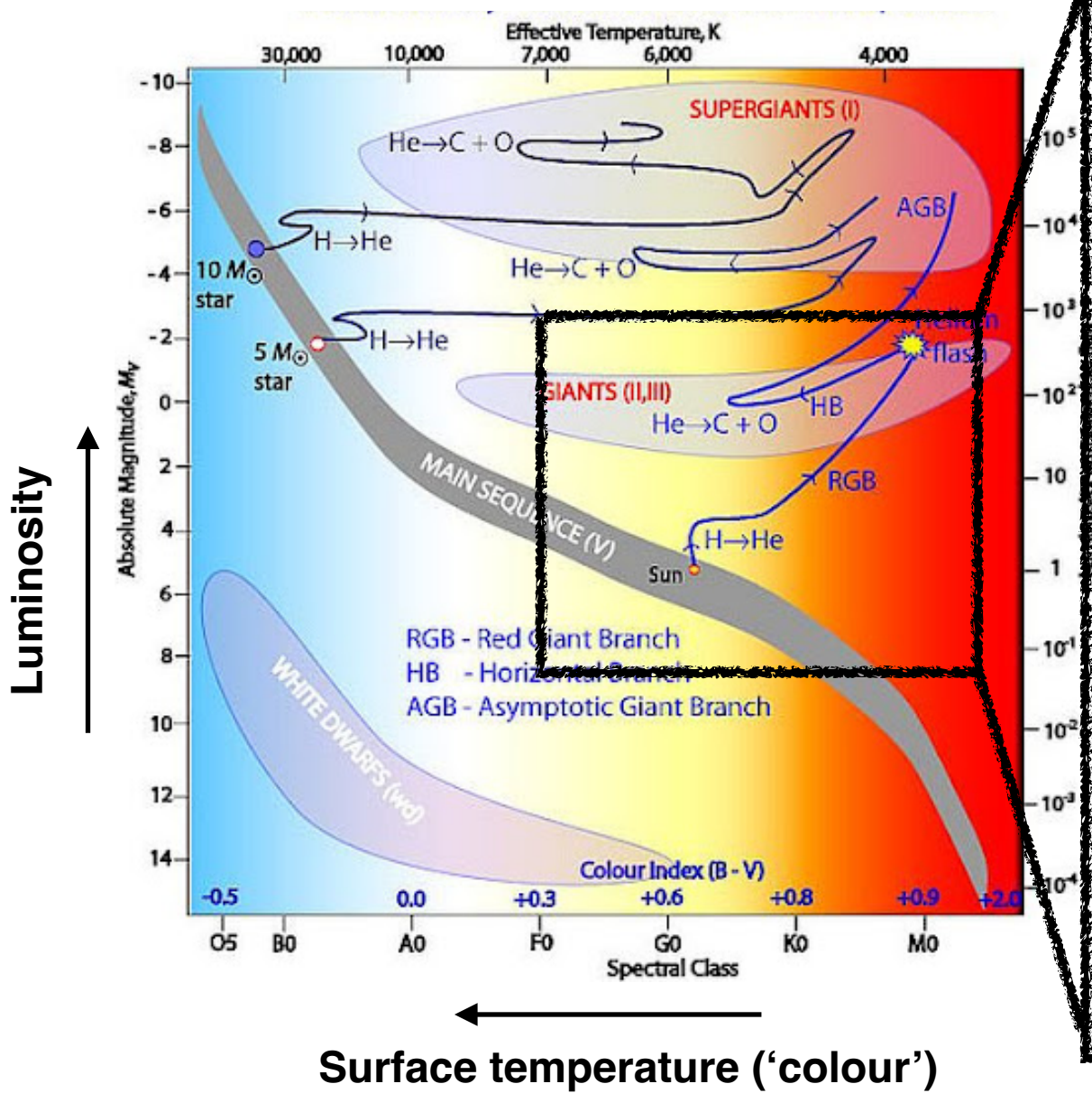
ALPs: Axion like-particles



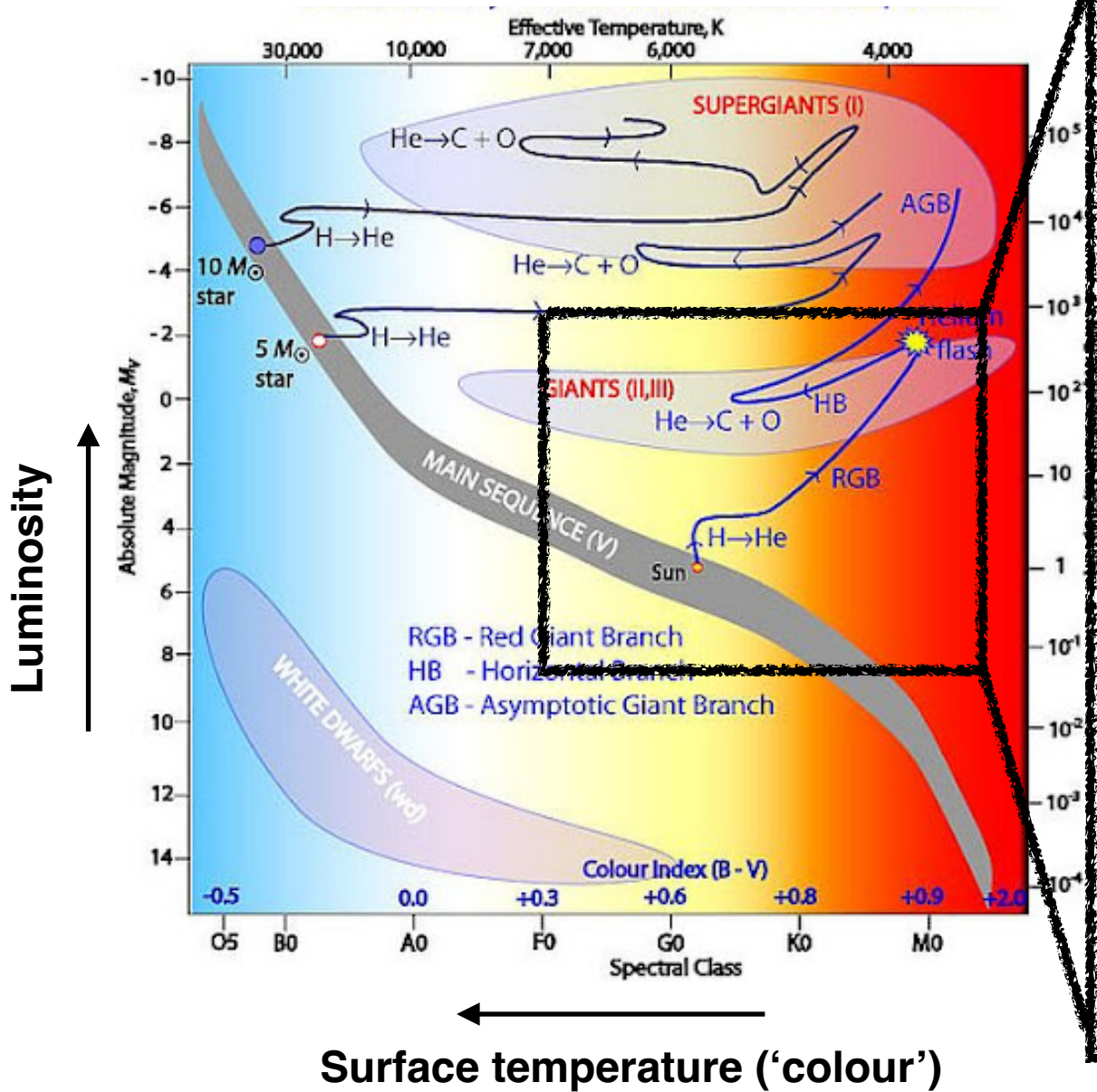
Hertzsprung-Russell diagram



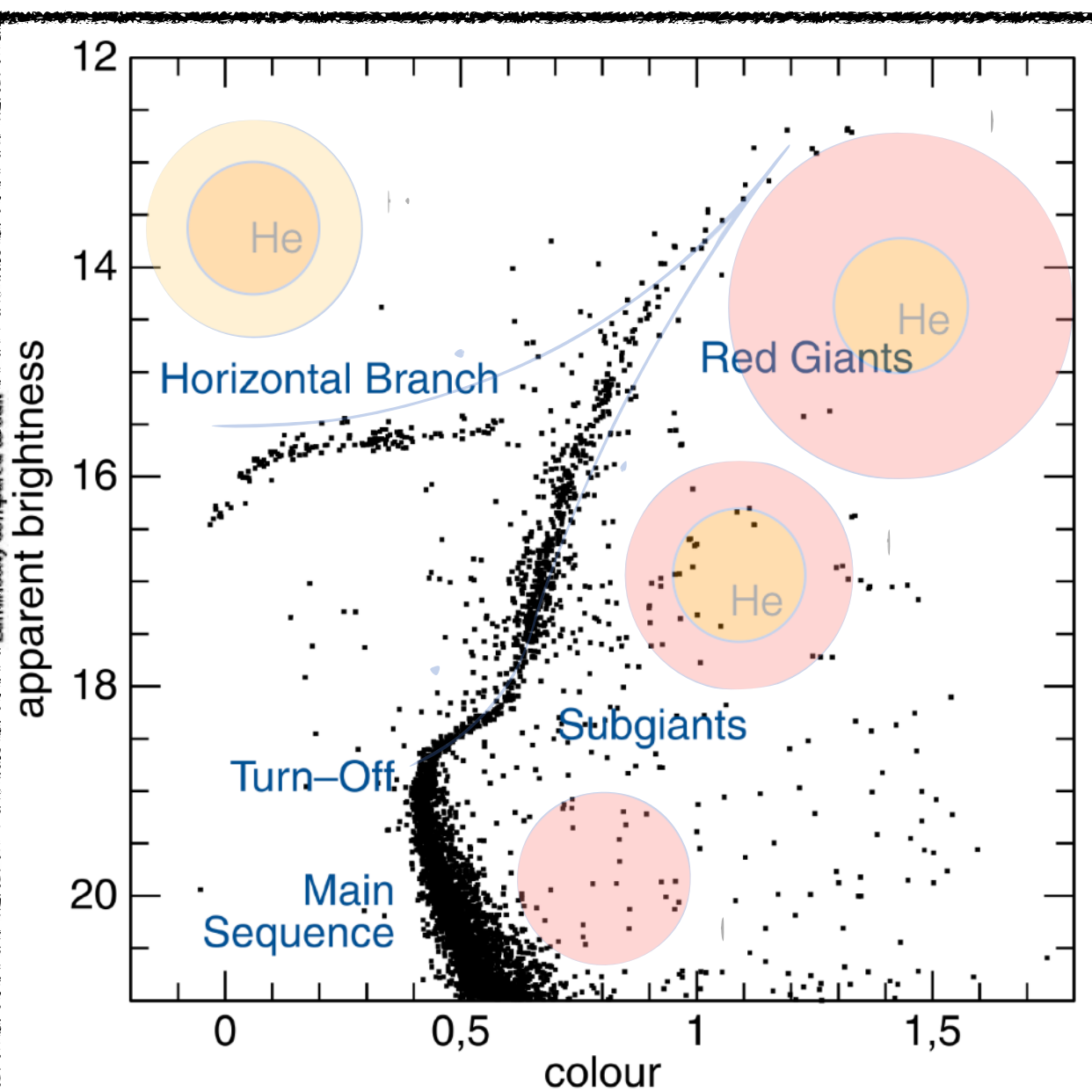
Hertzsprung-Russell diagram



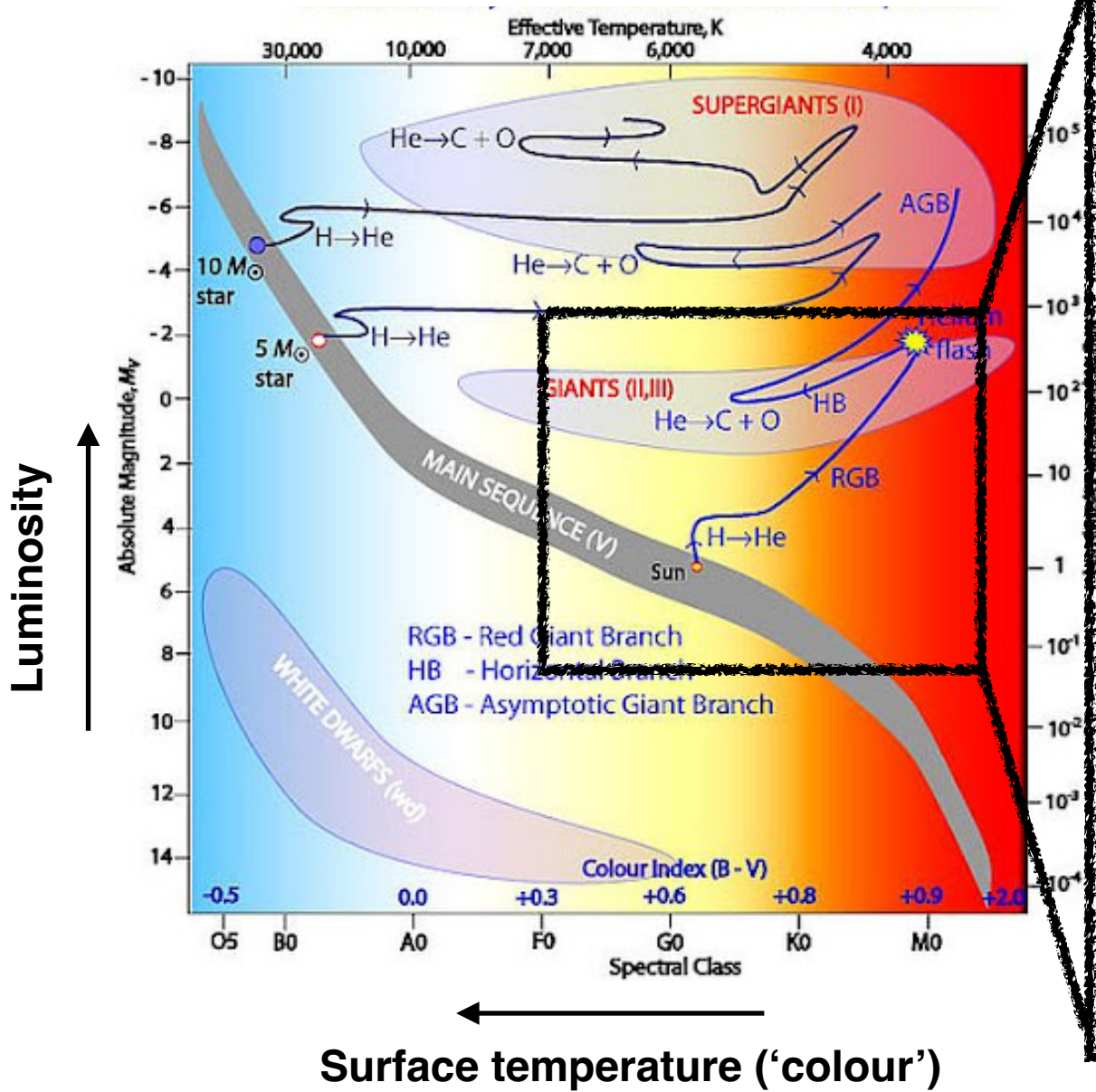
Hertzsprung-Russell diagram



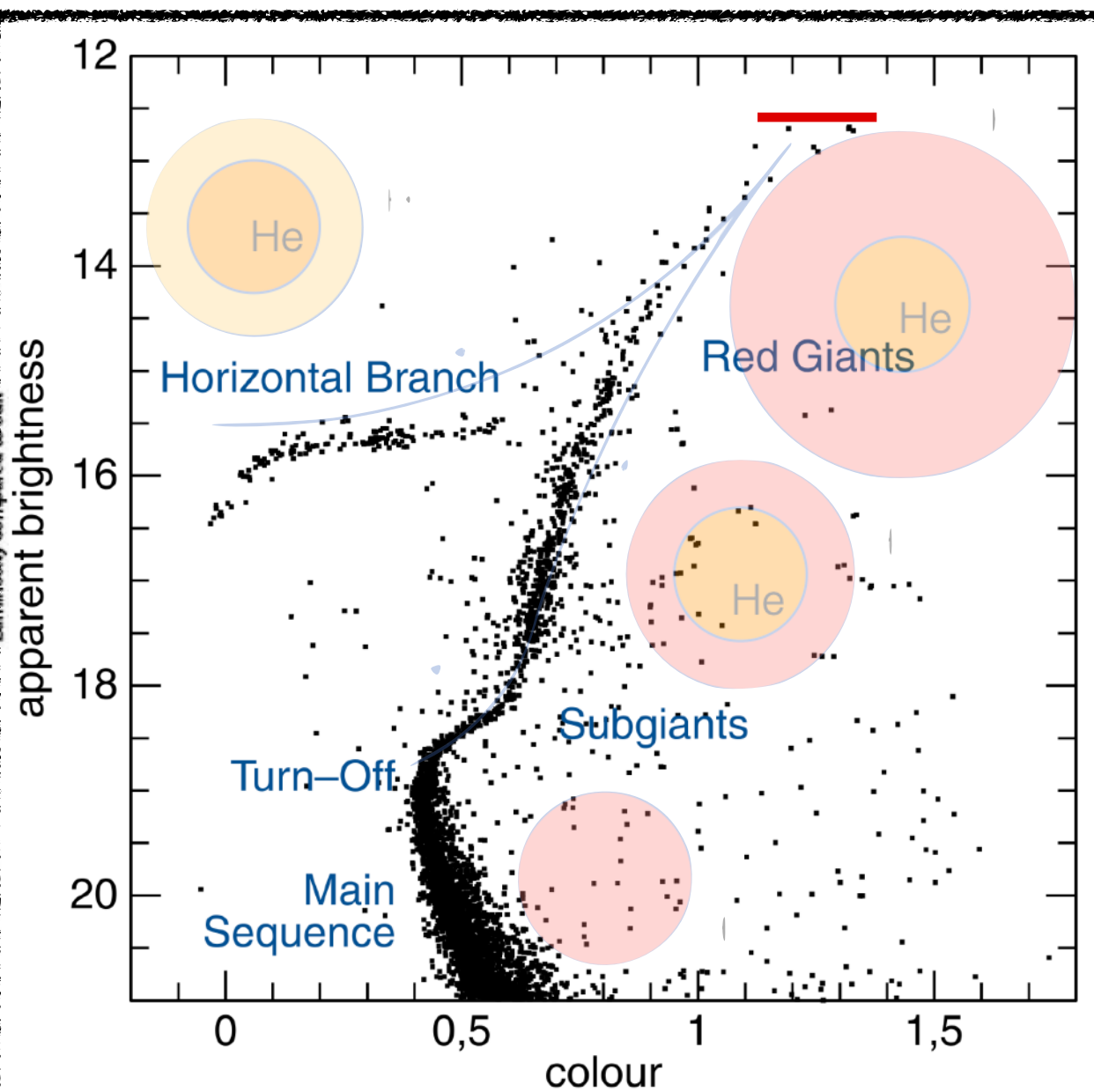
Globular Cluster M68



Hertzsprung-Russell diagram



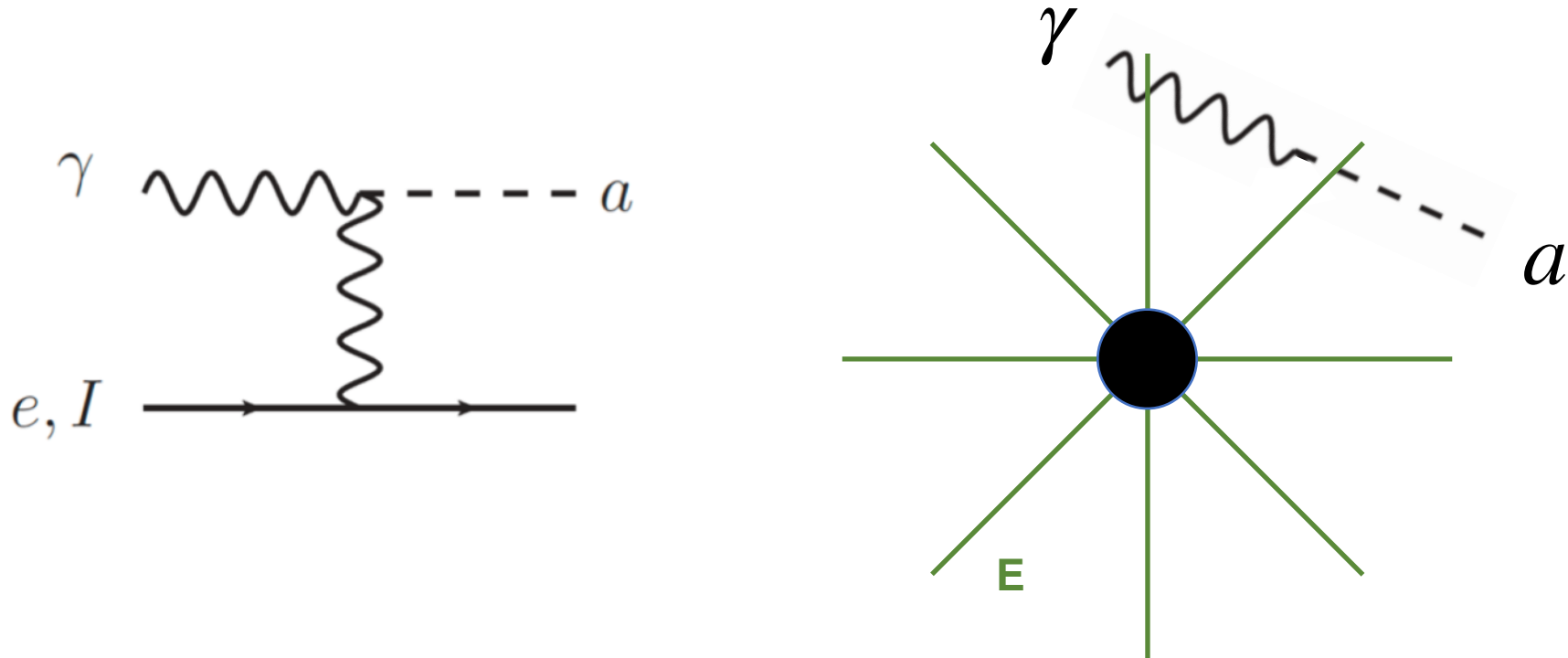
Globular Cluster M68



Stellar Emission

[Krauss, Moody & Wilczek (1984)]

In the electric fields of plasma in stars, photons can be converted to axions via the **Primakoff** process*:



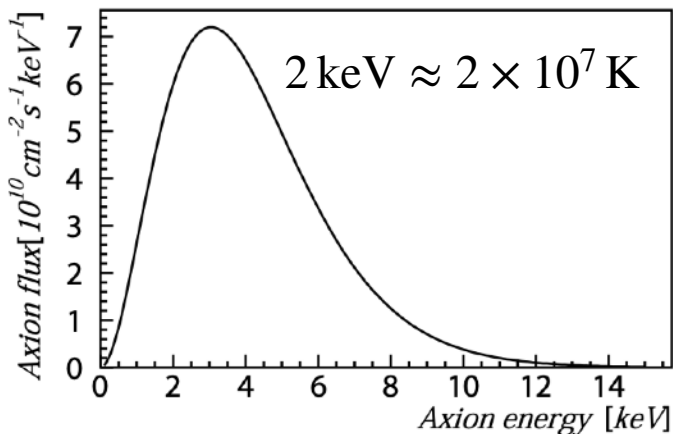
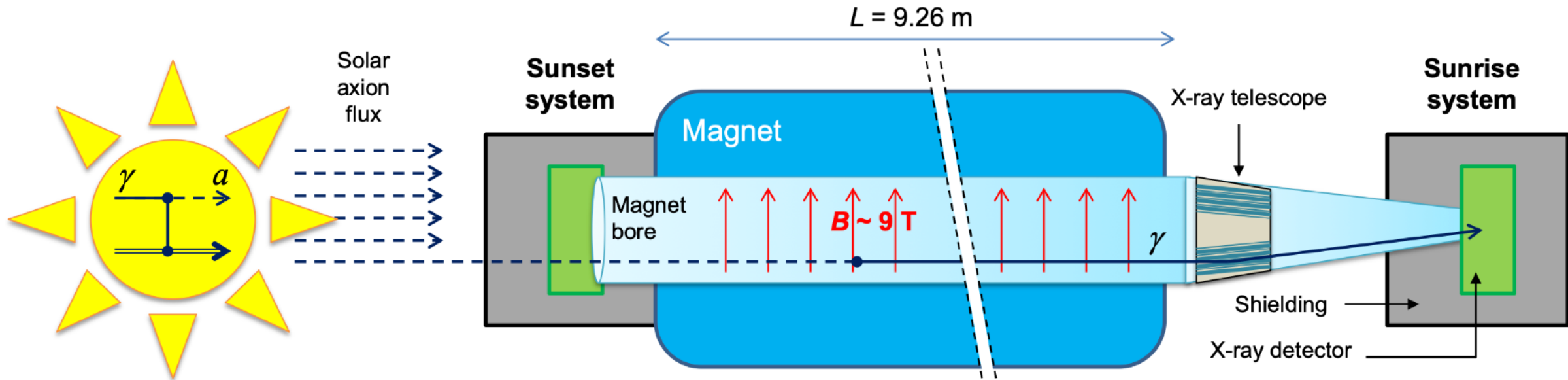
This provides an extra energy loss mechanism, allowing stars to cool more efficiently, which can delay the Helium Flash. Stellar population studies (especially in Globular clusters) constrains $g_{a\gamma\gamma} \lesssim 5 \times 10^{-11} \text{ GeV}^{-1}$

*if axion couples to electrons, other energy loss mechanisms are also possible

[1406.6053, 2109.10368]

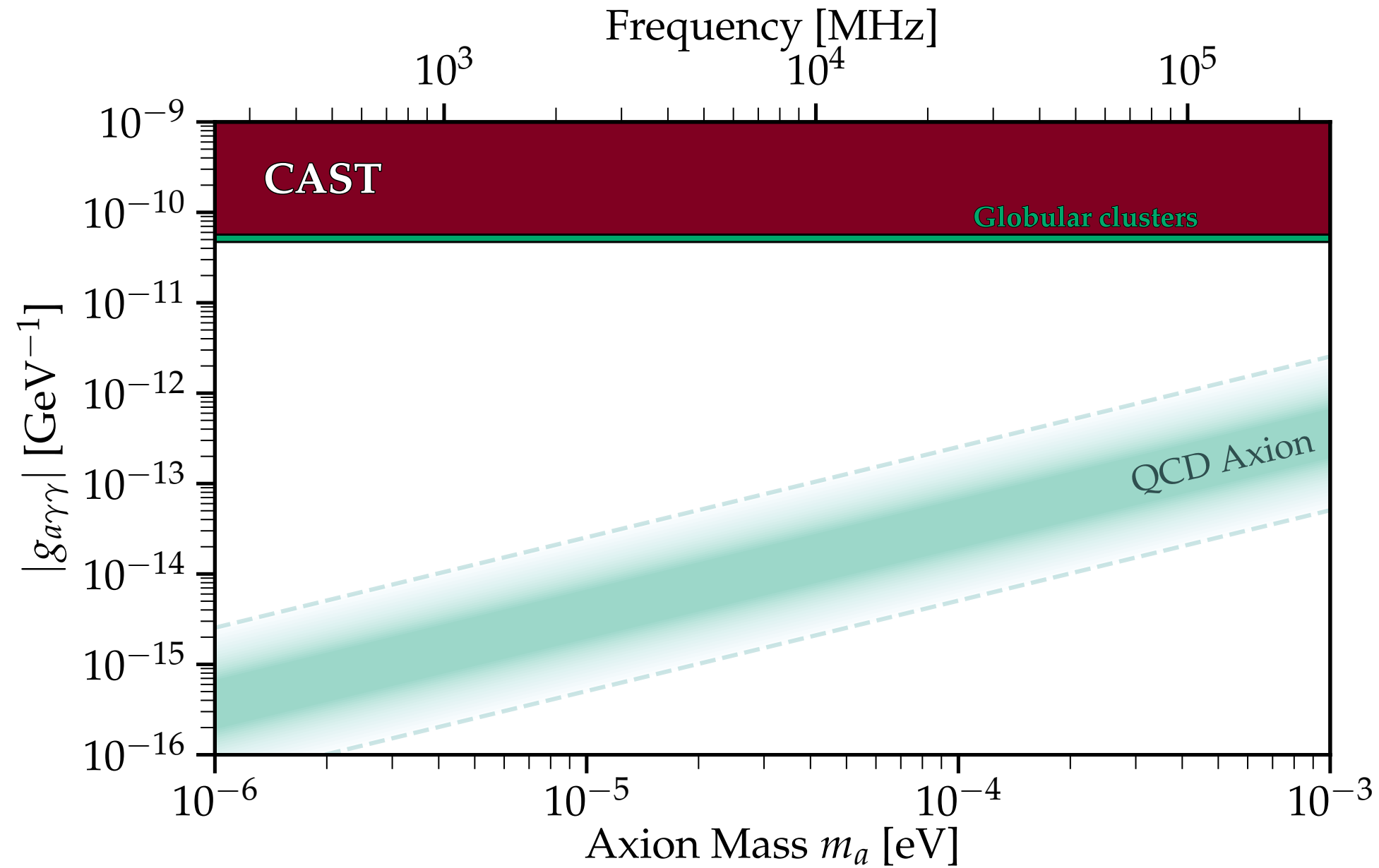
CERN Axion Solar Telescope (CAST)

[1705.02290, 2406.16840]



Non-observation of X-rays
from the Sun constrains:
 $g_{a\gamma\gamma} \lesssim 6 \times 10^{-11} \text{ GeV}^{-1}$

Axion Landscape



HALOSCOPES: Axions in the lab

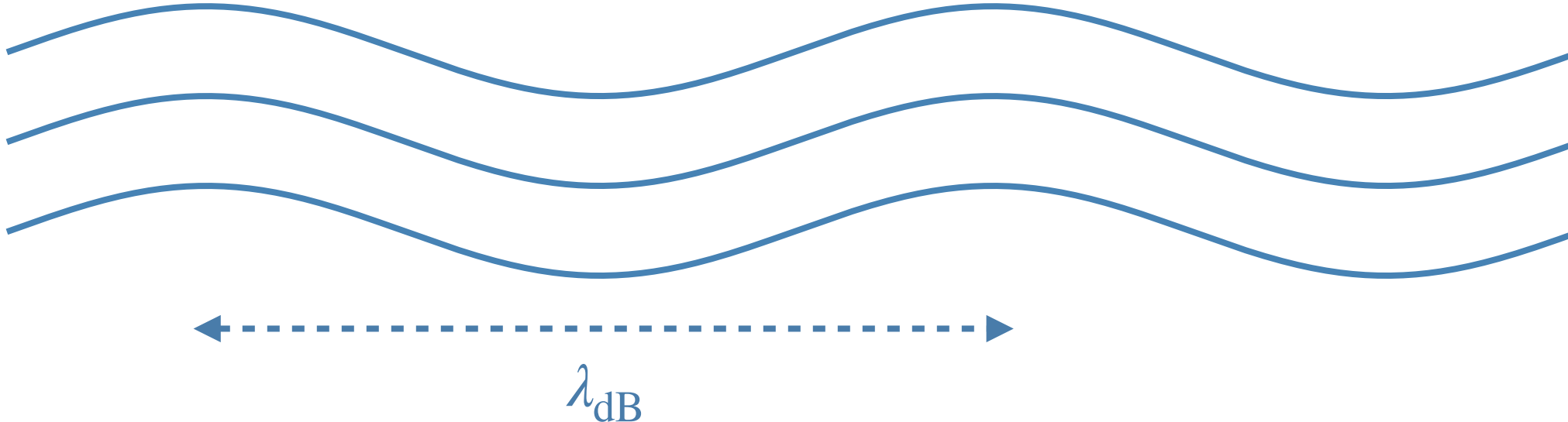
Axion-induced Electric Field

Dark Matter in the Milky Way is non-relativistic, with $v \sim 220 \text{ km/s} \sim 10^{-3} c$



$$a(\mathbf{r}, t) = a_0 \exp [-i (m_a t - \mathbf{p}_a \cdot \mathbf{r})] \approx \frac{\sqrt{2\rho_{\text{DM}}}}{m_a} \exp (-im_a t)$$

where we have made use of the fact that the axion Compton wavelength is: $\lambda_{\text{dB}} = \frac{2\pi\hbar}{m_a v} \approx (\mu\text{eV}/m_a) \cdot 2 \text{ km}$



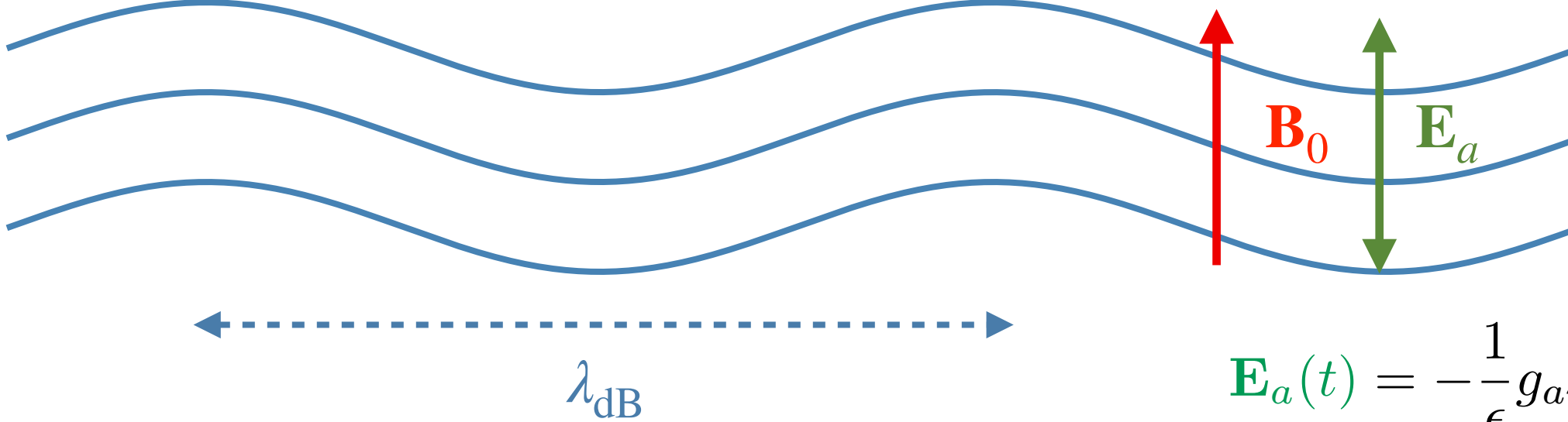
Axion-induced Electric Field

Dark Matter in the Milky Way is non-relativistic, with $v \sim 220 \text{ km/s} \sim 10^{-3} c$



$$a(\mathbf{r}, t) = a_0 \exp [-i (m_a t - \mathbf{p}_a \cdot \mathbf{r})] \approx \frac{\sqrt{2\rho_{\text{DM}}}}{m_a} \exp (-im_a t)$$

where we have made use of the fact that the axion Compton wavelength is: $\lambda_{\text{dB}} = \frac{2\pi\hbar}{m_a v} \approx (\mu\text{eV}/m_a) \cdot 2 \text{ km}$

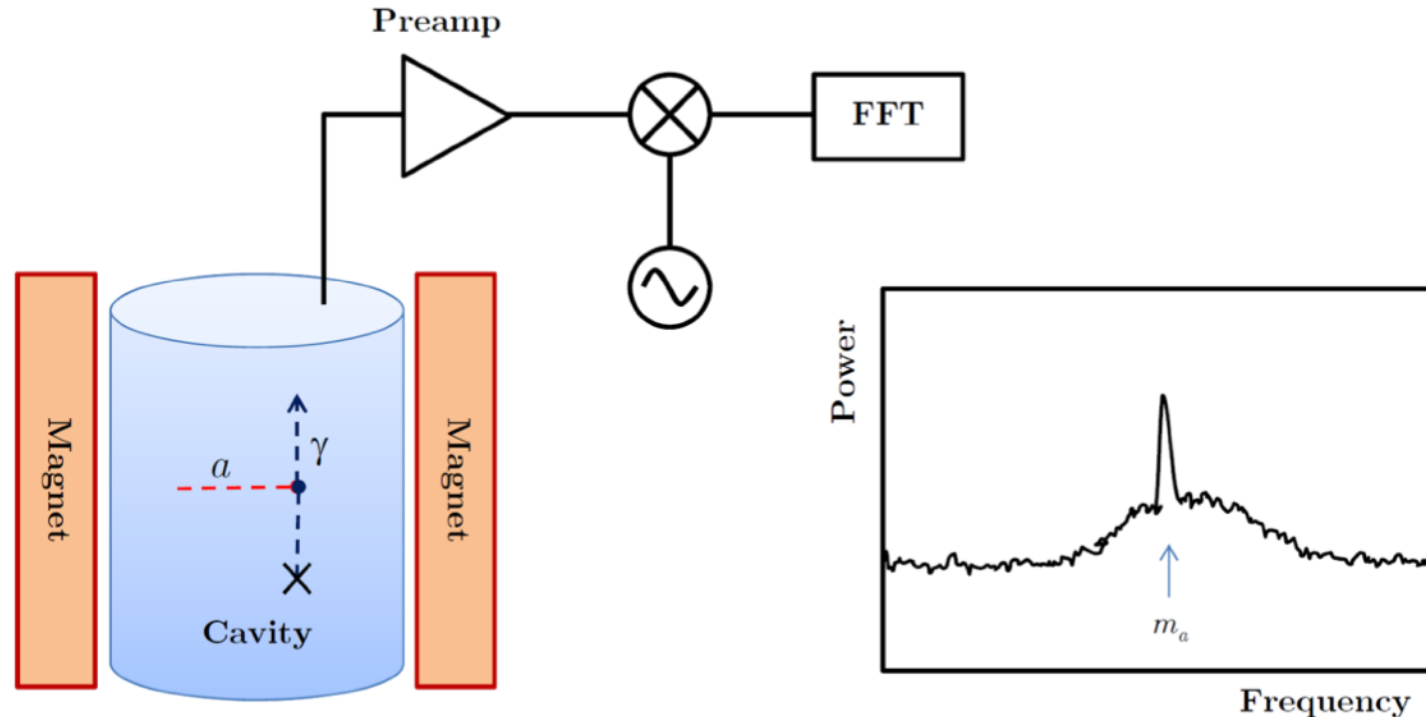


$$\mathbf{E}_a(t) = -\frac{1}{\epsilon} g_{a\gamma\gamma} a(t) \mathbf{B}_0$$

Axion-induced electric field oscillates at a frequency: $f = m_a/(2\pi) \approx (m_a/\mu\text{eV}) 0.242 \text{ GHz}$

Cavity Haloscopes

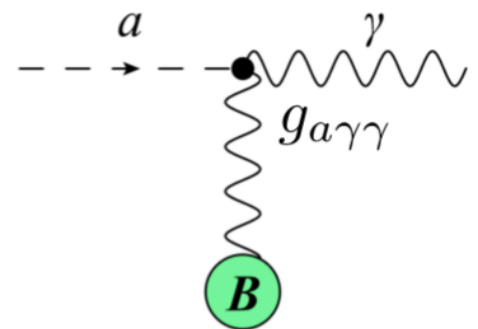
Immerse a **resonant cavity** in the magnetic field. If the resonant frequency of the cavity matches the mass of the axion, conversion can be resonantly enhanced by the quality factor $Q_0 \gtrsim 10^3$ of the cavity.



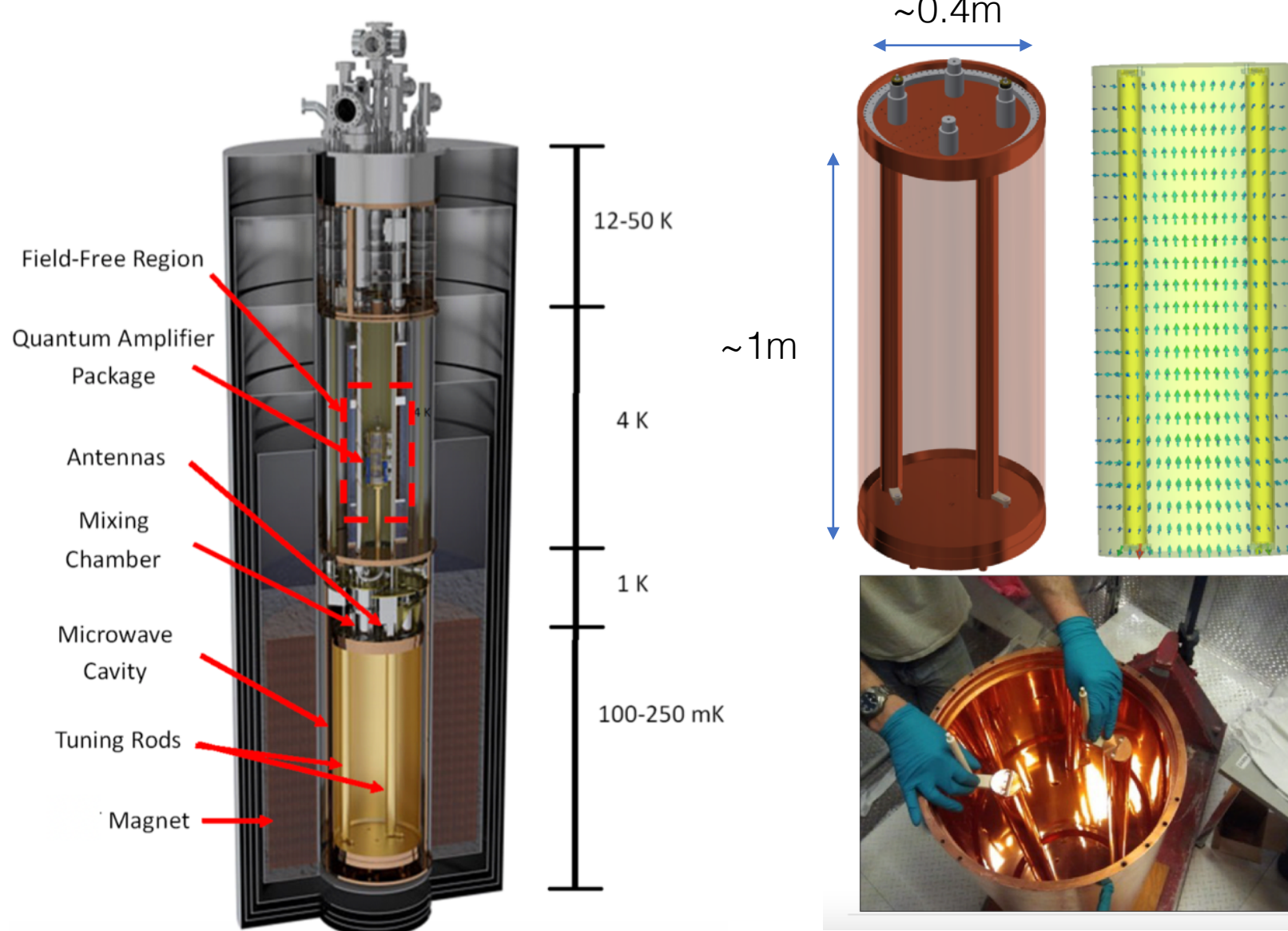
$$P_{a \rightarrow \gamma} \approx g_{a\gamma\gamma}^2 \frac{\rho_a}{m_a} B^2 C V Q_0 \lesssim 10^{-21} \text{ W}$$

$$C = \frac{\left| \int dV \mathbf{B}_0 \cdot \mathbf{E}_{mnp} \right|^2}{B_0^2 V \int dV \epsilon |\mathbf{E}_{mnp}|^2}$$

$$\begin{aligned}\mathcal{L} &\supset -\frac{1}{4} g_{a\gamma\gamma} a F_{\mu\nu} \tilde{F}^{\mu\nu} \\ &= -\frac{1}{4} g_{a\gamma\gamma} a \mathbf{E} \cdot \mathbf{B}\end{aligned}$$



Axion Dark Matter Experiment (ADMX)

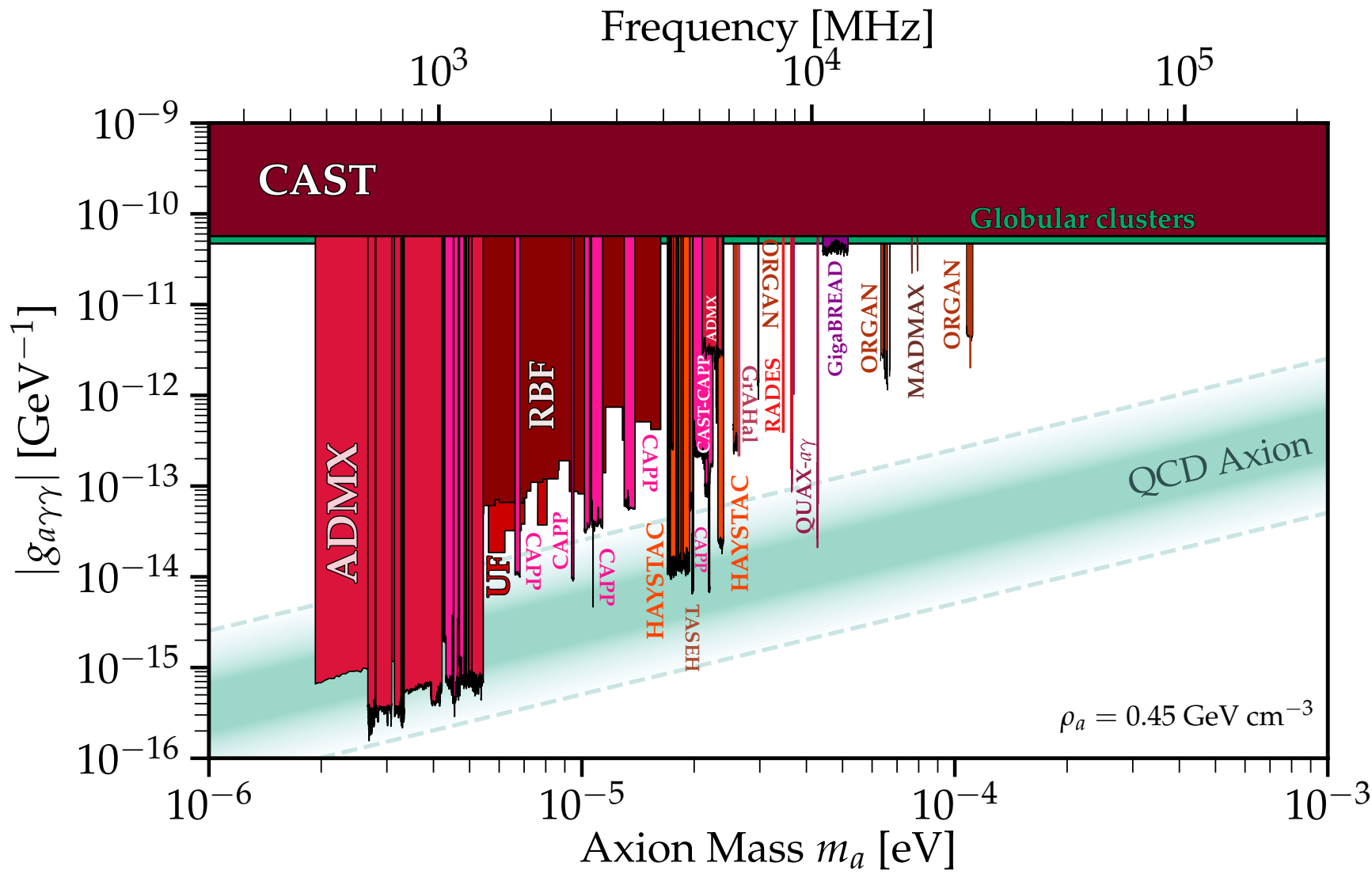


$$\lambda \sim 0.4 \text{ m} \rightarrow f \sim 750 \text{ MHz}$$

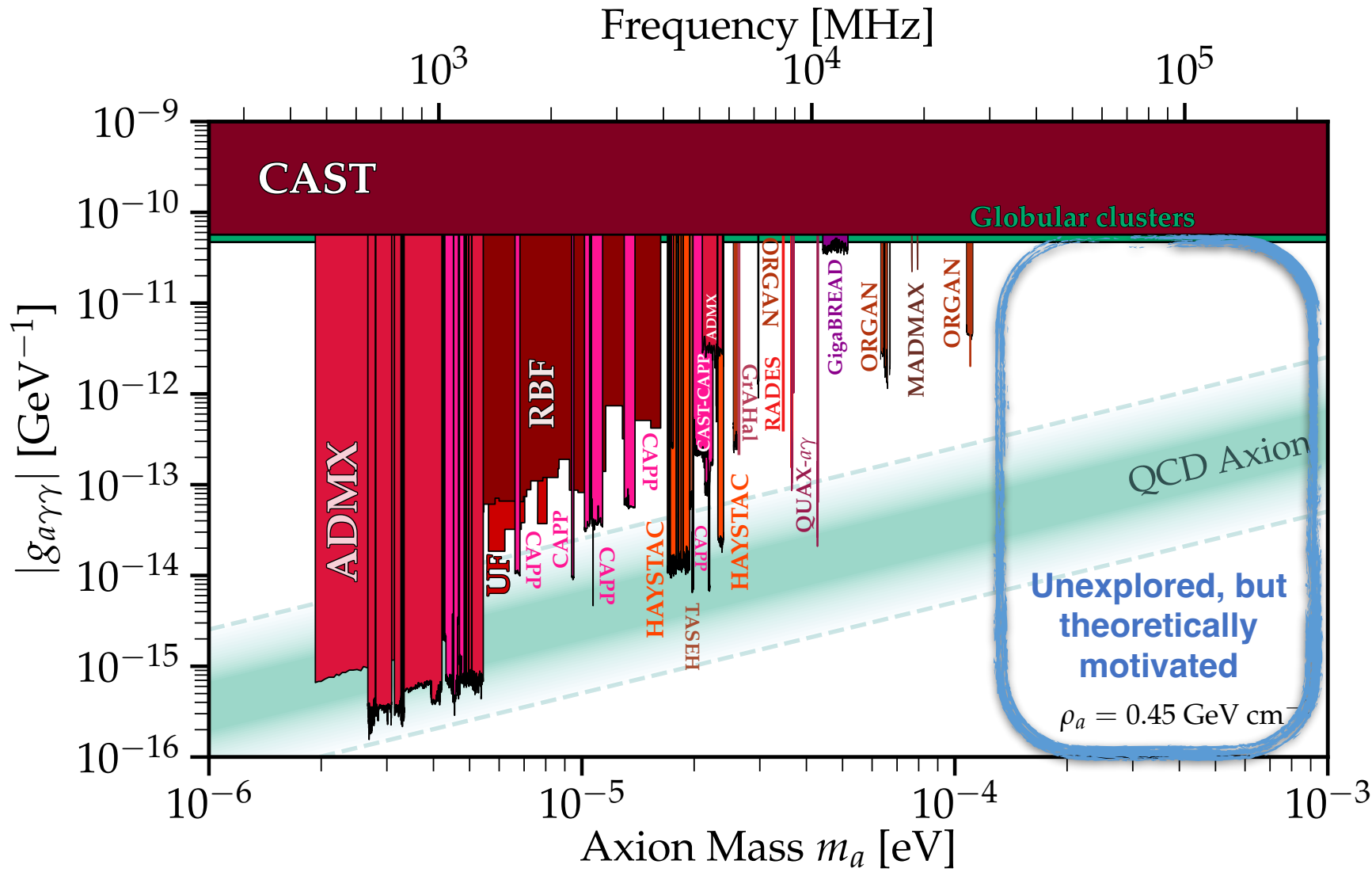
Use tuning rods to ‘scan’ resonant frequency in the range 580 MHz to 890 MHz.

[2010.00169]

Current Status of Haloscopes



Current Status of Haloscopes



High mass challenge!

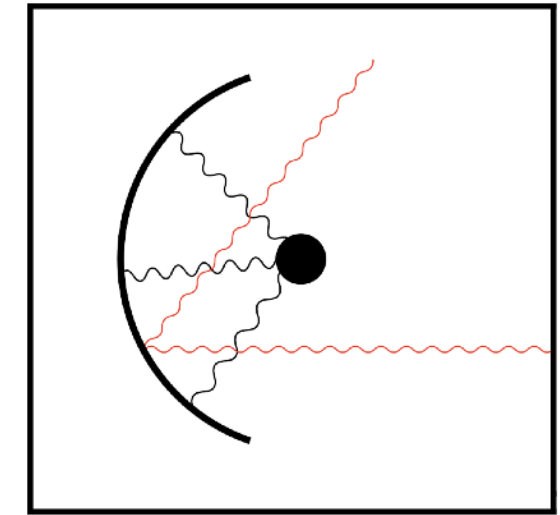
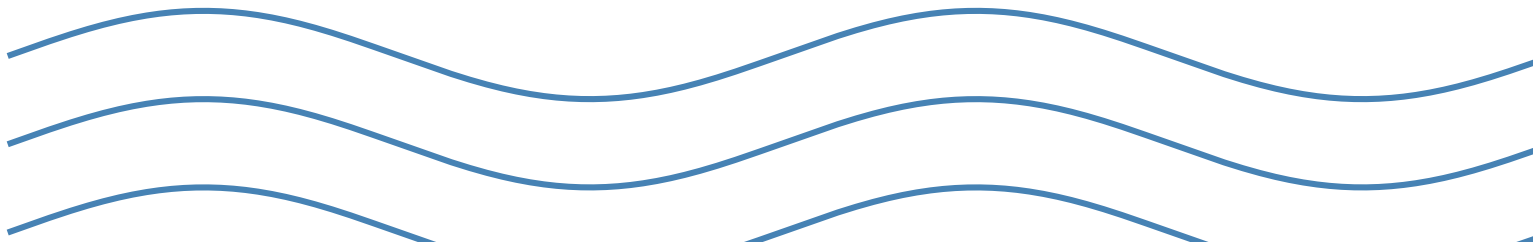
Cavity size (and therefore sensitive volume) decreases with increasing mass.

Coherent detection (using heterodyne amplification) run into the Standard Quantum Limit (SQL) as the frequency increases.

Dish Antenna Detectors

[1212.2970]

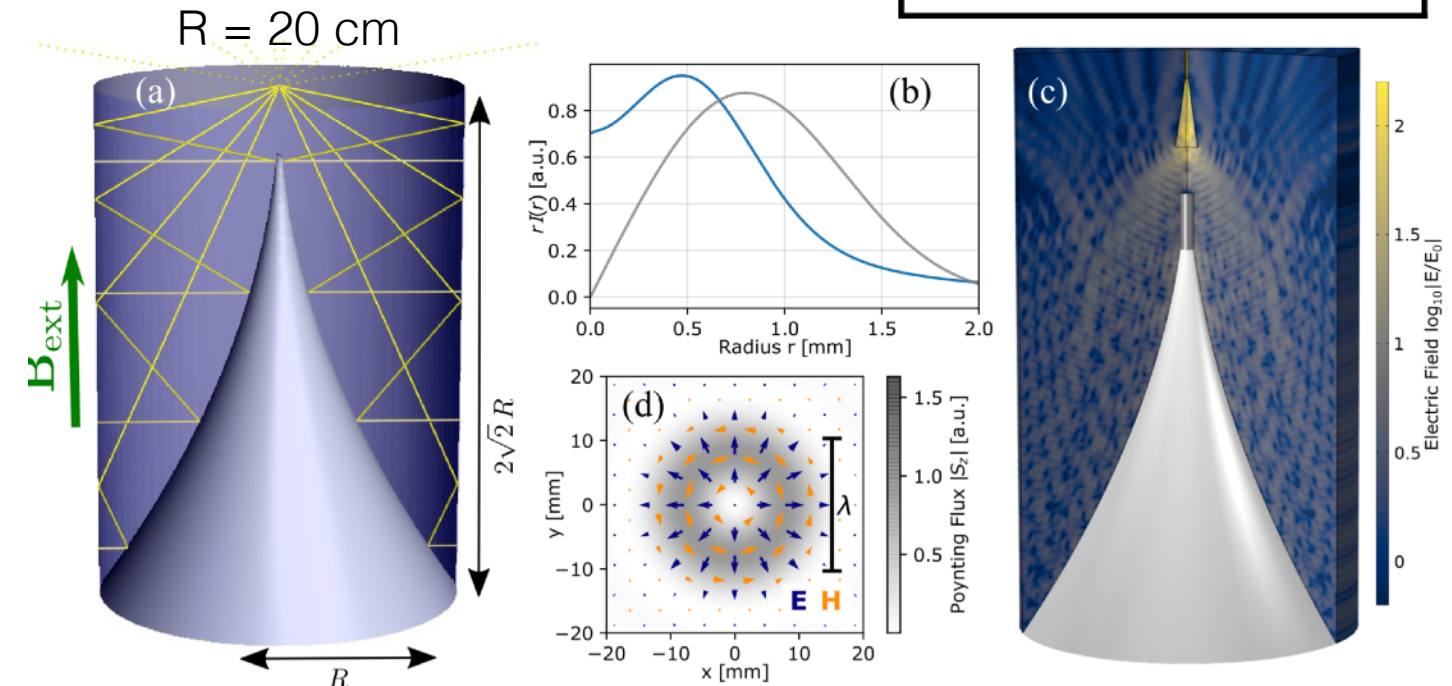
Dish antennas are ‘broadband’ (they avoid the need for resonant conversion)



But they need a large area to compensate - can be challenging to achieve inside a magnetic field

E.g. proposed BREAD Experiment

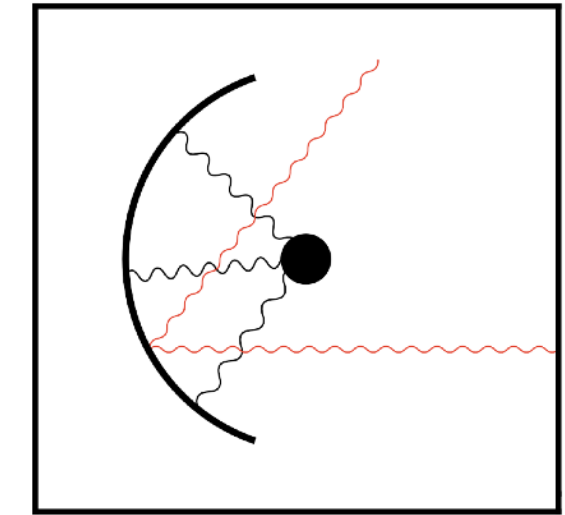
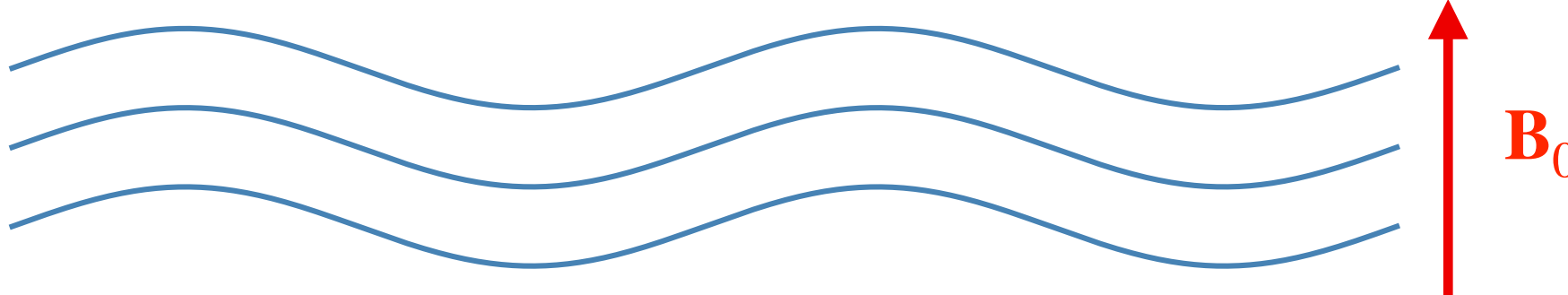
[2111.12103, 2501.17119]



Dish Antenna Detectors

[1212.2970]

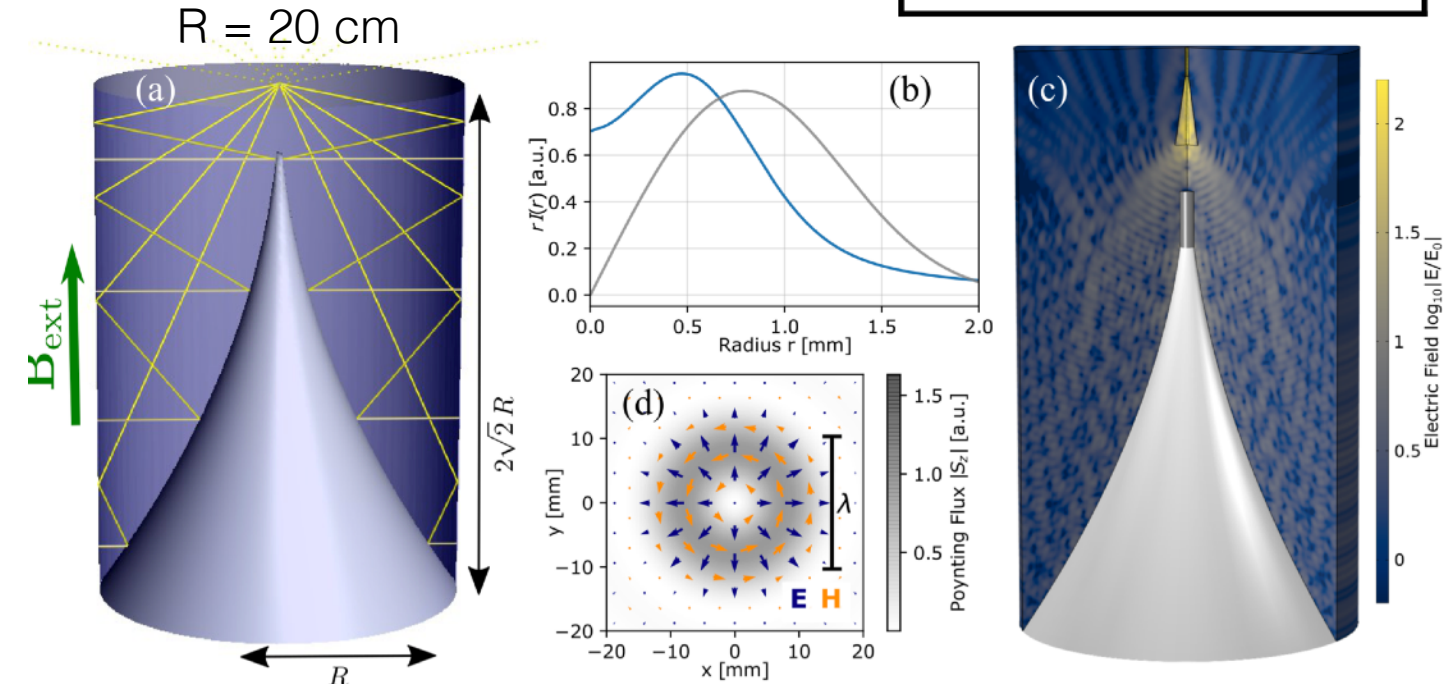
Dish antennas are ‘broadband’ (they avoid the need for resonant conversion)



But they need a large area to compensate - can be challenging to achieve inside a magnetic field

E.g. proposed BREAD Experiment

[2111.12103, 2501.17119]

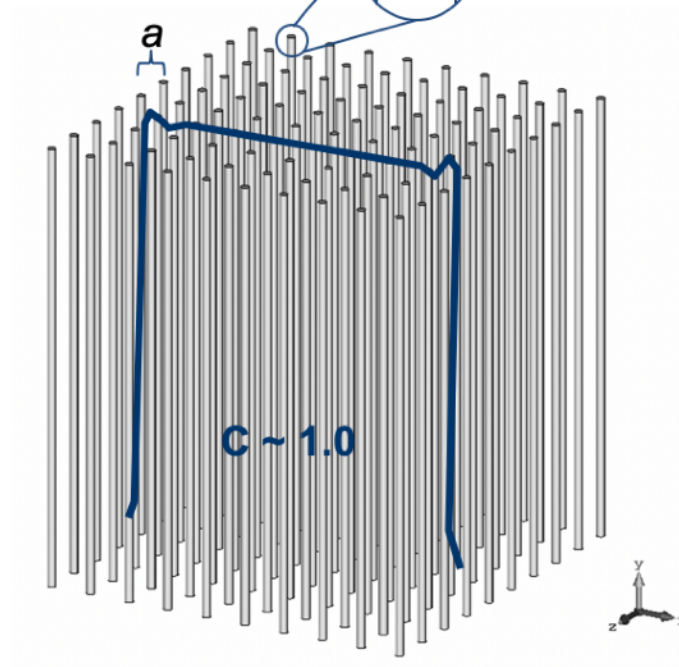


Plasma Haloscopes

[PATRAS Talk by Max Silva-Feaver]

[PATRAS Talk by Junu Jeong]

Use **wire metamaterials** inside the cavity. [\[1904.11872\]](#)



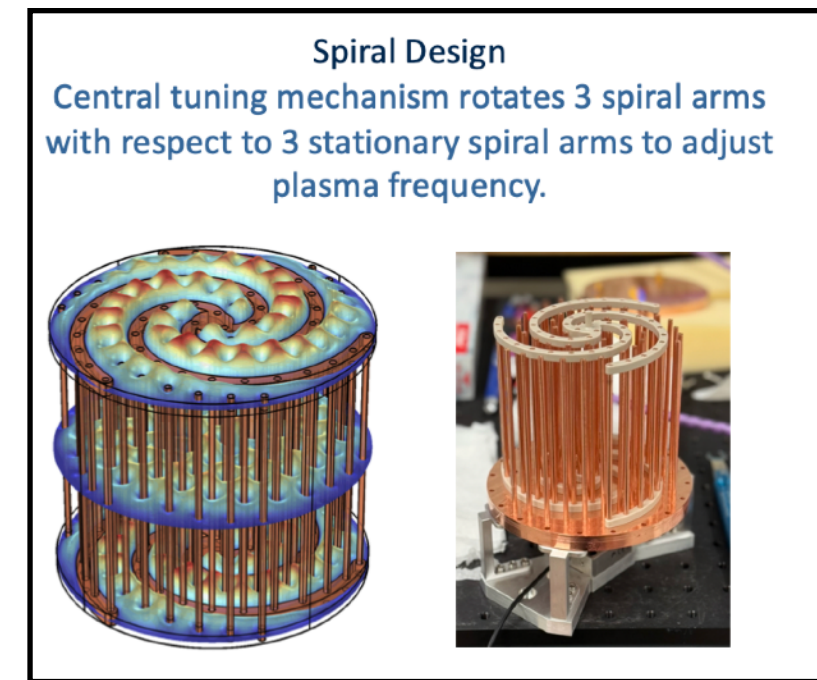
Lawson et al. (2019), PRL

$$f = \frac{c}{a} \sqrt{\frac{1}{2\pi \ln(a/r)}}$$

- Wires mutually induct, changing the plasma frequency
- Resonant **frequency is decoupled from the size of the system**
- A wire-spacing of 1 cm gives a plasma frequency of ~ 10 GHz
- **No theoretical volume limit**

Theory of wire metamaterial: [Pendry \(1998\)](#) and [Belov, et al. \(2003\)](#)

e.g. proposed ALPHA Experiment



Tuneable (?) $\sim 10 - 14$ GHz
[\[2210.00017\]](#), [\[2306.15734\]](#)

First ‘plasma haloscopes’ have yet to be demonstrated, and tuning may be challenging.

Canfranc Axion Detection Experiment

CADEX: a novel and challenging experiment to search for dark matter axions in the range $m_a = 330\text{--}460 \mu\text{eV}$ (W-band: 86–110 GHz). Also sensitive to dark photons.

Originally proposed and accepted by Canfranc Underground Laboratory (LSC) under [EoI-31-2021](#)

Novel Design:

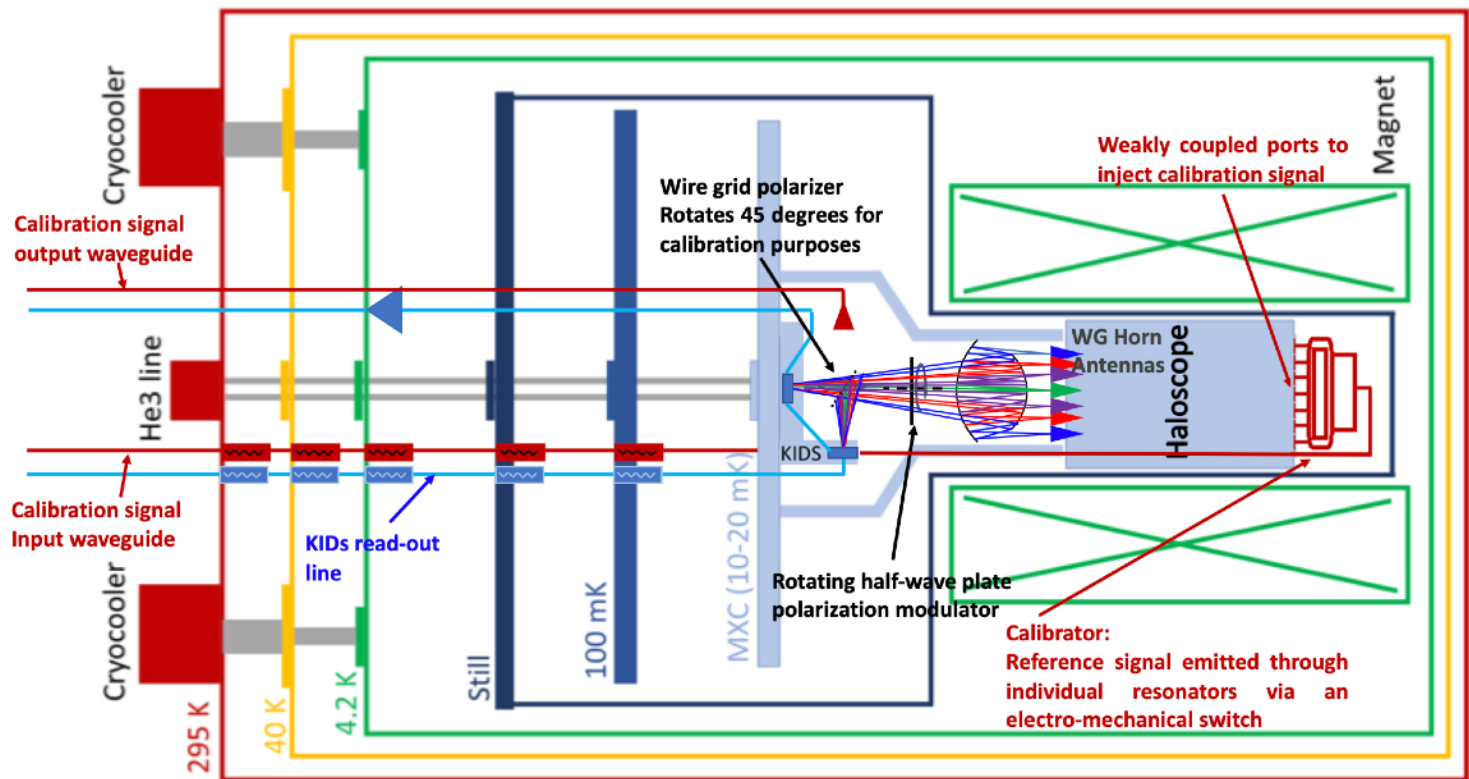
- Array of 7 high frequency, tuneable resonant cavities
- Superconducting Kinetic Inductance Detectors (KIDs)
→ broadband, polarisation detectors to go beyond the Standard Quantum Limit
- Eventually install and operate the CADEX experiment at LSC

CADEX as a technology platform!



[[JCAP 11 \(2022\) 044, arXiv:2206.02980](#)]

[[Cosmic WISPers 2024 Proceedings](#)]



More than 30 people from 11 institutions



Observatorio de Yebe
Infraestructura Científica
y Técnica Singular



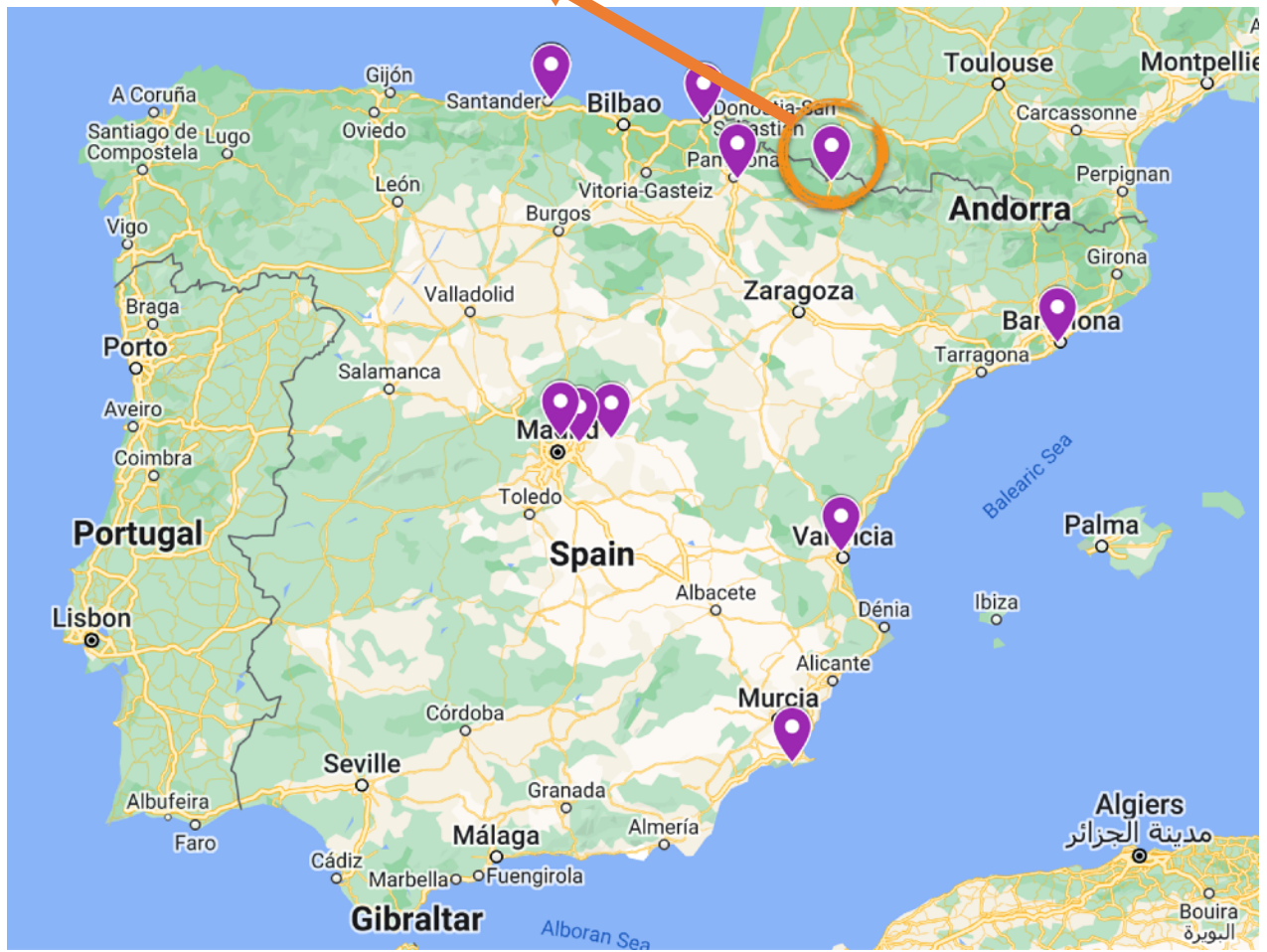
Innovative Antenna and Terahertz Imaging Technologies



INSTITUT DE FÍSICA
CORPUSCULAR



Universidad Pública de Navarra
Nafarroako Unibertsitate Publikoa



CADEx Sensitivity Projections

$$P_d = \frac{\beta}{(1 + \beta)^2} g_{a\gamma}^2 \frac{\rho_a}{m_a} B^2 C V Q$$

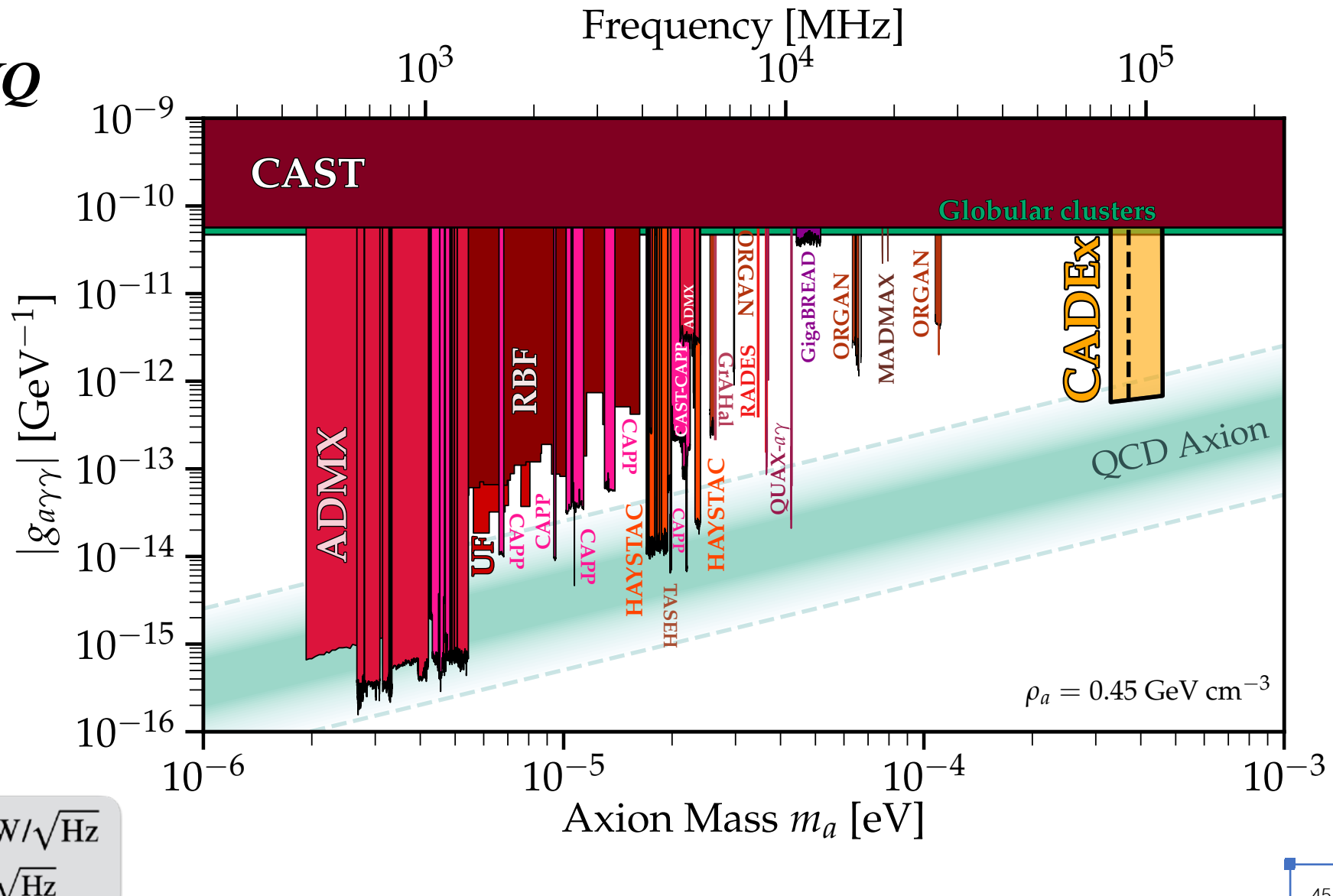
Magnetic field: $B = 8\text{ T}$

Total cavity volume: $V = 0.2L$

Cavity quality factor: $Q_0 = 2 \times 10^4$

Cavity coupling: $\beta \sim 1$

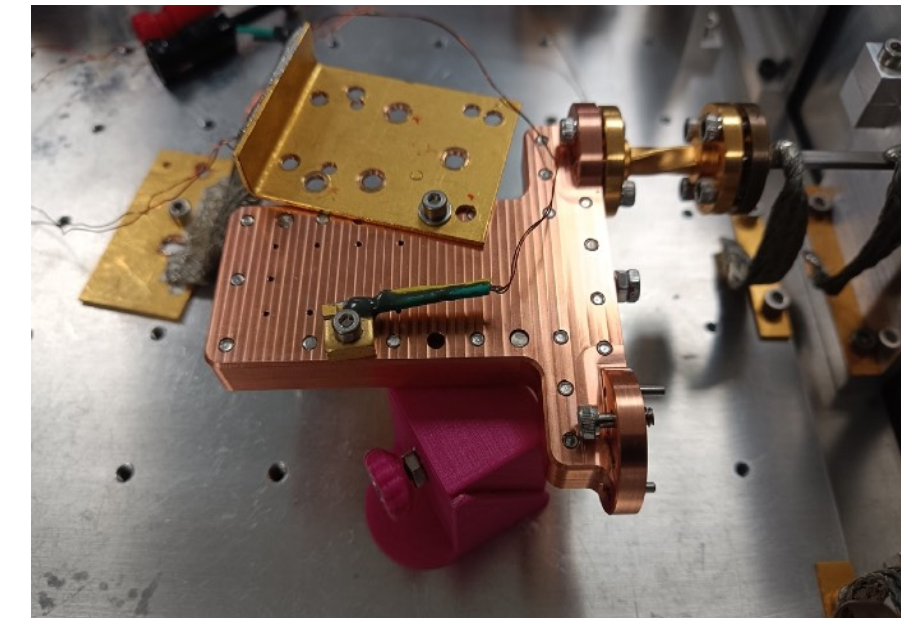
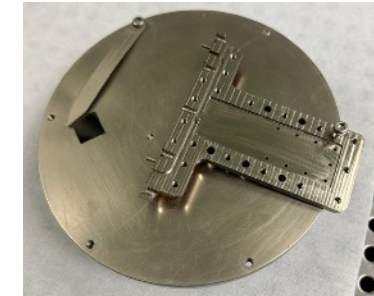
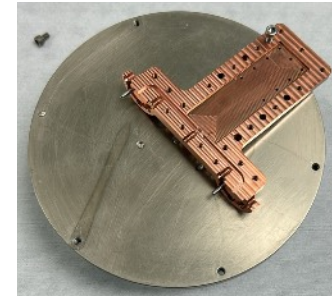
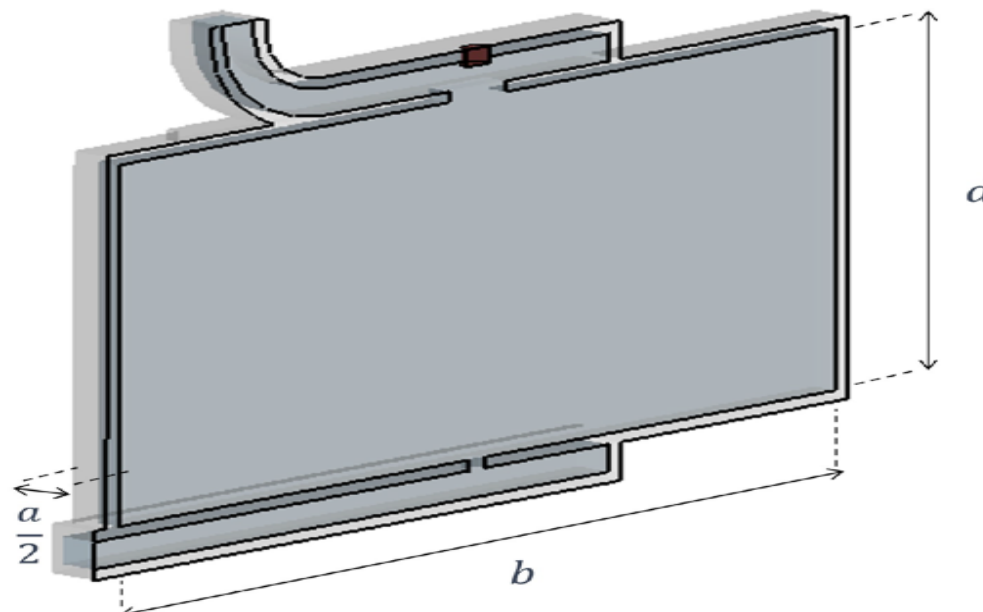
Cavity form factor: $C \sim 0.66$



- Pushing 3D Cavities to the **W-band**, two cavities have so far been fabricated, coated with **superconducting NbTiN film** to enhance Q.

$$f_r = \frac{c}{2} \sqrt{\frac{1}{a^2} + \frac{1}{b^2}}$$

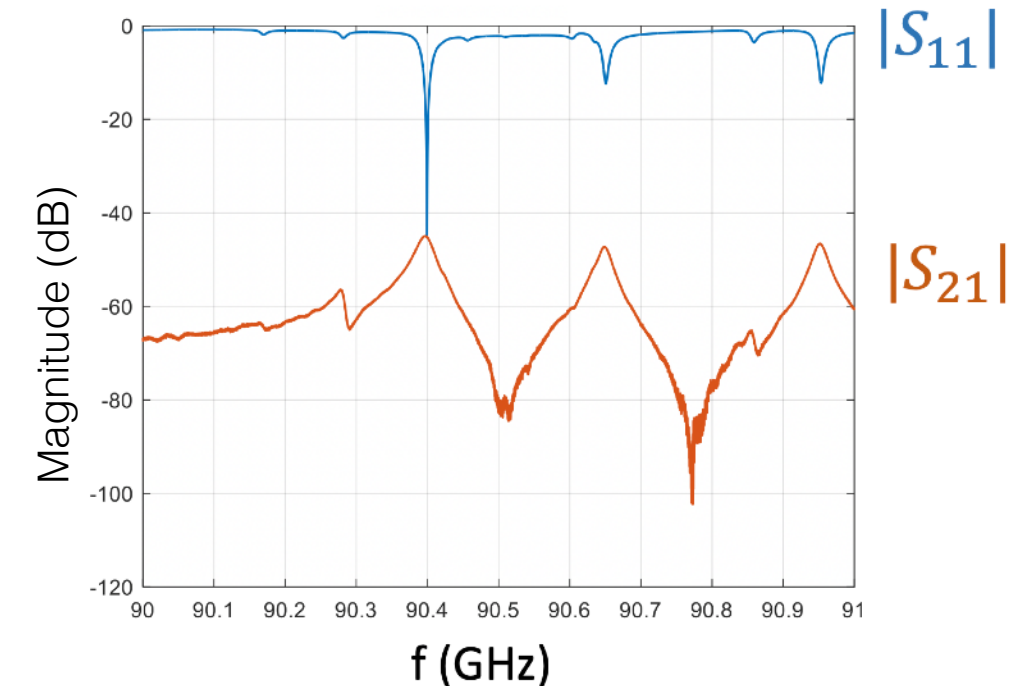
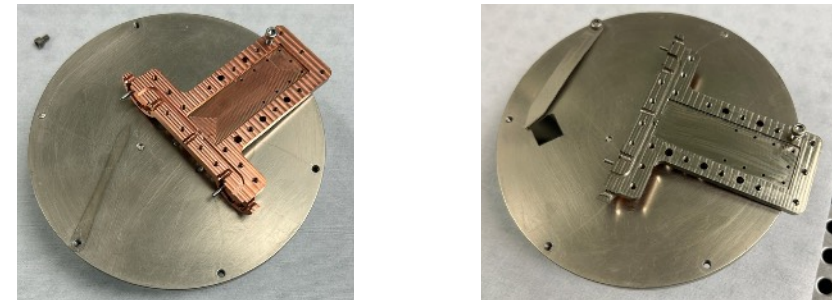
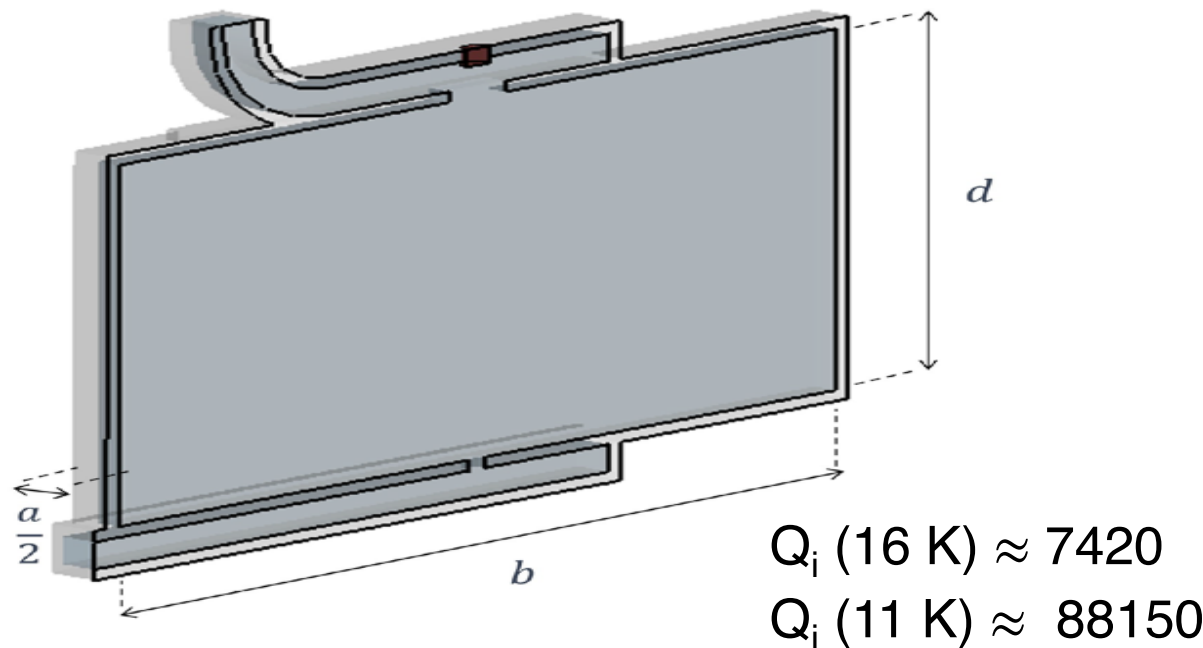
$a \approx 1.7 \text{ mm}$
 $b = 40a$
 $f_r = 90\text{GHz}$



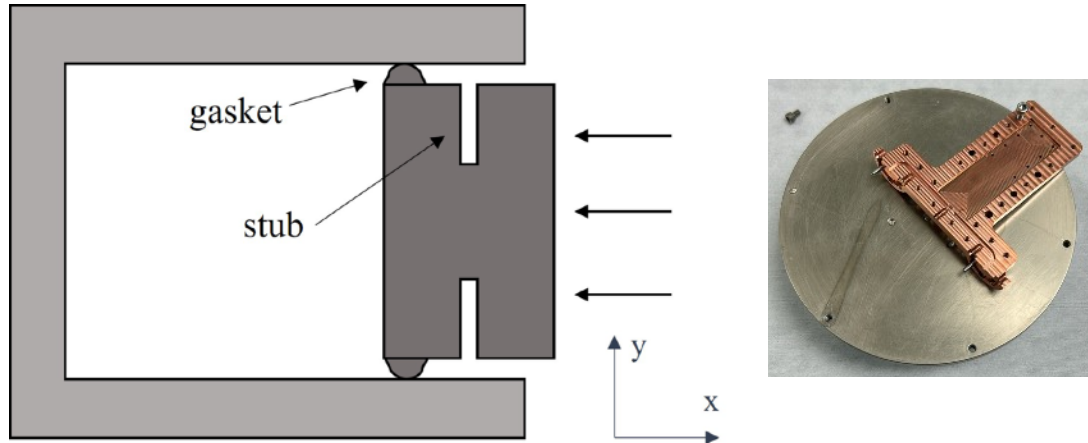
- Pushing 3D Cavities to the **W-band**, two cavities have so far been fabricated, coated with **superconducting NbTiN film** to enhance Q.

$$f_r = \frac{c}{2} \sqrt{\frac{1}{a^2} + \frac{1}{b^2}}$$

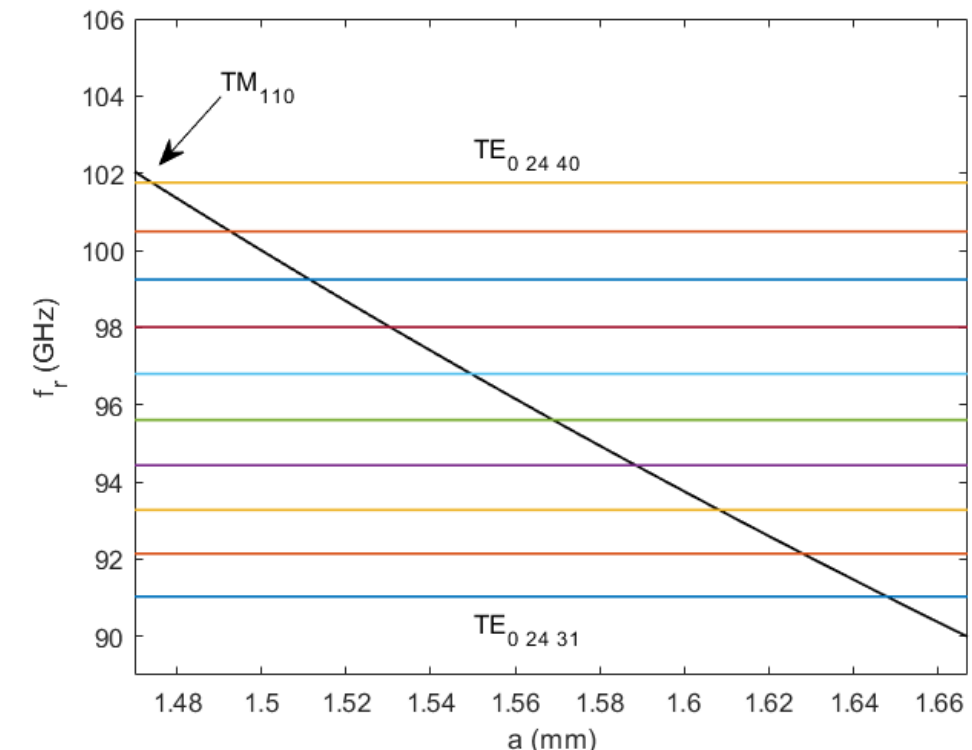
$a \approx 1.7 \text{ mm}$
 $b = 40a$
 $f_r = 90\text{GHz}$



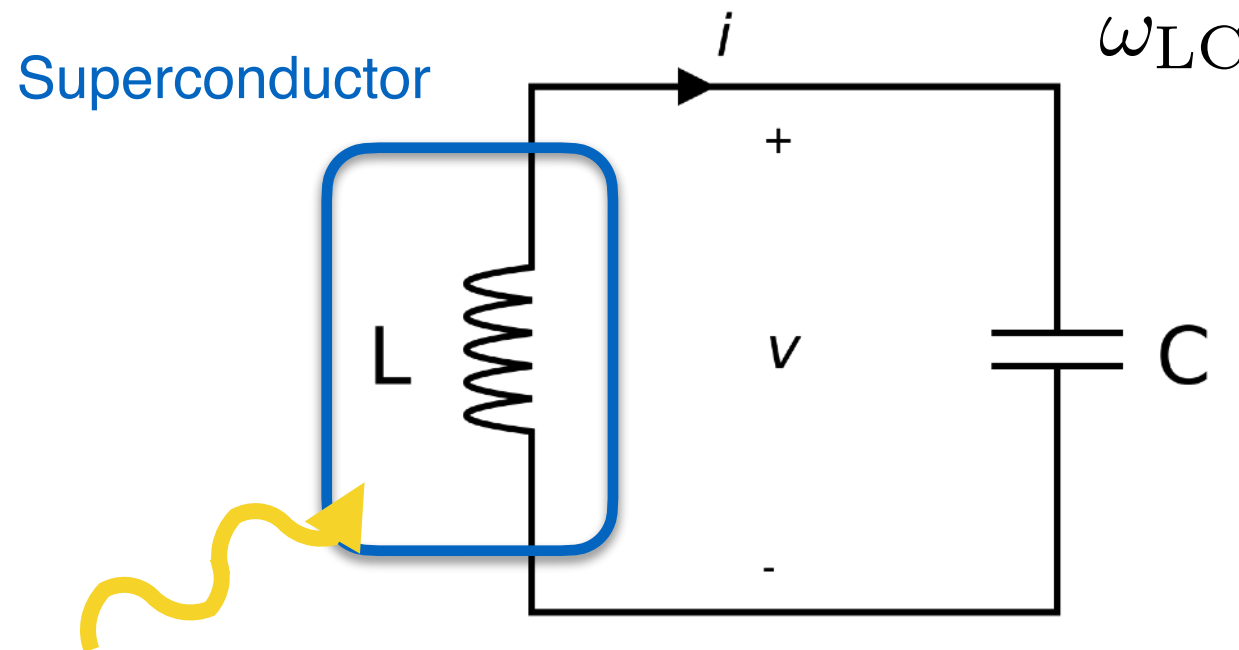
- Pushing 3D Cavities to the **W-band**, two cavities have so far been fabricated, coated with **superconducting NbTiN film** to enhance Q.
- Next generation of cavities are **about to be machined**, with quality factor measurements in the coming months (Q4 2025)
- Ultimately aim to develop **tunable cavities** to scan frequency range $f_r \in [86, 111]$ GHz



[See e.g. McAllister et al., [2309.12098](#)]



Kinetic Inductance Detectors (KIDs)



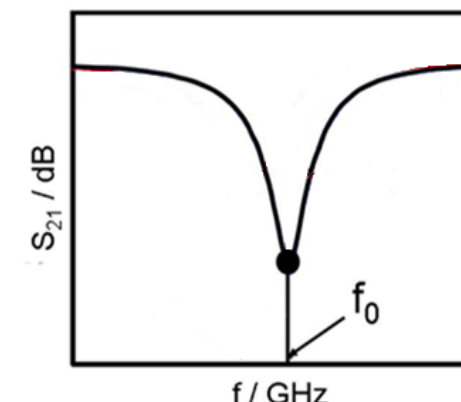
Photon absorbed by superconductor breaks Cooper pairs,
reducing kinetic inductance

Sensitivity described by
Noise-equivalent power (NEP):

$$\delta P_{\text{noise}}^{\text{inc}} = \frac{\text{NEP}}{\sqrt{2\Delta t}}$$

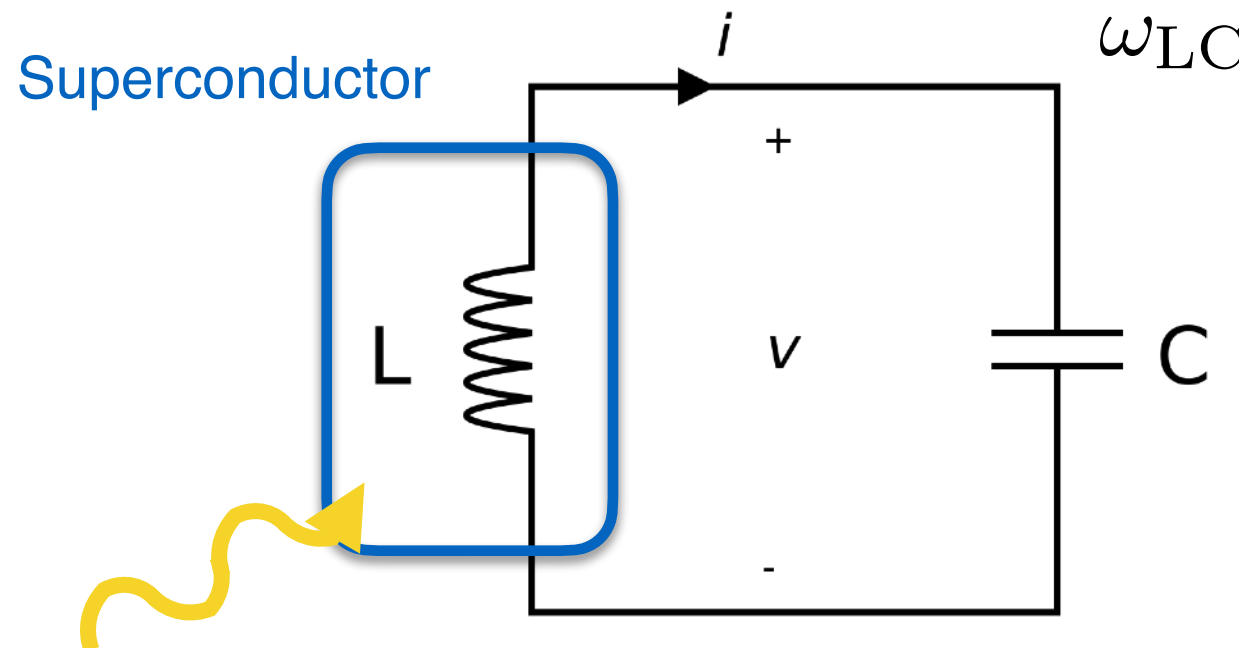
$$f_0 = \frac{1}{\sqrt{LC}}$$

$$f' = \frac{1}{\sqrt{L'C}}$$



Detection by monitoring the
resonant frequency of the LC
circuit

Kinetic Inductance Detectors (KIDs)



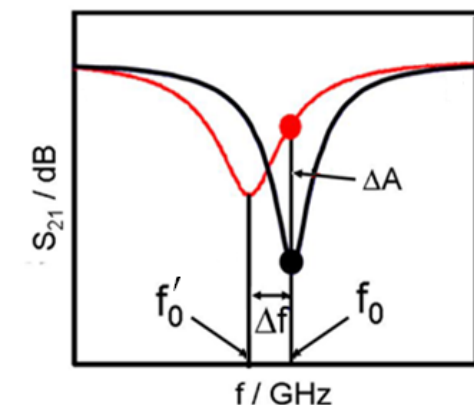
Photon absorbed by superconductor breaks Cooper pairs, reducing kinetic inductance

Sensitivity described by Noise-equivalent power (NEP):

$$\delta P_{\text{noise}}^{\text{inc}} = \frac{\text{NEP}}{\sqrt{2\Delta t}}$$

$$f_0 = \frac{1}{\sqrt{LC}}$$

$$f' = \frac{1}{\sqrt{L'C}}$$



Detection by monitoring the resonant frequency of the LC circuit

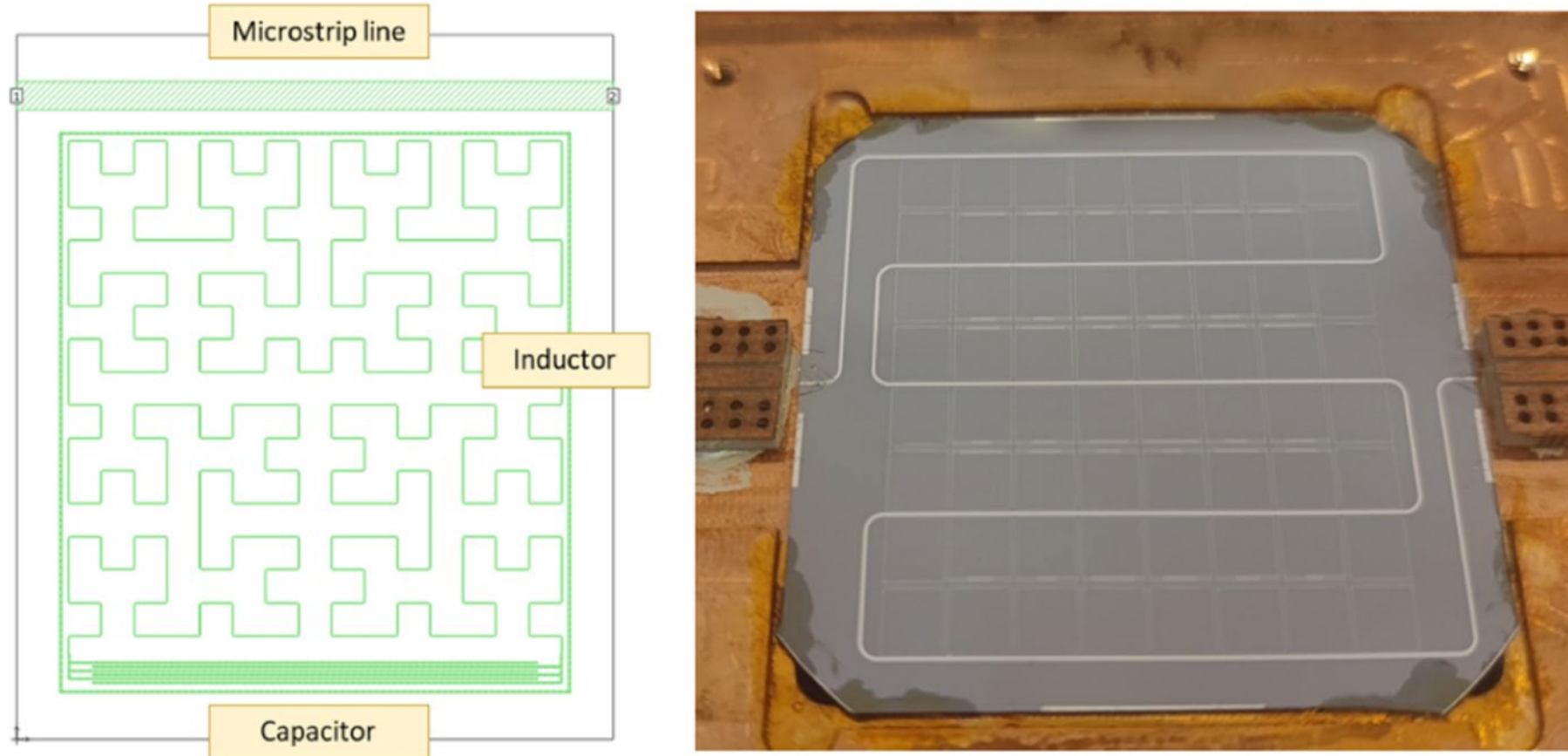


Fig. 1 *Left* schematic of a LEKID coupled to a microstrip read-out line, with the inductor and the inter-digital capacitor. *Right* photograph of the 64 LEKIDs prototype fabricated on a silicon substrate of size $40 \times 40 \text{ mm}^2$

[See also [Journal of Low Temperature Physics \(2024\)](#)]

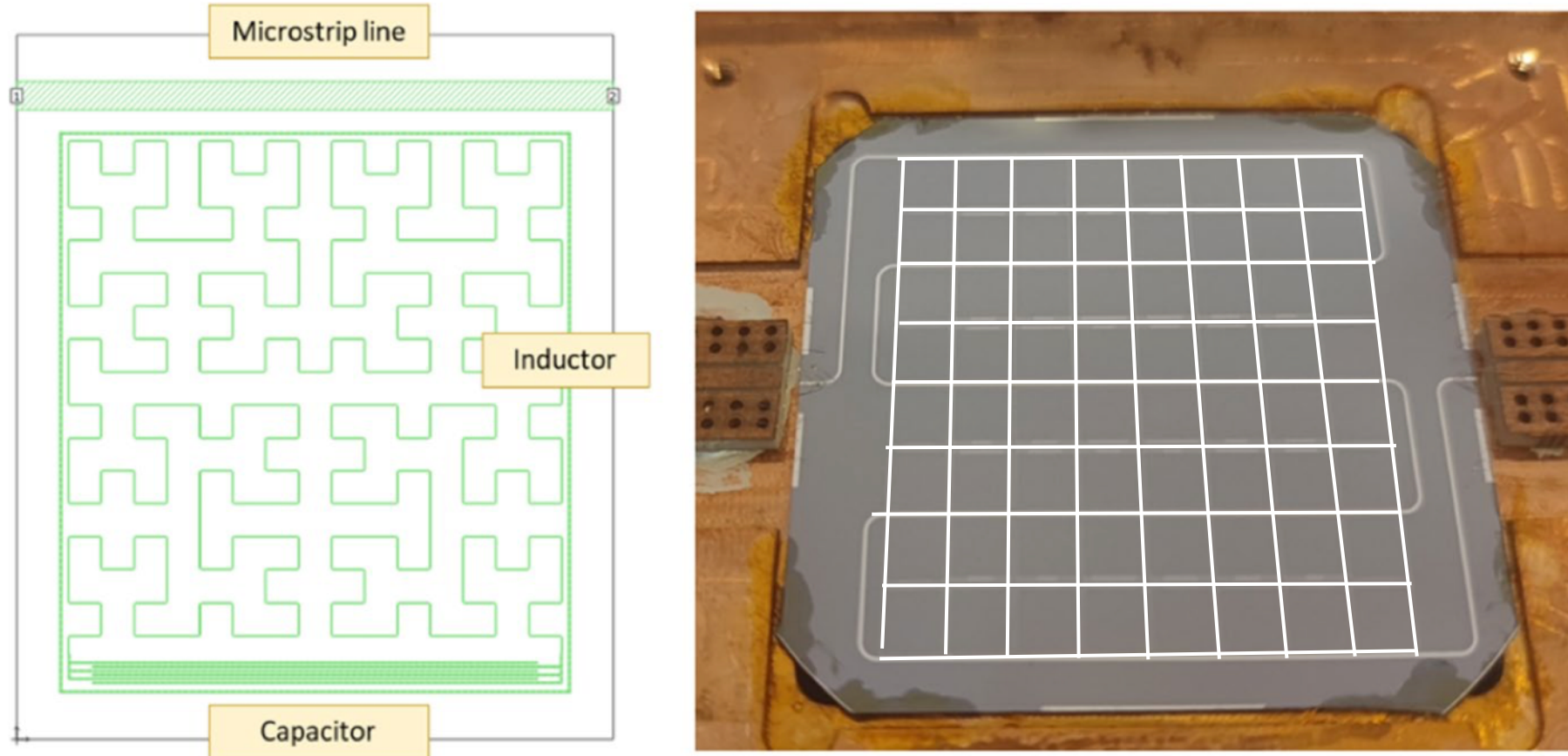
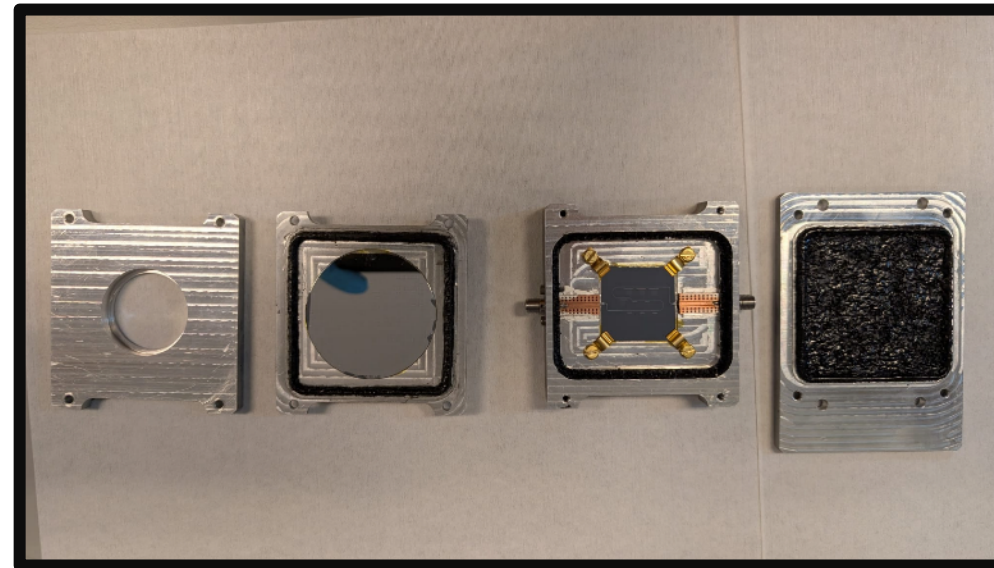


Fig. 1 *Left* schematic of a LEKID coupled to a microstrip read-out line, with the inductor and the inter-digital capacitor. *Right* photograph of the 64 LEKIDs prototype fabricated on a silicon substrate of size $40 \times 40 \text{ mm}^2$

[See also [Journal of Low Temperature Physics \(2024\)](#)]

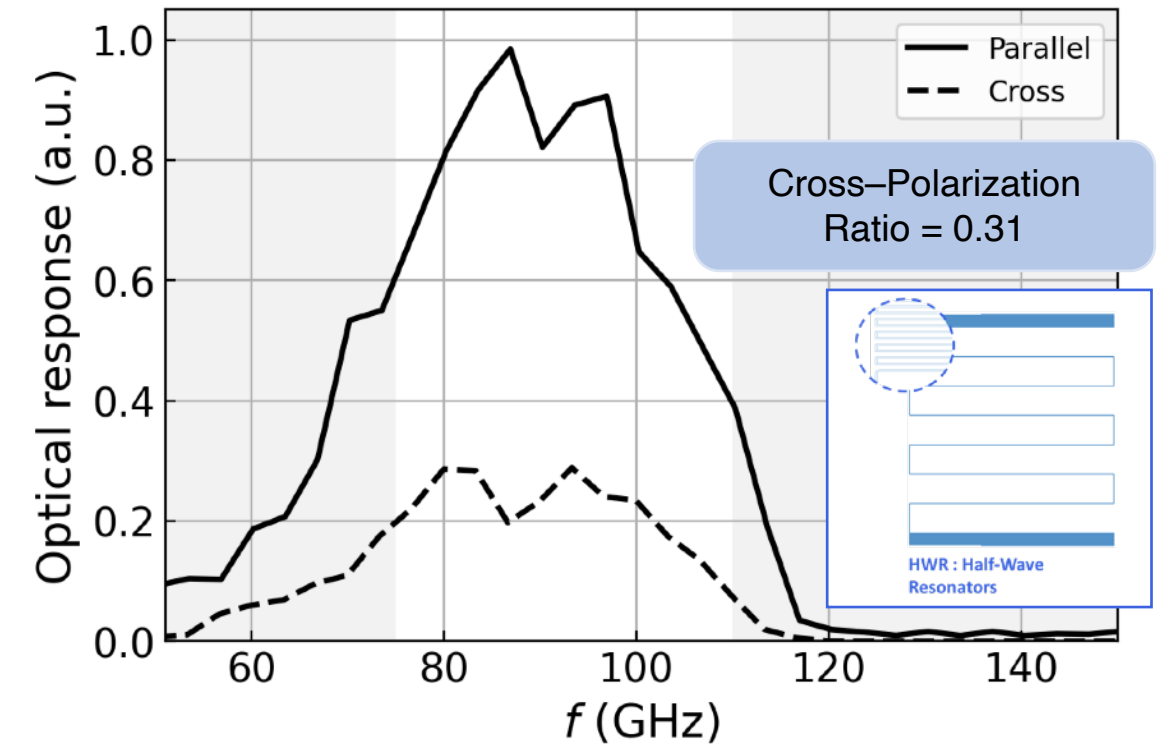
- **Broadband** detection system based on superconducting **Kinetic Inductance Detectors**
- First demonstrators based on **Ti/Al bilayer** have been developed and characterized
- Cryogenic response confirms **W-band detection**.
- KIDs demonstrated **background limited performance** ($T_{bb} = 50$ K).
- **Low background set-up** under test



Target NEP $\leq 10^{-19}$ W/ $\sqrt{\text{Hz}}$

15 nm Al ($T_c \approx 1.2$ K)
15 nm Ti ($T_c \approx 0.4$ K)

[See also [Journal of Low Temperature Physics \(2024\)](#)]



- **IFCA Cryolab:** New cryogenic laboratory at IFCA will host CADEx technology demonstrator - civil work recently completed in Summer 2025*
- Installation of dilution refrigerator now completed
- Cryolab will be a **test bed of quantum sensor technologies**. Pathfinder setup will be used to test, compare and optimise detectors
- Currently tendering for the magnet.



*IFCA cryolab also to be used for e.g. development of the thermal monitoring and control system (TMCS) system for the LiteBird experiment (CMB polarisation satellite, Cosmology Group)

CADEx Timeline

Existing EoI with LSC runs through 2026. What does the future look like?

- **Design and Demonstration Phase (2 years)**

Cryostat acquisition, installation and operation

Full quasi-optical design

Demonstration of key technology (haloscope and detectors) in the lab.

- **Pathfinder Phase (2 years)**

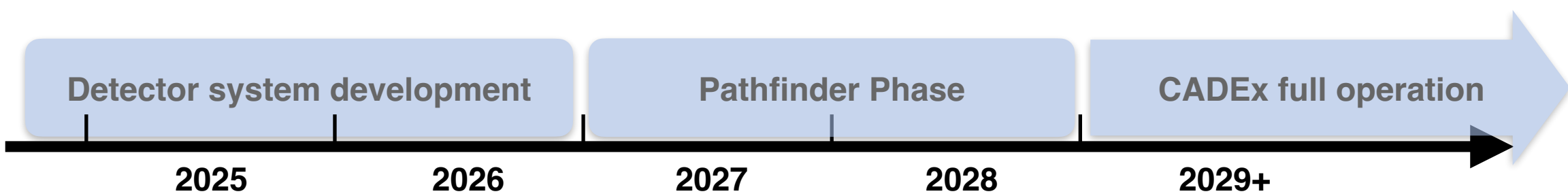
First CADEx prototype (pathfinder) to be installed & tested in IFCA Cryolab

First science results in 2027/2028

- **Operation Phase (8 years)**

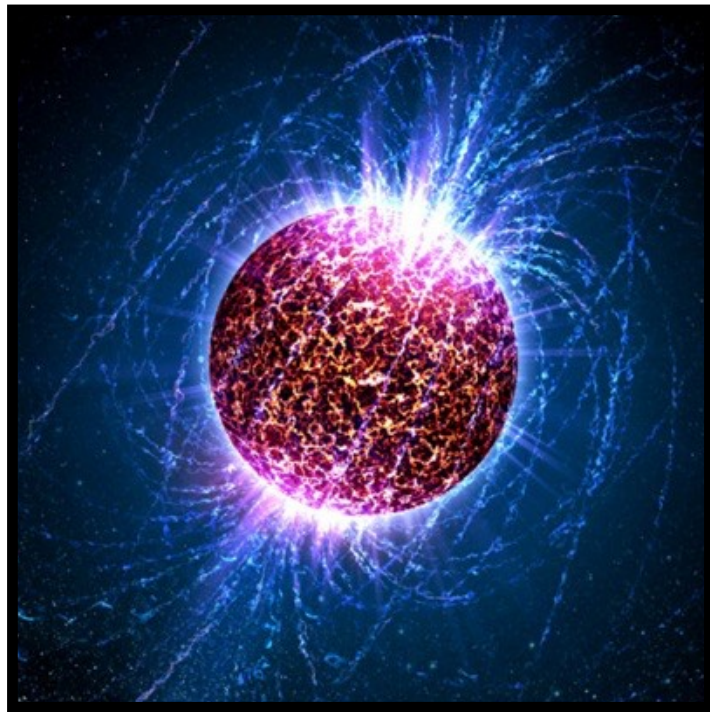
Upgrade the experiment to improve the sensitivity

Installation & Commissioning at LSC. Full Operation



Complementary Searches

Neutron Stars



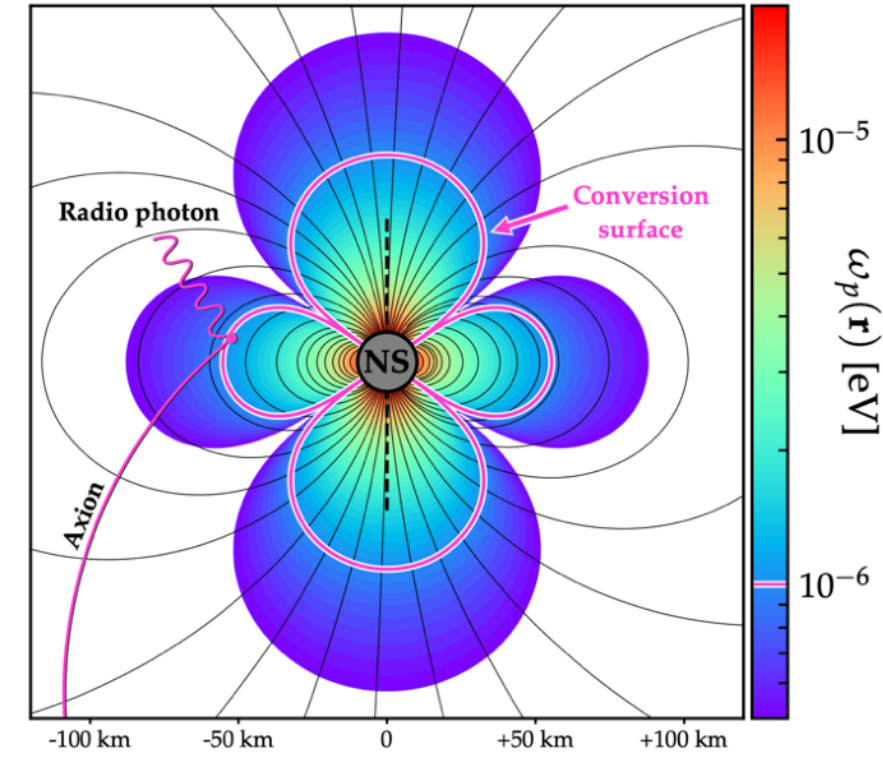
[Credit: Casey Reed (Penn State University), Wikimedia Commons]

[For recent modeling developments, see also Battye et al., [1910.11907](#), [2104.08290](#); Leroy et al., [1912.08815](#)]

Strong gravitational field

compresses DM phase space, enhancing DM density near NS surface

Young neutron stars can have **extremely high magnetic fields**
($B_0 = 10^8 - 10^{11}$ T)

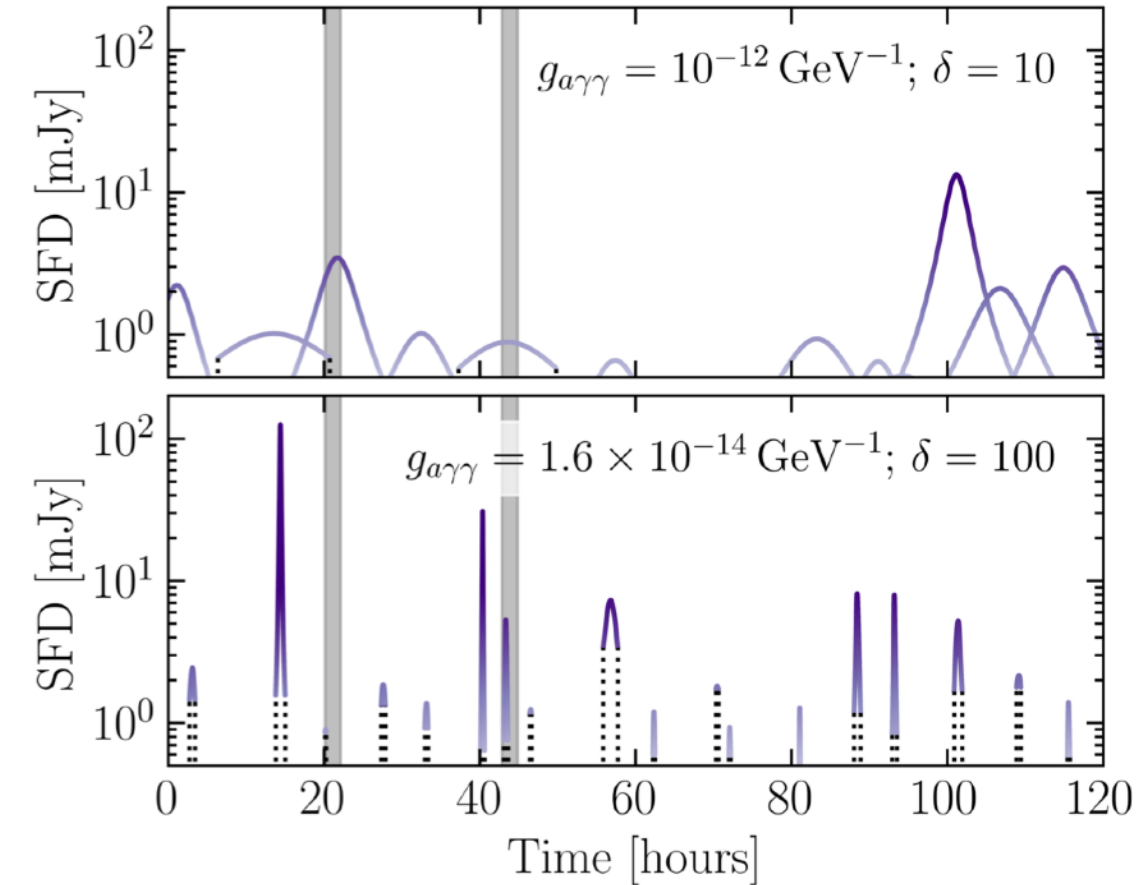
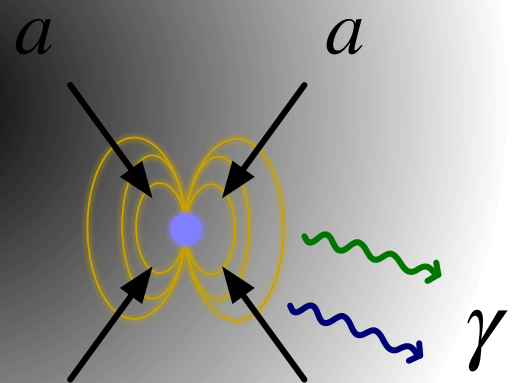


NS surrounded by a dense plasma which allows ‘resonant’ conversion, when **axion mass matches plasma mass**:
 $\omega_p(B_0, P) = m_a/2\pi$

[Search in the Galactic Centre, Foster et al., [2202.08274](#)]

Radio Transients

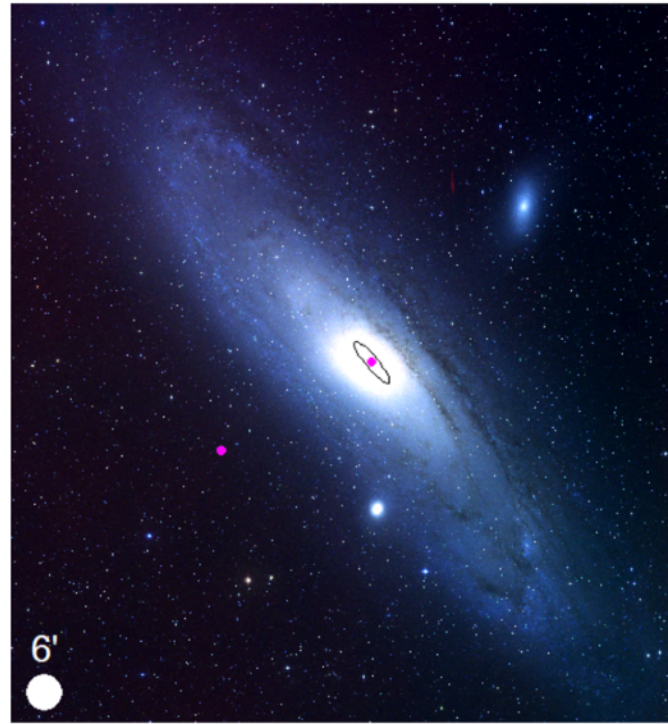
If it turns out that most of the axion density is locked up in axion miniclusters, one promising way to find it would be in **radio transients**.



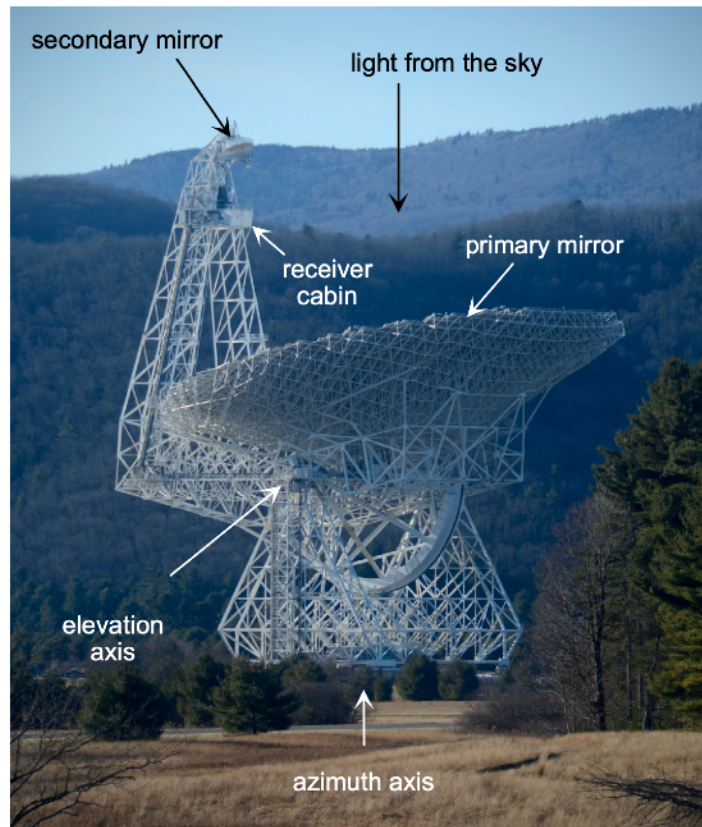
Expect rates of $O(1)$ per day per galaxy

[**BJK**, Edwards, Visinelli, Weniger,
[2011.05377](https://arxiv.org/abs/1105.377), [2011.05378](https://arxiv.org/abs/1105.378)]

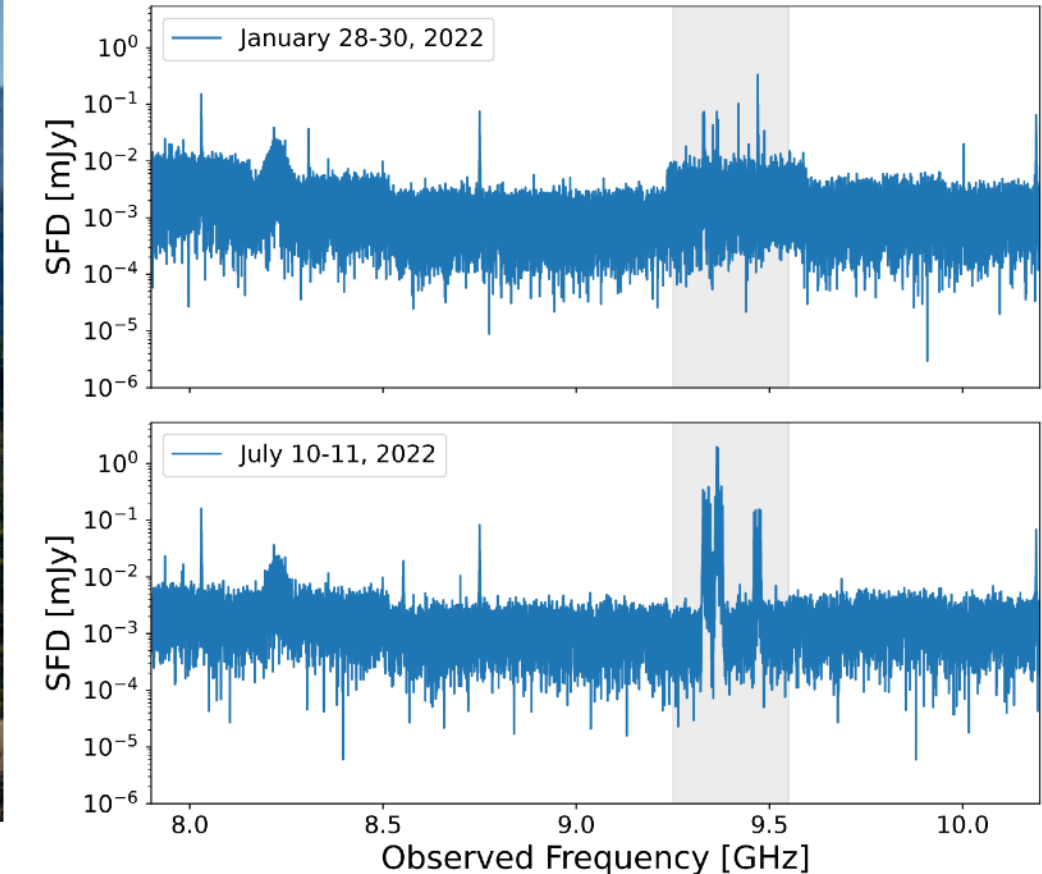
Axions in Andromeda



Andromeda (M31)



Green Bank Telescope (GBT)

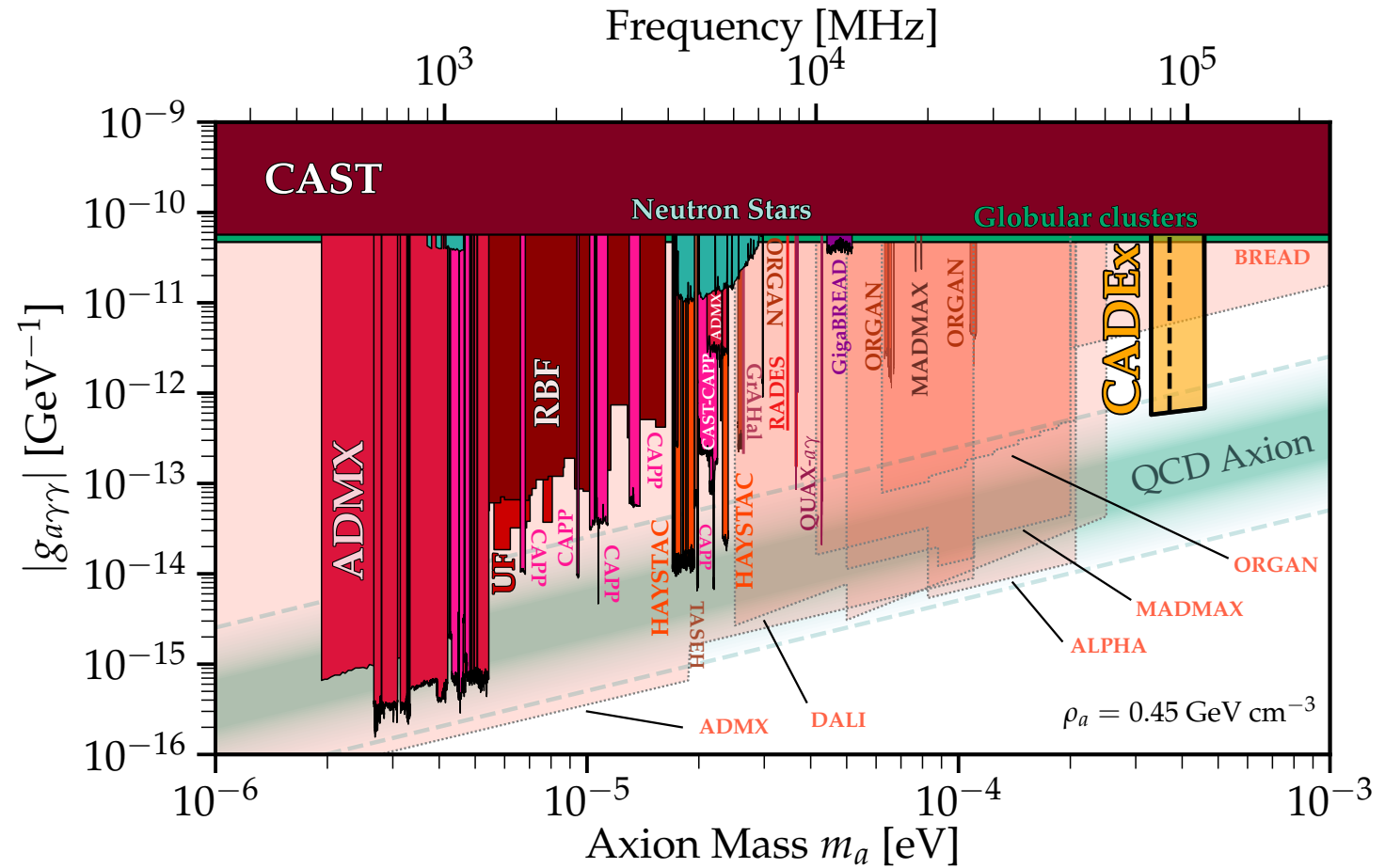


No axion-like transients observed in X-band ($\sim 8\text{-}10$ GHz)

[Walters et al. (including **BJK**), [2407.13060](#)]

Summary

- Axions are a well-motivated Dark Matter candidate, but **high-mass axions ($\gtrsim 100 \mu\text{eV}$) are unexplored.**
- **CADEX**: a novel search for DM axions (and more?) using a resonant cavity array
- Substantial **technological challenge** (but also a platform for development and testing of new sensors)
- **Complementary** to proposed non-cavity high-frequency axion searches
- Development of haloscopes, optics and detectors are underway, with **installation of the pathfinder planned for 2026** → first science results expected in 2027/2028

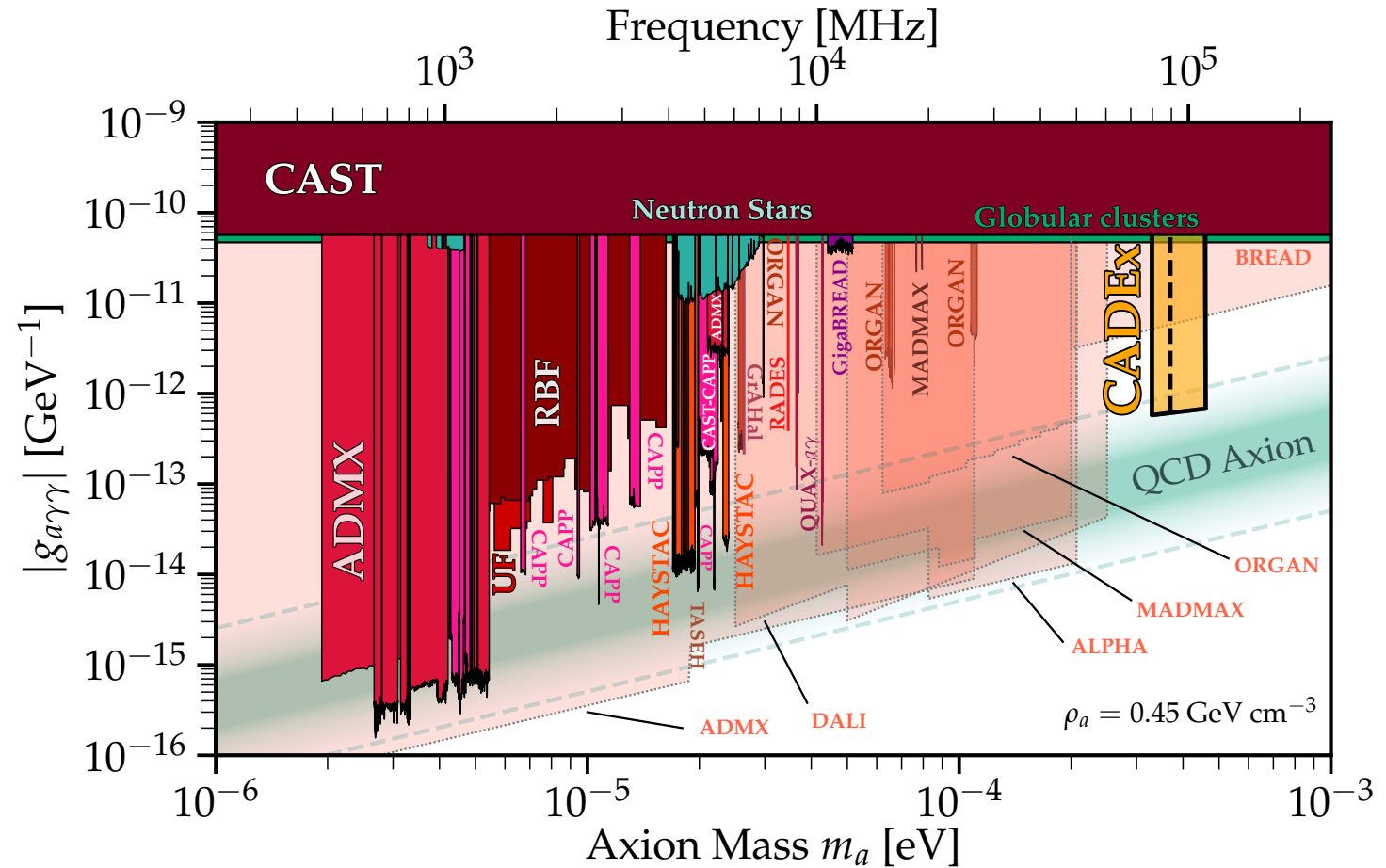


Thanks to the CADEX Team. And a special thanks to Ciaran O'Hare and to Igor Irastorza.

Summary

- Axions are a well-motivated Dark Matter candidate, but **high-mass axions ($\gtrsim 100 \mu\text{eV}$) are unexplored.**
- **CADEX**: a novel search for DM axions (and more?) using a resonant cavity array
- Substantial **technological challenge** (but also a platform for development and testing of new sensors)
- **Complementary** to proposed non-cavity high-frequency axion searches
- Development of haloscopes, optics and detectors are underway, with **installation of the pathfinder planned for 2026** → first science results expected in 2027/2028

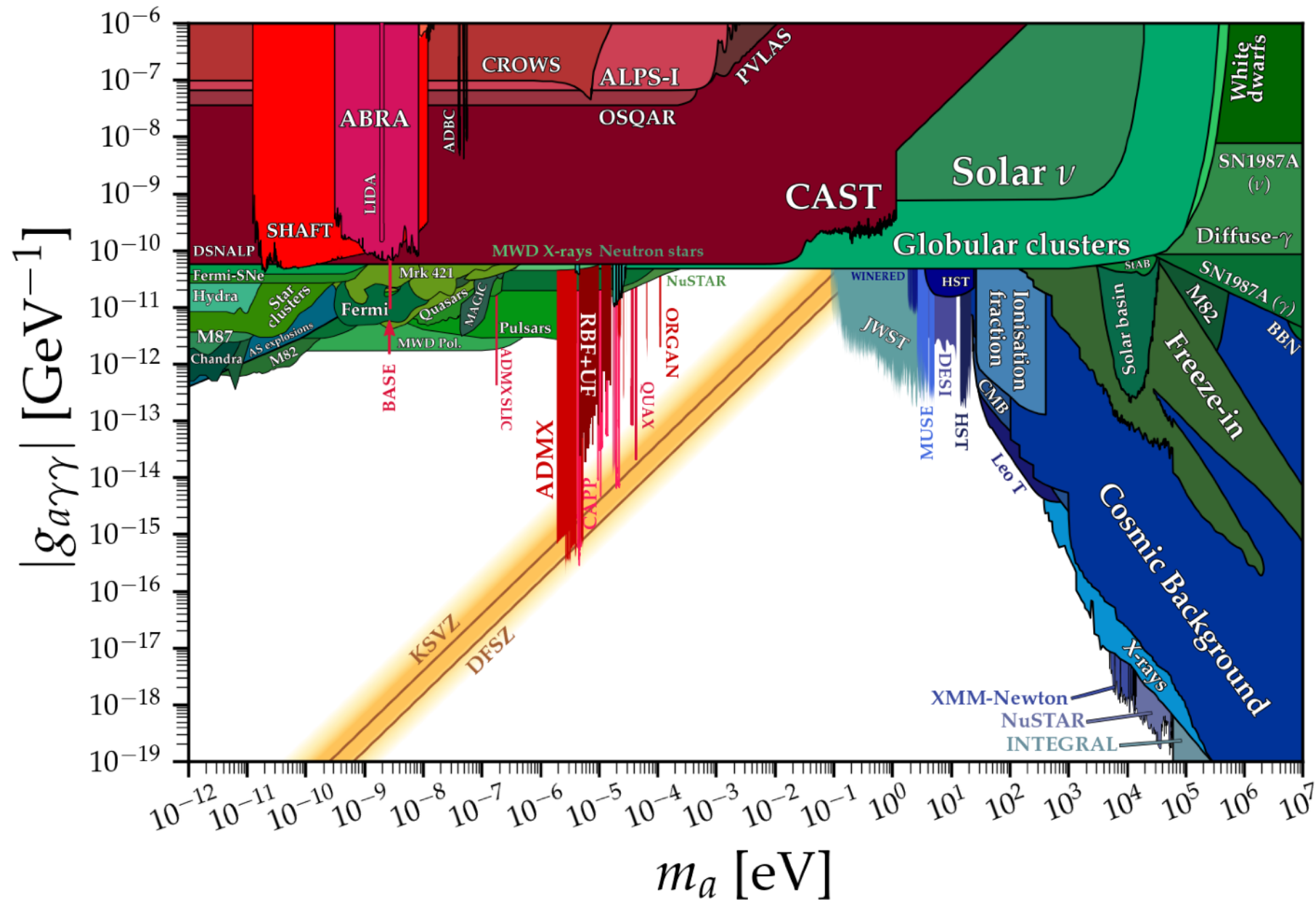
Thank you!



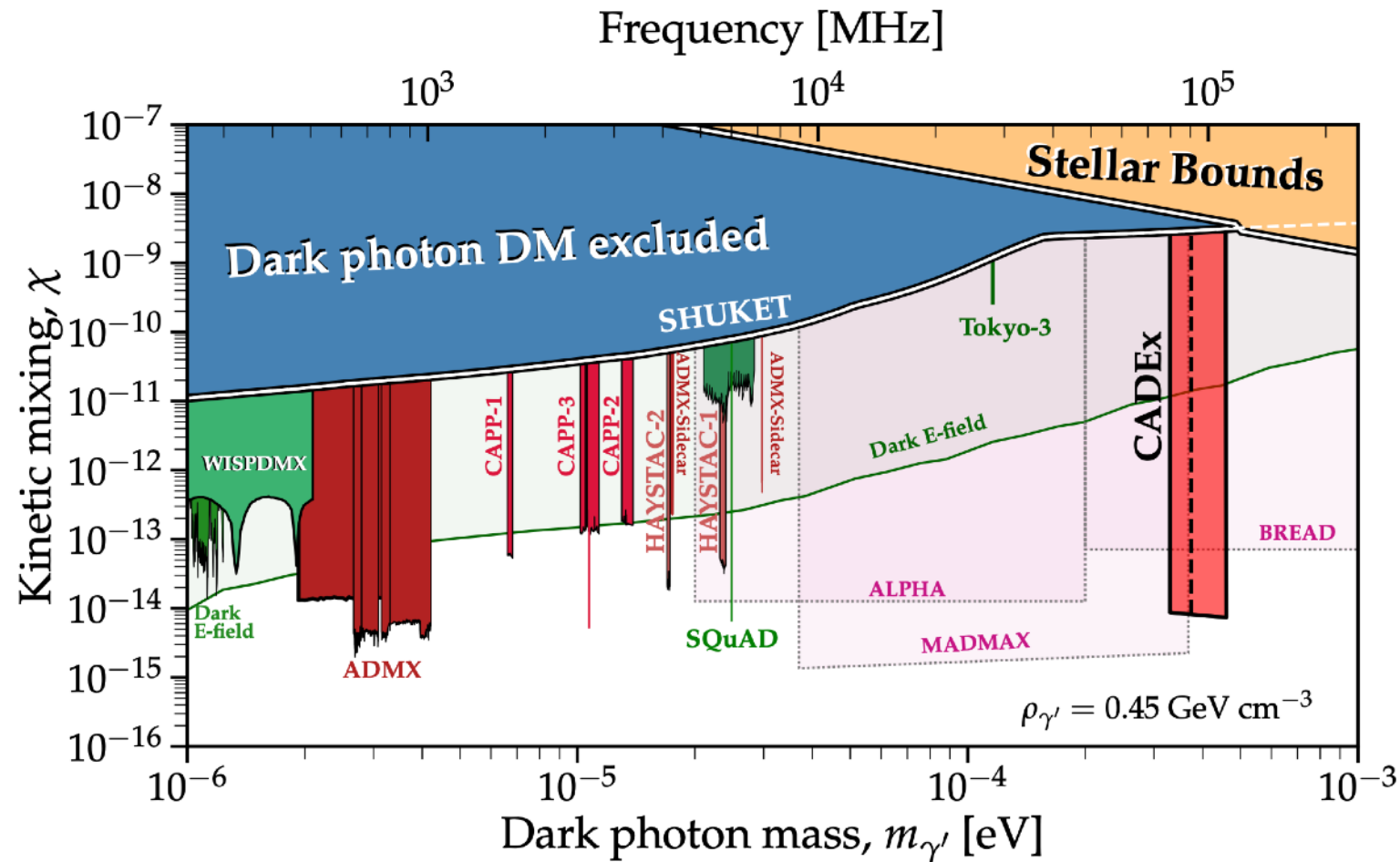
Thanks to the CADEX Team. And a special thanks to Ciaran O'Hare and to Igor Irastorza.

Backup Slides

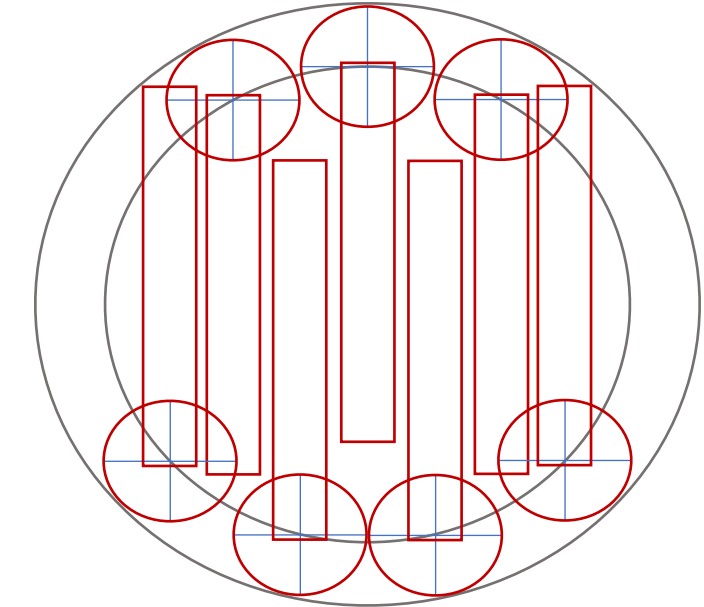
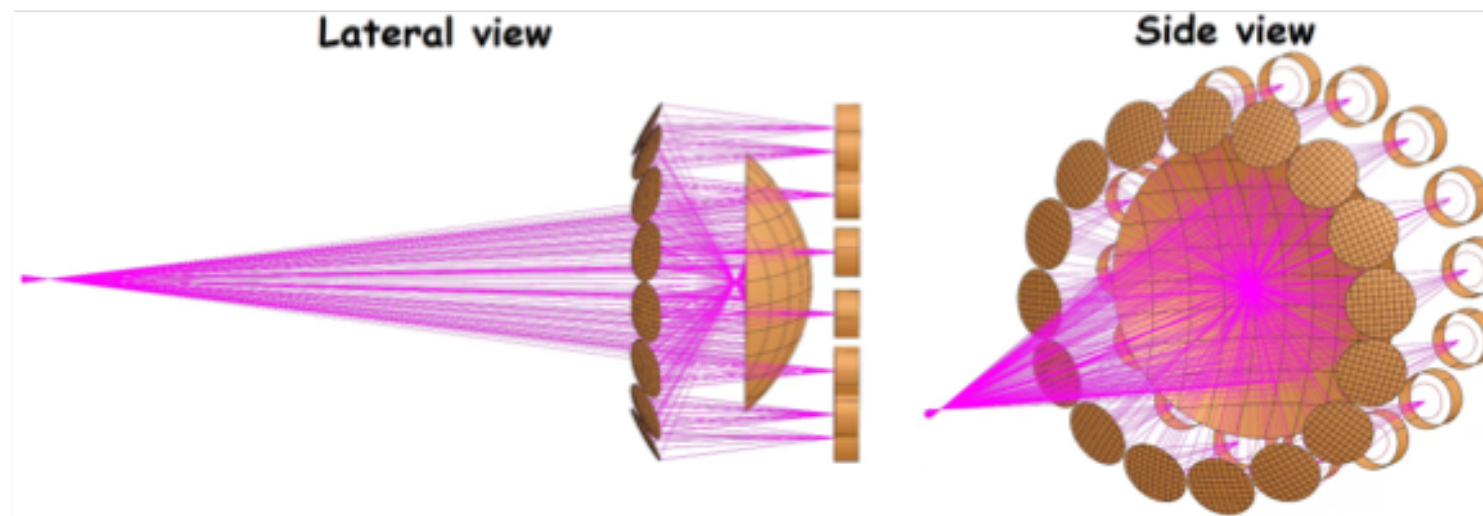
Axion Landscape (writ large)



- Updating sensitivity estimates, as design is updated and finalised
- Developing the **data analysis strategy** - broadband detection means spectral information of signal cannot be used to discriminate from background!
- Expanding the proposed search beyond axion (Dark Photons? Scalars? Gravitational Waves?)



- Need to **maximize volume** → haloscope array!
- **Quasi-optical system** based on 7 horn antennas apertures focus signal going out from the haloscopes to the detection system.
- Polarization needs to be preserved.
- To be fitted in the 100 mK space within the cryogenic system.
- Filters are mandatory to diminish out-of-band background signal.



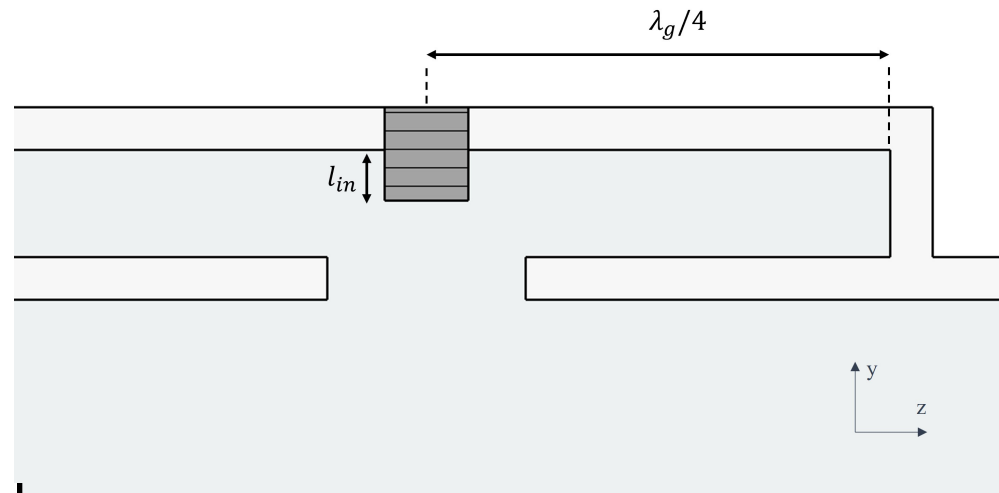
$$P_d = \frac{\beta}{(1 + \beta)^2} g_{a\gamma}^2 \frac{\rho_a}{m_a} B^2 C V Q$$

Old design with 16 cavities
(New design is for **7 cavities**)

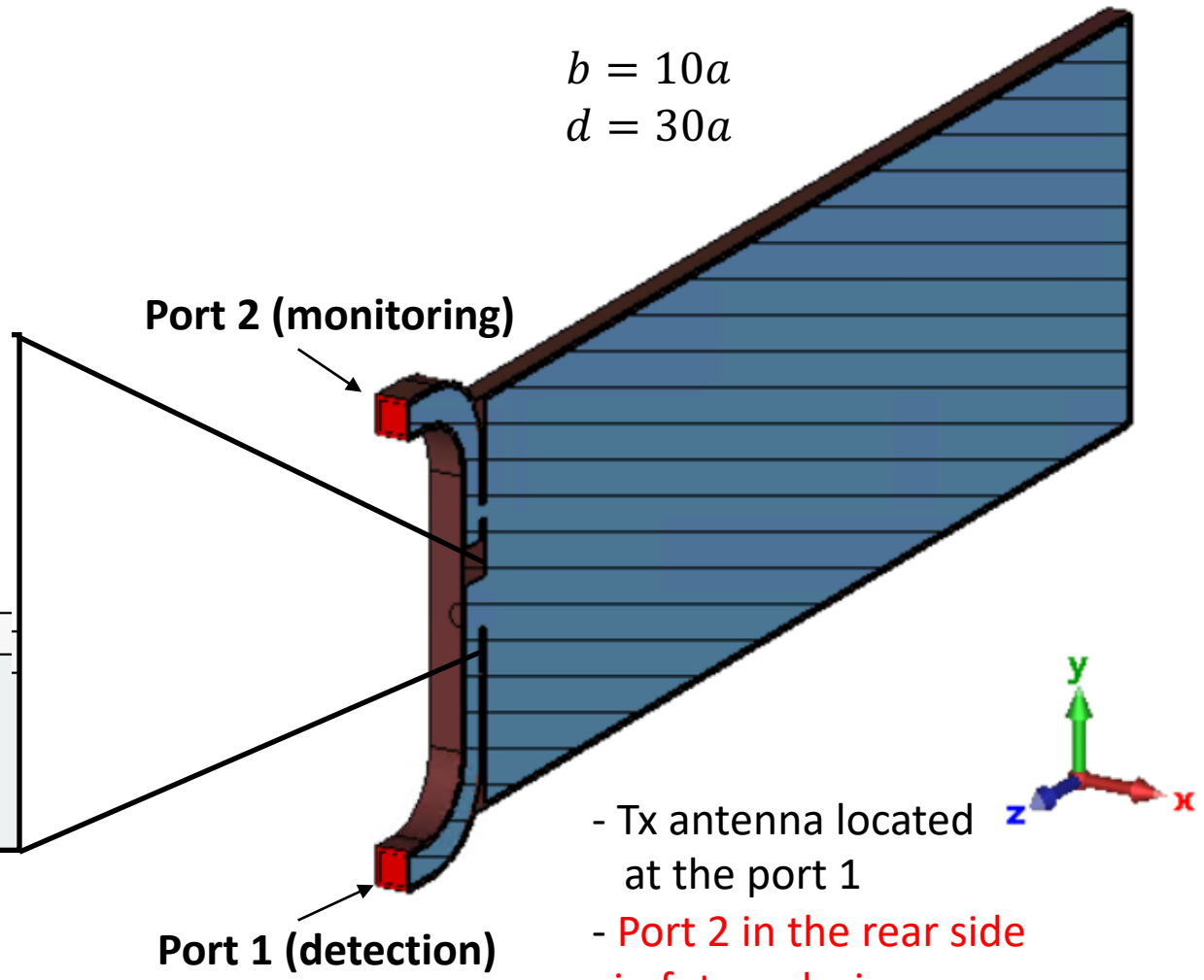
Haloscope Coupling

Bended waveguides are needed to orient the signal to the horn antennas

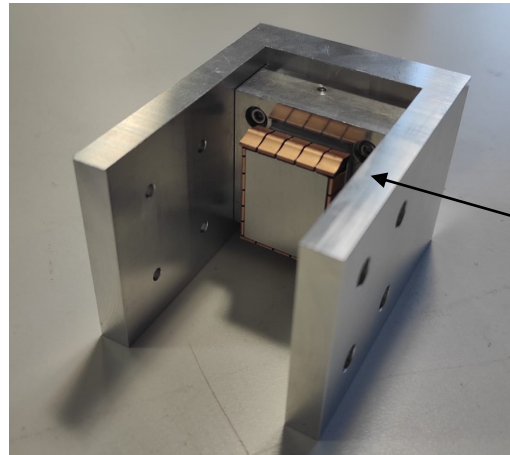
Coupling screw system



Needed to recouple the waveguide to the cavity

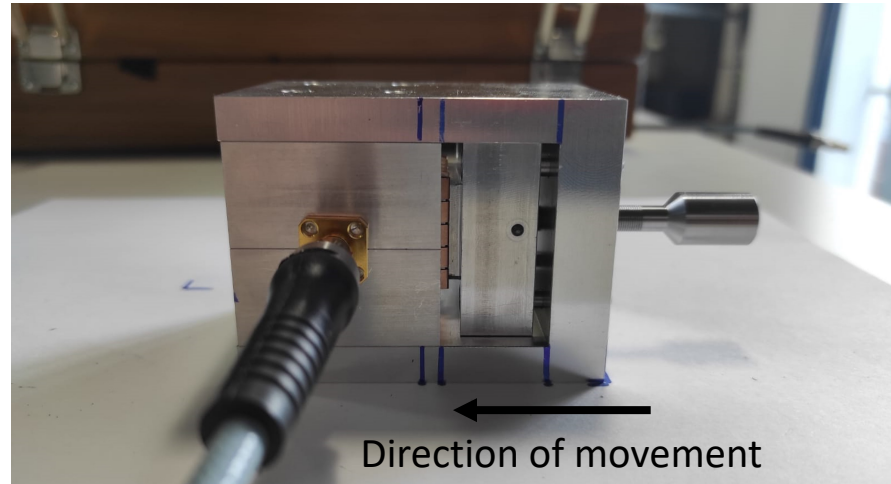


Tuneable Cavities

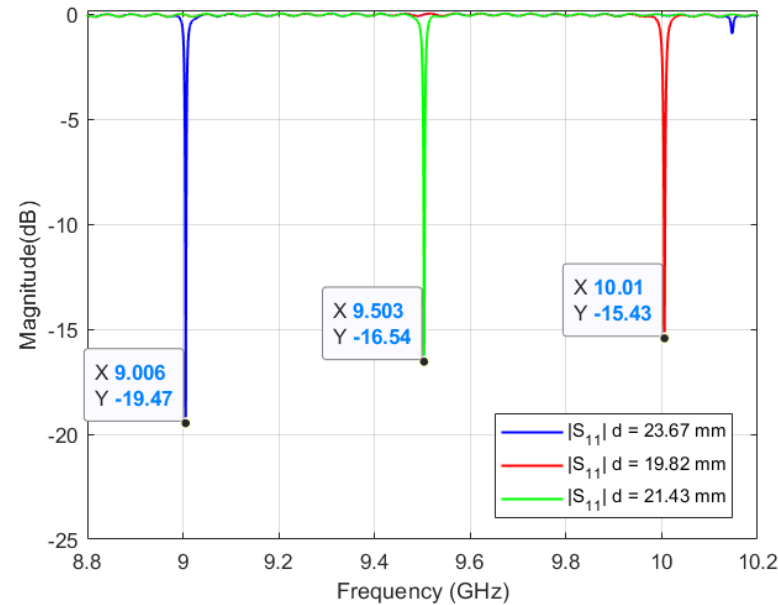


Manufactured sliding wall + gaskets prototype in X-Band (9-10 GHz)

Gaskets



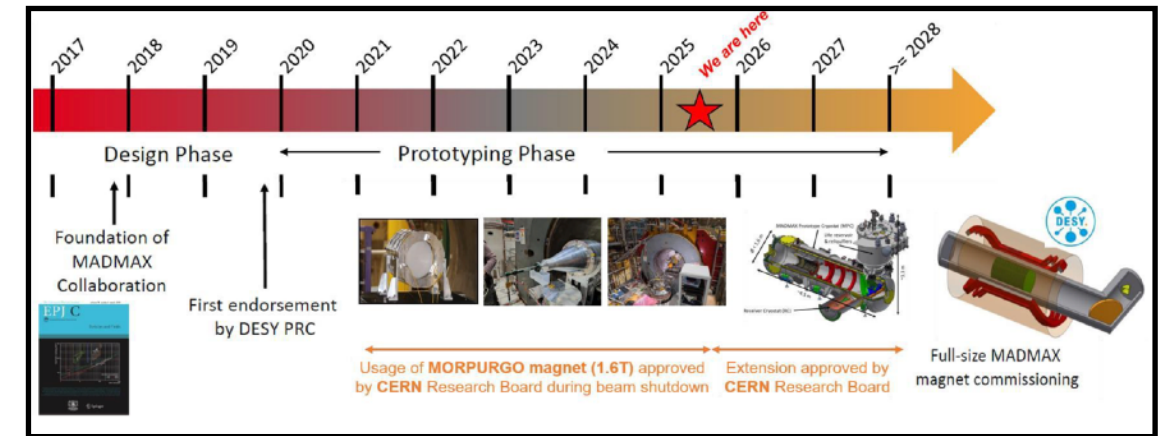
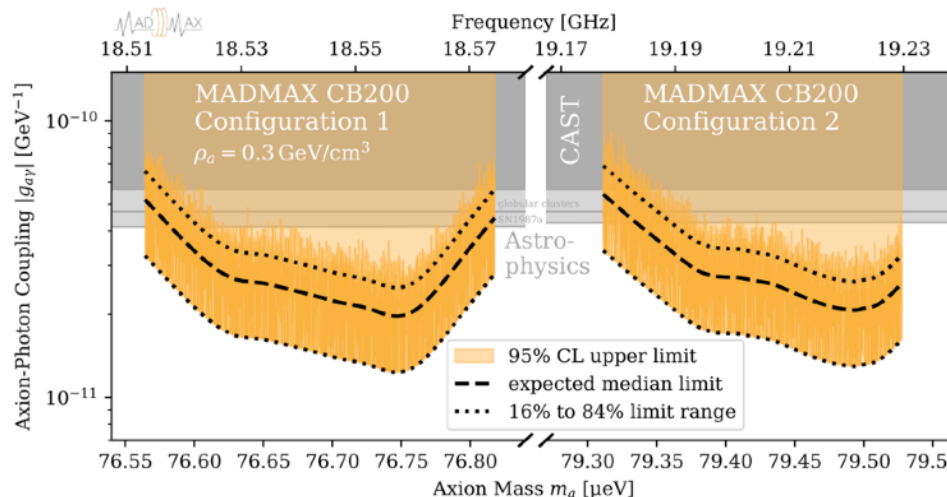
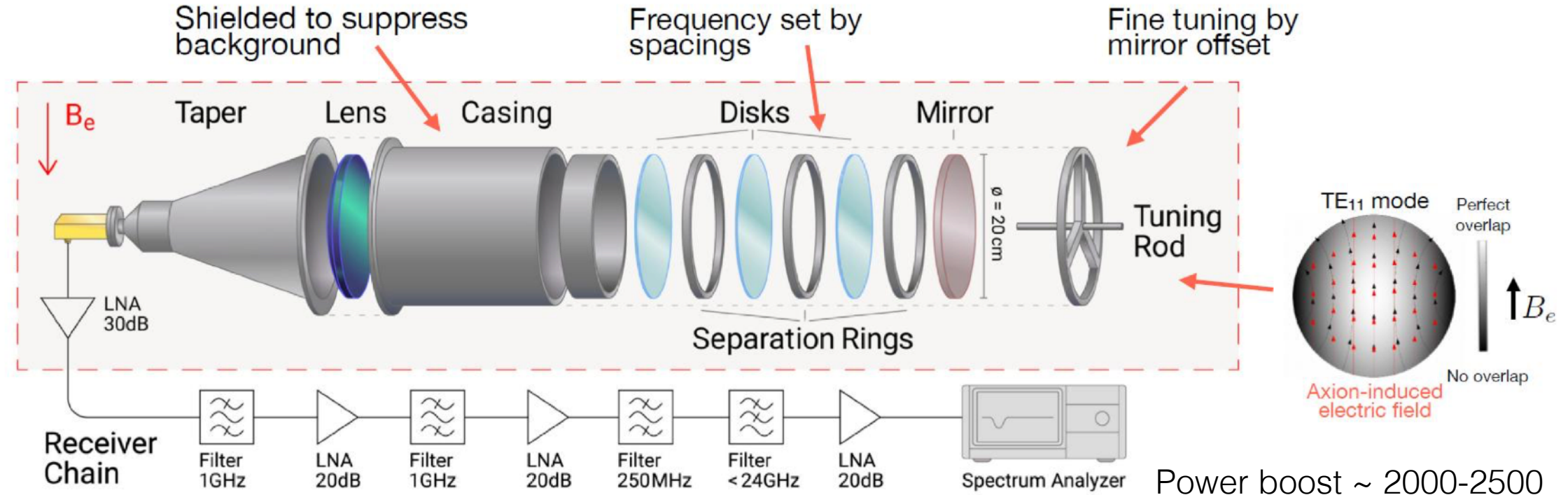
Direction of movement



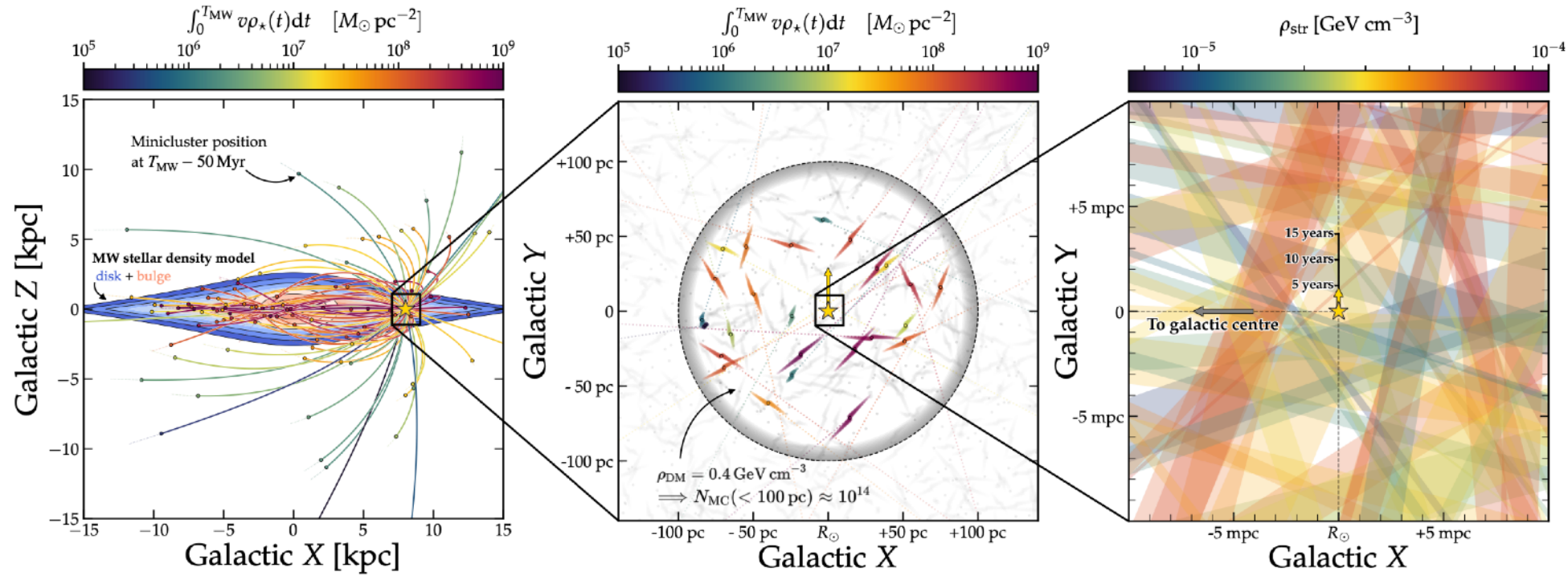
Compared with theoretical Q_0

Gaskets maintain **56%** of the theoretical Q_0

↓
Need to test combination of **gaskets + stub**



Axion Minicluster Streams and Voids



[2311.17367]

